A chromatin-modifying protein is a context-dependent modulator of cell survival in hematopoietic malignancies

by

Jennifer Ricks Shingleton

B.S. Biochemistry
B.A. Chemistry
North Carolina State University, 2008

Submitted to the Department of Biology
in Partial Fulfillment of the Requirements for the Degree of

Doctor of Philosophy

at the

MASSACHUSETTS INSTITUTE OF TECHNOLOGY

September 2014

Signature of Author .... Signature redacted .....
Department of Biology
July 1, 2014

Certified by ..... Signature redacted .....
Michael Hemann
Associate Professor of Biology
Thesis Supervisor

Accepted by ..... Signature redacted .....
Michael Hemann
Associate Professor of Biology
Co-Chair, Biology Graduate Committee

Abstract

Proteins that modify chromatin architecture are important drivers of leukemia. Many genetic lesions in hematopoietic malignancies lead to altered function of one or more chromatin-modifying proteins, often resulting in less differentiated cells that are more therapy-resistant. While a number of these lesions have led to development of effective targeted therapies, most have not. Identification of additional chromatin modifiers that affect disease progression may result in more amenable drug targets. With this in mind, our group carried out a large-scale RNA interference (RNAi) screen for factors influencing disease progression in a murine model of BCR-Abl+ B-ALL, a disease with low long-term survival rates despite treatment with inhibitors targeting the BCR-Abl kinase. This screen identified two chromatin-modifying genes, *Chd8* and *Sin3a*, as necessary for growth and survival of leukemic cells. While SIN3A is a well-characterized transcriptional co-repressor, the exact mechanism and relevance of CHD8 is less clear.

Here we demonstrate that RNAi-mediated depletion of CHD8 in BCR-Abl+ B-ALL cells leads to cell death, most likely in a caspase-independent manner and without a preceding cell cycle arrest. While multiple kinds of B cell malignancies were dependent on CHD8 expression for survival, two T cell malignancies displayed significantly milder phenotypes upon CHD8 knockdown. In addition, ectopic expression of the intracellular domain of Notch (ICN) in one of these T cell malignancies partially alleviated the detrimental effect of CHD8 depletion. Although CHD8 has been shown to bind to many active promoter sites, results of RNA-Seq analysis did not show significant expression changes of any particular genes upon CHD8 depletion, suggesting that CHD8 may act to regulate transcription of a large number of genes in a modest way. We show evidence that CHD8 promotes NF-κB signaling, as levels of phosphorylated RelA decrease upon CHD8 knockdown and addition of recombinant TNFα partially rescues the CHD8-depletion phenotype in BCR-Abl+ B-ALL cells. Our results demonstrate that CHD8 has a crucial role in cell survival, and its inhibition may be an effective treatment for B lymphoid malignancies that circumvents resistance to current therapies.

Table of Contents

Acknowledgements

I would like to thank...

My advisor, Dr. Michael Hemann, for his constant support throughout my graduate career. I am grateful for the freedom he gave me to pursue this project, as well as his friendship.

The members of my thesis committee, Dr. Tyler Jacks and Dr. Laurie Boyer, for their very helpful insights into my project over the years. I would also like to thank Dr. Michael Lee for graciously agreeing to serve on my thesis defense committee.

The members of the Koch Institute core facilities, especially Glenn Paradis, Mike Jennings, Michele Griffin, Charlie Whittaker, and Vincent Butty. Glenn and Mike do a fantastic job running the flow cytometry facility, and Mike and Michele sorted many millions of cells for me over the course of my graduate career. Charlie and Vincent, as well as Stuart Levine of the BioMicro Center, helped with RNA-Seq and subsequent expression analyses.

My fellow Hemann lab members, who have made my time at MIT an unforgettable experience. They created a scientifically rigorous but fun and supportive lab environment.

Peter Bruno, Yadira Soto, Eric Bent, Eleanor Cameron, Jordan Bartlebaugh, and Simona Dalin for critical readings of this document.

My fellow members of the incoming Biology Class of 2008. This is an incredible group of colleagues who quickly became great friends.

My family, especially my parents who have always supported my love of science. They chaperoned every trip to a Science Olympiad competition for 7 years, and have been an unfailing source of encouragement throughout graduate school. I would finally like to thank my husband Will. I am extremely grateful for his encouragement and support, especially during the thesis-writing process. I look forward to the next phase of our adventure.

Chapter 1: Introduction

Leukemic cell-of-origin vs. leukemia-initiating cell

Leukemia is largely a disease of interrupted differentiation. Differentiation can be stalled at multiple points along the hematopoietic lineage and by a number of different events, resulting in a wide array of malignancies. Decades of investigation into the process of hematopoietic differentiation have facilitated the use of morphology and cell surface marker expression to assign leukemia subtypes to corresponding stages of normal hematopoiesis. In particular, lineage- and stage-specific cell surface markers have been invaluable tools in investigating the developmental blocks that occur in leukemia. Despite this wealth of knowledge, determining the leukemic cell-of-origin, or the cell type in which the first transforming event took place, can still be challenging. Acquisition of an oncogenic mutation can lead to a leukemia that has de-differentiated back toward a stem cell state or a leukemia that results from arrest of forward progress. Thus the cell-of-origin in human leukemias cannot always be determined by examining the differentiation status of the bulk disease. In leukemias of the lymphoid lineage, B cell and T cell receptor status and clonality can help determine the origin of the disease. In addition, mouse models of various leukemias have allowed investigation into the ability of hematopoietic stem cells (HSCs) and more differentiated progenitor cells to give rise to disease upon introduction of an oncogene. For example, several studies have determined that both HSCs and granulocyte-macrophage progenitors (GMPs) can give rise to acute myeloid leukemia (AML) in mice when transduced with MLL fusion proteins, which are frequent drivers of AML (Cozzio *et al.* 2003; Hess 2004; Chen *et al.* 2008; Krivtsov *et al.* 2013). These studies also demonstrated certain differences between leukemias that arose from the two populations: HSCs were more efficiently transformed

by expression of MLL fusion proteins *in vitro*, were more capable of initiating leukemia upon transplant into mice, and gave rise to leukemias that were more resistant to chemotherapy (Cozzio *et al.* 2003; Chen *et al.* 2008; Krivtsov *et al.* 2013). In addition, Krivtsov and colleagues determined that AML patients exhibiting a genetic signature more similar to HSCs than GMPs had a worse prognosis (2013). These results suggest that determining the leukemic cell-of-origin can be clinically relevant by conferring prognostic information and potentially informing the course of treatment.

The same oncogenic event can give rise to different leukemic subtypes when it occurs in distinct stages of hematopoietic differentiation. A t(9;22) chromosomal translocation generating the BCR-Abl fusion protein can lead to either chronic myeloid leukemia (CML) or B-cell acute lymphoblastic leukemia (B-ALL). It has been demonstrated that CML arises when this translocation occurs in an HSC, while B-ALL arises from a progenitor B cell (Castor *et al.* 2005; Wang *et al.* 2008; Williams and Sherr 2008). The cell-of-origin of many other leukemia subtypes is still unclear. However, whether the leukemic cell-of-origin is an HSC or a committed progenitor, the resulting malignancy is composed of cells that cannot undergo terminal differentiation. The outgrowth of these less-differentiated, non-functional cells overwhelms normal hematopoietic populations and their functions.

Leukemia-initiating cells (LICs), on the other hand, are any cells within the tumor that have the ability to seed the disease. While LICs more closely resemble, transcriptionally and morphologically, cells in progenitor or stem cell states rather than terminally differentiated cell types (Crews and Jamieson 2013), they may no longer exactly correspond to the leukemic cell-of-origin. LICs can arise by alteration of committed progenitor cells to express a more stem-like state while maintaining other characteristics of the progenitor transcriptional program (Krivtsov *et al.* 2006).

Alternatively, HSCs themselves can be transformed through a series of mutations to give rise to LICs (Sloma *et al.* 2010; Jan and Majeti 2013). In both scenarios, the resulting cell type is able to self-renew indefinitely, giving rise to a bulk tumor population with either similar or lessened self-renewal potential, depending on the disease. One mechanism by which LICs achieve this stem-like state is through alterations in the genome itself. In many cases of AML, a chromosomal translocation fuses the *MLL* gene to a partner and alters its effect on target gene expression (Krivtsov and Armstrong 2007). These target genes include the *HOX* family, resulting in an aberrant self-renewal transcriptional program that prevents differentiation.

In addition to alterations in genomic sequence, changes in epigenetic patterning can also drive leukemogenesis. Aberrant methylation of promoters can alter the expression of genes that promote more differentiated states or maintain stemness without modifying the actual genetic code (Jones and Baylin 2007; Chan and Majeti 2013). The *de novo* DNA methyltransferase DNMT3A is frequently mutated or epigenetically silenced in AML, suggesting that misregulated DNA methylation is a driving force in leukemogenesis (Ley *et al.* 2010; Jost *et al.* 2013). Challen and colleagues found that conditional deletion of *Dnmt3a* in mice resulted in impaired HSC differentiation and an expanded pool of HSCs, similar to that seen in AML patients with *DNMT3A* mutations (Challen *et al.* 2012; Chan and Majeti 2013). Although these mice did not develop leukemia, this expanded pool of HSCs represents an increased opportunity for acquisition of additional mutations that can lead to disease. While DNMT3A inhibitors are frequently used to treat AML (Fathi and Abdel-Wahab 2011), our understanding of DNMT3A's mechanism of stem cell maintenance is far from complete.

A thorough understanding of the relationship and relative differentiation status between LICs and the bulk tumor population is critical to designing more effective

therapeutic regimens for hematopoietic malignancies. Certain leukemias follow the cancer stem cell model in which only a rare population of less differentiated cells has tumor-initiating potential and gives rise to a bulk population of non-tumorigenic cells (Shackleton *et al.* 2009). In other leukemias however, a large fraction of cells have tumor-initiating potential (Kelly *et al.* 2007; Williams *et al.* 2007; Rehe *et al.* 2012). These models dictate somewhat varying treatment strategies: in malignancies following the cancer stem cell model, traditional anti-mitotic chemotherapeutics alone would be less effective on these rare, slowly-dividing or dormant LICs and relapse would quickly ensue (Ravandi and Estrov 2006). On the other hand, anti-mitotic drugs would more clearly benefit patients suffering from malignancies in which LICs constitute a large fraction of the rapidly proliferating disease burden. This variance is illustrated in the different therapeutic regimens administered to patients with chronic myeloid leukemia (CML) and Philadelphia chromosome-positive acute lymphoblastic leukemia (Ph+ B-ALL). Although the same oncogenic fusion protein (BCR-Abl) is present in both diseases, CML follows a cancer stem cell model while Ph+ B-ALL does not (Sloma *et al.* 2010; Rehe *et al.* 2012). Accordingly, treatment for Ph+ B-ALL is more aggressive, with patients receiving cytotoxic chemotherapy in addition to a kinase inhibitor targeting BCR-Abl and/or allogeneic stem cell transplant (Fielding and Zakout 2013).

However, whether LICs are rare or abundant in a particular malignancy, any tumor cells with the potential to re-propagate the disease burden following therapy must be eradicated to achieve a long-term cure. Whether rare or not, LICs are often resistant to therapy, either due to intrinsic properties or location within a protective niche (Bradstock and Gottlieb 1995; Crews and Jamieson 2013; Krause *et al.* 2013). An attractive strategy for eradicating LICs in either leukemic model consists of forcing them to undergo differentiation (Crews and Jamieson 2013). The resulting more highly

differentiated cells would be unable to revert to an undifferentiated state and self-renew, re-seeding the disease after termination of therapy. Two major categories of proteins, transcription factors and epigenetic regulators, are highly involved in the process of differentiation and have been functionally implicated in leukemogenesis, providing a number of prospective and realized drug targets. Numerous therapeutic agents inhibiting these factors are currently in use, and some have proved highly effective at treating certain hematopoietic malignancies. However, there is still much room for improvement and development as long-term cure rates remain abysmally low for many leukemias.

Transcription factor mediators of differentiation are deregulated in leukemia

Extensive research has elucidated the function of a number of prominent transcription factors that are mediators of differentiation and drivers of leukemogenesis. For some leukemias, this understanding has translated into more effective therapies that have radically altered prognoses. Unfortunately, most transcription factors are as yet "undruggable," making the search for inhibitors that are effective in large patient populations a challenging endeavor.

RARα

Acute promyelocytic leukemia (APL) is one of the most striking examples of how the adoption of differentiation therapy can alter a disease history. APL is a malignancy characterized by a balanced chromosomal translocation fusing the N-terminus of the *PML* (promyelocytic leukemia) gene on chromosome 15 to the C-terminus of the retinoic

acid receptor-alpha (RARα) gene on chromosome 17 (Borrow *et al.* 1990; Kakizuka *et al.* 1991; de Thé *et al.* 1991; dos Santos *et al.* 2013). RARα normally functions as a transcriptional repressor that recruits additional co-repressors and histone deacetylases (HDACs) to inhibit expression of target genes. In the presence of retinoic acid (RA), RARα becomes a transcriptional activator, recruiting histone acetyltransferases (HATs) and turning on expression of genes that lead to differentiation along the myeloid lineage. However physiological levels of RA are unable to convert the PML-RARα fusion protein into an activator, thus keeping target gene promoters inaccessible to transcription machinery, stalling cellular differentiation, and maintaining cells in a state resembling the promyelocytic stage (Wang and Chen 2008; de Thé and Chen 2010; de Thé *et al.* 2012).

Discovery of this translocation several decades ago gave a mechanistic rationale for the use of all-trans RA (ATRA) as a frontline therapeutic, which had been used for several years to induce remission in patients with APL (Wang and Chen 2008). ATRA is able to induce differentiation of leukemia-initiating cells into granulocytes, leading to complete remission in almost all cases (Chomienne *et al.* 1990). However, most patients on ATRA monotherapy eventually relapse due to the acquisition of resistance and the presence of minimal residual disease (MRD), demonstrating that granulocyte differentiation alone is not sufficient to cure this malignancy (Nasr *et al.* 2008). Arsenic trioxide (ATO) was added to ATRA therapy several years later in hopes of improving patient response (Wang and Chen 2008). This regimen proved to be a synergistic combination, shortening the time to complete remission and decreasing the incidence of relapse compared to ATRA or ATO monotherapy. ATO binds directly to PML-RARα and induces structural changes that result in the formation of PML nuclear bodies (Jeanne *et al.* 2010; Zhang *et al.* 2010). PML-RARα is sumoylated within these nuclear bodies, leading to ubiquitination and proteasomal degradation (Lallemand-Breitenbach *et al.*

2008; Tatham *et al.* 2008). The importance of PML-RARα degradation in the effective treatment of APL is demonstrated in that synthetic retinoids that cause differentiation but do not lead to PML-RARα degradation are less effective therapeutics (Ablain *et al.* 2013). It has been shown that ATRA and ATO are synergistic in that the transcriptional response induced by ATRA and the proteomic changes effected by ATO reinforce each other, resulting in death of cells expressing PML-RARα (Zheng *et al.* 2005).

"Undrugged" transcription factors involved in leukemia

Unfortunately the success of ATRA/ATO therapy in treating APL has not been replicated in cases of leukemia driven by other transcription factors. Although we have a detailed understanding of the structure and mechanism of many of these proteins, the development of effective small molecule inhibitors has remained elusive. A small number of transcription factors responsible for HSC population maintenance are very frequently altered in AML, including EVI1 and RUNX1, suggesting that new therapies targeting these factors may have a clinical effect in a large percentage of patients.

EVI1 was first identified in murine models of myeloid leukemia as a site of ecotropic retroviral integration leading to disease (Morishita *et al.* 1988; Mucenski *et al.* 1988; Goyama and Kurokawa 2010). It is frequently activated as a result of chromosomal translocations in AML, CML, and myelodysplastic syndrome (MDS) (Morishita *et al.* 1992; Mitani *et al.* 1994), or aberrant transcription driven by MLL fusion proteins (Arai *et al.* 2011). AML patients with high EVI1 expression have a poor prognosis (Barjesteh van Waalwijk van Doorn-Khosrovani *et al.* 2003). The normal function of EVI1 is to promote HSC proliferation and maintenance through transcriptional activation of *GATA-2* and other target genes involved in these processes (Yuasa *et al.* 2005), thus the effect of EVI1 overexpression is enhanced self-renewal and leukemia-

initiating potential (Sato *et al.* 2014). High EVI1 expression in a murine model of CML was also associated with resistance to tyrosine kinase inhibitor (TKI) therapy and progression to CML blast crisis, highlighting the link between LIC self-renewal and drug resistance properties. A recent study identified two serine phosphorylation sites on EVI1 that regulate its ability to bind to DNA (Bard-Chapeau *et al.* 2013). Inhibition of phosphorylation at these sites may be a promising strategy for abolishing EVI1 activity and inducing differentiation of LICs in malignancies that overexpress this factor.

The transcription factor RUNX1 (AML1) is the most common target of chromosomal translocation in AML, as well as a frequent target in CML and pediatric B-ALL (Okuda *et al.* 1996; Wang *et al.* 1996). RUNX1 is a member of the runt-related heterodomain transcription factor family and is required for HSC generation in embryos. However in adult HSCs, RUNX1 negatively regulates self-renewal (Ichikawa *et al.* 2004; Ichikawa *et al.* 2008; Kumano and Kurokawa 2010). Most RUNX1 alterations found in AML involve a chromosomal translocation that creates a fusion protein that can bind to DNA but is unable to activate transcription, resulting in a dominant negative protein that competes away wild-type, functional RUNX1 from target promoters (Koh *et al.* 2013). One of the most common fusion proteins, RUNX1-ETO, has been shown to increase the number of early progenitor cells, which in turn increases the available pool of cells that can undergo further mutation to generate leukemia (Nimer and Moore 2004). Several large-scale screens with chemical compound libraries have yielded a number of promising drugs with efficacy against AML with RUNX1-ETO translocations (Hatlen *et al.* 2012). In one such screen, corticosteroids and dihydrofolate reductase inhibitors were shown to decrease colony formation ability and facilitate myeloid differentiation and apoptosis in Kasumi-1 AML cells, which express this translocation (Corsello *et al.* 2009). In addition, HDAC and HSP90 inhibitors have been shown to reduce the half-life of the

RUNX1-ETO fusion protein, thus alleviating its aberrant self-renewal transcriptional program (Lutterbach *et al.* 1998; Yang *et al.* 2007). Further clinical studies will be needed to establish the potency of these compounds in AML patients with a variety of RUNX1 lesions. However it is clear that induction of differentiation is a necessary component of therapy in these AML subtypes.

Epigenetic mediators of differentiation are deregulated in leukemia

In recent years the importance of epigenetic regulation in cancer has gained greater appreciation as more leukemic drivers with histone-modifying activity have been discovered, including those that regulate differentiation status (Popovic and Licht 2012). Histone methyltransferases such as MLL and EZH2, as well as several histone deacetylases are just a few examples of regulators of hematopoietic differentiation that have epigenetic functions.

MLL

One of the most frequently mutated histone modifiers in leukemia is MLL (mixed lineage leukemia). Chromosomal abnormalities involving MLL are common in both pediatric and adult AML cases, and are also found in ALL (Biondi *et al.* 2000; Hess 2004; Zhang *et al.* 2012). The normal function of MLL is to maintain expression of *HOX* genes in hematopoietic stem and progenitor cells through methylation of lysine 4 on histone H3 (H3K4) (Krivtsov and Armstrong 2007; Chi *et al.* 2010), a marker associated with actively transcribed genes. Fusion of the N-terminus of MLL to one of several fusion partners

results in loss of H3K4 methyltransferase activity, but leads to H3K79 methylation (another marker of active transcription) at target gene promoters, thus retaining transcriptional activity but possibly altering its control (Krivtsov and Armstrong 2007). The most common MLL fusion partner genes include *AF4*, *AF9*, *AF10*, *ELL*, and *ENL*, all of which encode proteins with transcription elongation or activation functions (Meyer *et al.* 2006; Krivtsov and Armstrong 2007). In addition, the AF4 and AF9 fusion partners are able to recruit the H3K79 methyltransferase DOT1L to promoters of *HOX* genes and *MEIS1*, a HOX co-factor (Schnabel *et al.* 2000; Krivtsov and Armstrong 2007; Bernt *et al.* 2011). The end result of each of these chromosomal abnormalities is the creation of a population of leukemia-initiating cells with an aberrant self-renewal transcriptional program. Studies have shown that expression of MLL fusion proteins in HSCs, common myeloid progenitors (CMPs), and granulocyte-macrophage progenitors (GMPs) can give rise to AML (Cozzio *et al.* 2003; Krivtsov *et al.* 2006).

While no therapies targeting MLL itself have been generated, a number of drugs inhibiting MLL-interacting proteins are under investigation (Zhang *et al.* 2012). A small molecule that inhibits the interaction of MLL with the transcription factor Menin has been shown to induce terminal differentiation and growth arrest in human leukemia cells (Grembecka *et al.* 2012). This molecule, MI-2, prevents the Menin-MLL-AF9 complex from binding to the *HOXA9* and *MEIS1* loci and activating transcription. An inhibitor of DOT1L has also shown efficacy in MLL fusion-driven xenograft models of AML, and is specific to cells expressing MLL translocations (Daigle *et al.* 2011). In addition, an RNAi screen performed in an MLL-AF9 driven mouse model of AML identified a dependency on Brd4 (bromodomain-containing 4) activity for proliferation and survival (Zuber *et al.* 2011). Accordingly, treatment with the bromodomain inhibitor JQ1 resulted in growth inhibition and apoptosis in both murine and human AML cell lines and primary patient

samples. Further elucidation of the mechanisms responsible for MLL-driven leukemogenesis and maintenance will hopefully yield additional candidate drug targets.

EZH2

EZH2 (Enhancer of Zeste Homologue 2) is the catalytically active subunit of the Polycomb repressor complex 2 (PRC2) (Lund *et al.* 2014). PRC2 functions as a transcriptional repressor by methylating lysine 27 of histone 3 (H3K27), thus creating a more compact chromatin environment, as well as by directly inhibiting RNA polymerase II (Cao *et al.* 2002; Francis *et al.* 2004; Min *et al.* 2011). PRC2 has been shown to be necessary for the initiation of transcriptional repression, while PRC1 is recruited by the H3K27me3 marks deposited by PRC2 and is responsible for maintaining repression (Cao *et al.* 2002; Lund *et al.* 2014). EZH2 also recruits DNA methyltransferases, thus initiating an additional mechanism of transcriptional repression (Viré *et al.* 2006).

Hematopoietic stem cells (HSCs) exhibit high levels of EZH2 as this protein is required for maintenance of the HSC compartment (Kamminga *et al.* 2006). EZH2 represses the expression of genes involved in differentiation in order to preserve stem cell potential, and leads to increased expression of cell cycle genes to prevent stem cell exhaustion (Ezhkova *et al.* 2009; Bracken *et al.* 2003). This anti-differentiation role of EZH2 is deregulated in several hematopoietic malignancies including diffuse large B cell lymphoma (DLBCL) and follicular lymphoma, either through overexpression or gain-of-function mutations (van Kemenade *et al.* 2001; Morin *et al.* 2010). A number of mutations at Tyr641 result in alteration of the preferred substrate of EZH2 (Sneeringer *et al.* 2010). Wild-type EZH2 is most efficient at methylating H3K27me0, and catalytic efficiency decreases as additional methyl groups are bound to H3K27. However, Tyr641 mutations greatly increase the efficiency of the trimethylation reaction, resulting in

increased levels of H3K27me3 and transcriptional repression of genes involved in differentiation. Interestingly, Tyr641-mutant alleles of EZH2 are always expressed in conjunction with a wild-type EZH2 allele, suggesting that both alleles with their complementary substrate specificities are required for target gene repression.

A number of small molecule inhibitors of EZH2 are in development. The first to be developed, DZNep, induces degradation of PRC2 but has broad inhibitory effects on other protein methyltransferases (Tan *et al.* 2007; Miranda *et al.* 2009). More recently identified EZH2 inhibitors, including EPZ005687 and GSK126, are more specific (Knutson *et al.* 2012; McCabe *et al.* 2012). Both of these compounds inhibit the methylation activity of EZH2, thus reducing H3K27me3 levels and relieving transcriptional repression. EPZ005687 specifically inhibits Tyr641-mutant EZH2, thus inducing apoptosis in mutant lymphoma cells while largely sparing wild-type cells (Knutson *et al.* 2012). GSK126 has been shown to reduce tumor burden and extend the lifespan of xenograft mouse models of mutant EZH2-driven DLBCL (McCabe *et al.* 2012).

While EZH2 appears to act as an oncogene in a number of malignancies, loss of EZH2 function has also been observed in cancers, including AML and T-ALL (Lund *et al.* 2014). It has been hypothesized that loss of EZH2 in myeloid malignancies contributes to the cancer stem cell state by increasing expression of *HOX* genes that promote self-renewal (Khan *et al.* 2013). Given the ability of EZH2 to act as a tumor suppressor gene or an oncogene in different cellular contexts, greater understanding of the drivers determining the different roles of this protein will help predict which malignancies to treat with EZH2 inhibitors.

Histone deacetylases

While effective drugs targeting histone methyltransferases remain elusive, small molecule inhibitors of histone deacetylases (HDACs) have been in use in the clinic for years (Rosenberg 2007). Their mechanism of action was only discovered relatively recently and is still only partially understood. Histone deacetylation is yet another epigenetic modification that plays a role in impairing cellular differentiation in leukemia. HDACs are recruited by transcription factors to promoters of target genes to repress transcription through the creation of a closed chromatin conformation (Mummery *et al.* 2011). It has been shown that the PML-RARα, PLZF-RARα, and RUNX1-ETO fusion proteins facilitate transcriptional repression through recruiting HDACs, supporting their inclusion in combination therapies for leukemias driven by these oncogenes (Minucci and Pelicci 2006). In addition to their role in histone acetylation, HDACs also deacetylate numerous non-histone protein substrates including p53, pRb, and Myc, and part of their clinical efficacy is attributed to these non-histone related functions (Minucci and Pelicci 2006; Mummery *et al.* 2011). Unfortunately the promise of HDAC inhibitors has not yet been borne out by clinical trial results. Additional research into HDAC biology is required to fully understand the effects of these enzymes on cellular transformation and maintenance of the malignant state.

Functional genetic screening to identify modulators of leukemia progression

Although numerous transcriptional and epigenetic regulators of differentiation have been identified as drivers of leukemogenesis, most of these factors remain poor

drug targets. Additional investigation is required to uncover factors that may be easier to inhibit in order to induce differentiation of LICs. The importance of driving LICs towards differentiation has been shown by studies demonstrating that leukemic relapse can be initiated by relatively minor subclones of the bulk population at the time of diagnosis (Mullighan *et al.* 2008b). Thus, the leukemic cells that should be targeted for eradication are not necessarily the ones constituting the majority of the disease burden, but any cells with leukemia-initiating potential (although cells with this potential may make up a large fraction of the burden in certain malignancies) (Shackleton *et al.* 2009). Factors that are responsible for maintaining the self-renewal ability of leukemic blasts should be identified and targeted as a means to eradicate the minimal residual disease burden that leads to relapse.

Deep sequencing and copy number analysis are powerful tools for identifying genetic alterations in tumor samples. However complementary approaches should also be used, as the power of high-throughput sequencing to discover factors responsible for LIC self-renewal is limited. LICs harboring mutations in these factors may constitute a small minority of the disease burden and may not be distinguishable from the bulk population. In addition, large-scale transcriptional changes caused by mutations in chromatin-modifying genes are often responsible for enhanced self-renewal. While sequencing can identify alterations in the chromatin-modifying genes responsible for these changes, this approach would not yield information on their downstream effects or whether the mutations conferred loss or gain of function.

RNA interference (RNAi) screening in mouse models is a complementary approach that can functionally identify genes or pathways critical for leukemic self-renewal. Crucially, RNAi screens enable the examination of loss-of-function effects of genes, providing much more information than sequencing alone. Recent advances in

screening protocols have made this approach even more tractable on a high-throughput scale. Massively parallel sequencing allows one to determine the relative expression of multiple short hairpin RNA (shRNA) constructs pooled within a single sample, with each cell expressing a single shRNA. In this way the behavior of hundreds or even thousands of shRNAs within a single tumor or cell culture plate can be simultaneously assessed rather than measuring the behavior of a single shRNA in each population. In these pool-based screens it is possible to query the effect of knocking down several thousand genes in a single population, increasing the scale of RNAi library feasible for investigation (Meacham 2012).

In addition to being able to represent a highly complex library, an effective mouse model for RNAi screening must also closely recapitulate a human disease. To meet both of these criteria, we selected a mouse model of Philadelphia chromosome-positive (Ph+) B-ALL, another example of a leukemia driven by over-proliferation of less differentiated cells. In contrast to other B cell malignancies such as diffuse large B-cell lymphomas and chronic lymphocytic leukemia, Ph+ B-ALL is composed of pre-B rather than mature B cells (Young and Staudt 2013). The hallmark genetic event of this disease is a balanced chromosomal translocation between the breakpoint common region (BCR) on 22q11 and the *ABL1* gene on 9q34 that generates the characteristic Philadelphia chromosome and results in a constitutively active Abl tyrosine kinase due to loss of its N-terminal autoregulatory region (Groffen *et al.* 1984; Clark *et al.* 1987; Pluk *et al.* 2002). Ph+ B-ALL accounts for approximately 20% of adult ALL cases and 5% of pediatric cases, while another 10% of adult B-ALL cases that are Philadelphia chromosome-negative manifest the BCR-Abl fusion gene (Kurzrock *et al.* 2003). While the BCR-Abl translocation is sufficient to generate the indolent phase of chronic myeloid leukemia (CML), an additional genetic lesion is necessary to generate Ph+ B-ALL or trigger

lymphoid blast crisis CML. These lesions are commonly found in the *IKAROS*, *PAX5*, and *INK4A-ARF* loci, and contribute to maintenance of the immature lymphoid state of these cells (*IKAROS* and *PAX5*) or avoidance of apoptosis (*INK4A-ARF*) (Heerema *et al.* 2004; Mullighan *et al.* 2008a; Mullighan *et al.* 2008b; Mullighan *et al.* 2008c; Williams and Sherr 2008).

Tyrosine kinase inhibitors (TKIs) have been developed that specifically target BCR-Abl, and Ph+ B-ALL patients generally respond well initially (Boulos *et al.* 2011; Liu-Dumlao *et al.* 2012). However, patients quickly relapse, usually acquiring drug resistance due to mutations in the kinase domain of ABL that prevent TKI binding, upregulation of drug efflux pumps, or activation of compensatory cell signaling pathways (Hu *et al.* 2006; Talpaz *et al.* 2006; Boulos *et al.* 2011; Liu-Dumlao *et al.* 2012). Even the combination of TKI therapy with conventional chemotherapeutics has not substantially altered long term survival rates, especially in elderly patients who are poor candidates for allogeneic stem cell transplant (Ravandi *et al.* 2010; Fielding and Zakout 2013). A large-scale RNAi screen was carried out in a model if this disease in order to identify additional factors that promote progression of Ph+ B-ALL and could serve as novel drug targets, including factors that contribute to self-renewal or leukemia-initiating processes (Meacham 2012).

This model of Ph+ B-ALL was generated by transducing $Arf^{-/-}$ murine bone marrow cells with a *BCR-Abl* human transgene and culturing these cells under conditions selective for pre-B cell growth (Williams *et al.* 2007). Upon transplant of as few as 20 cells into immunocompetent, syngeneic recipient mice, an aggressive pre-B ALL develops within three weeks, allowing the study of this disease in the context of a normal microenvironment and fully functional immune system. This property confers a distinct advantage over cell culture and xenograft systems that lack the full complement of

environmental signals and cellular interactions. In addition, the capacity of a significant percentage of cells to seed disease in this model renders it amenable to screening with highly complex RNAi libraries in that a large proportion of the transplanted cells will be represented in the population upon disease presentation.

Our group previously screened such a complex RNAi library (approximately 20,000 unique constructs) in these BCR-Abl+ *Arf*$^{-/-}$ cells (Meacham 2012). Populations of shRNA-expressing leukemia cells representing the entire library were injected into syngeneic mice or plated in order to carry out parallel *in vivo* and *in vitro* screens. Parallel screens were performed in order to identify shRNAs that confer different phenotypes in the *in vivo* setting due to environmental cues not present in normal cell culture conditions. Upon morbidity, mice were euthanized and leukemic cells from both environments were collected. shRNA sequences were isolated from these samples and underwent high-throughput sequencing to determine the representation of each shRNA at the endpoint of the screens relative to their representation in a population collected on the day of injection. shRNAs that confer a survival advantage (for example due to depletion of pro-apoptotic genes) would be expected to have an increased representation in the output population relative to the input. On the other hand, shRNAs that are detrimental to the cell through knockdown of genes necessary for survival would be expected to have a decreased representation at the end of the screen. In this screen, candidate hits were defined as shRNAs that decreased in representation ("depleted") in the output population relative to the input as these represent potential drug targets of interest.

Chromatin modifiers are mediators of disease progression in BCR-Abl+ B-ALL

Among the list of candidate hits were shRNAs targeting two chromatin modifiers, SIN3A and CHD8, underscoring the importance of epigenetic regulation in leukemia progression. The mechanism and scope of SIN3A's influence on gene expression has been well established. mSIN3A and mSIN3B, the mammalian homologs of the yeast repressor Sin3, were first identified in a yeast two-hybrid screen to identify interacting partners of MAD, a transcriptional co-repressor (Ayer *et al.* 1995). It was found that mSIN3A forms a ternary complex with MAD, MAX, and DNA, and that the transcriptional repressor function of the MAD-MAX complex required binding to mSIN3A or mSIN3B. Concurrently it was found that mSIN3 also associates with the MXI1-MAX transcriptional repressor complex, suggesting a mechanism for mSIN3-mediated tumor suppression in the repression of MYC-regulated genes involved in proliferation (Koskinen *et al.* 1995; Schreiber-Agus *et al.* 1995). Subsequent work showed that histone deacetylase (HDAC) activity is required for transcriptional repression mediated by SIN3A, and identified SIN3A domains responsible for association with HDACs (Alland *et al.* 1997; Hassig *et al.* 1997; Laherty *et al.* 1997). N-CoR and SMRT were identified as co-repressors that constitute complexes with mSIN3 and HDACs and are necessary for transcriptional repression by MAD-MAX (Heinzel *et al.* 1997; Nagy *et al.* 1997). Members of the nuclear receptor family of transcriptional repressors were also shown to utilize the SIN3A/N-CoR complex to mediate target gene suppression in the absence of their respective ligands (Heinzel *et al.* 1997). A large body of work supports the role of SIN3A in facilitating association of HDACs with multiple transcription factors that utilize this protein to repress

transcription including p53, Rb, PLZF, LAZ3, TAL1, ETO, RUNX1, and Menin (David *et al.* 1998; Dhordain *et al.* 1998; Lutterbach *et al.* 1998; Wang *et al.* 1998; Murphy *et al.* 1999; Huang and Brandt 2000; Lutterbach *et al.* 2000; Lai *et al.* 2001; Kim *et al.* 2003; Zhao *et al.* 2008). Importantly for AML, the RUNX1-ETO oncogene requires SIN3A to facilitate transcriptional repression of target genes (Lutterbach *et al.* 1998; 2000). Dannenberg and colleagues found that approximately 1,300 genes were differentially expressed in MEFs lacking SIN3A, the majority of which were upregulated consistent with the role of SIN3A in transcriptional repression (2005). Pathways disrupted in these MEFs included DNA repair, the G2/M transition, replication, apoptosis, and both mitochondrial and cytosolic energy generation. *Sin3a*$^{-/-}$ mice do not survive beyond E6.5, underscoring the importance of SIN3A in cell survival and early embryonic development.

Despite the wide range of SIN3A interacting partners, it is possible to selectively inhibit certain interactions. Farias et al. transduced breast cancer cells with a vector encoding the SIN3A-interaction domain (SID) found in transcription factors that bind to the PAH2 domain of SIN3A, such as MAD (2010). Expression of this SID "decoy" prevented binding of SIN3A to PAH2-interacting transcription factors and induced cell cycle arrest and differentiation through upregulation of p27 and E-cadherin. Importantly, expression of the SID decoy or administration of cell-permeable SID peptides sensitized triple-negative breast cancer cells to retinoid and estrogen therapeutics, demonstrating that inhibition of a subset of SIN3A interactions is possible (at least *in vitro*) and leads to transcriptional alterations that render cells vulnerable to previously ineffective therapeutics. In addition to MAD, inhibiting the interaction between SIN3A and RUNX1-ETO could be effective in the treatment of leukemias driven by the transcriptionally repressive actions of this fusion gene, either by abrogating its repressor function or by promoting the degradation of RUNX1 (Imai *et al.* 2004; Zhao *et al.* 2008).

While there is abundant evidence for the importance of SIN3A in regulating expression of genes critical to cancer and development, there has been much less investigation into the role of CHD8 (chromodomain-helicase-DNA binding protein 8) in normal and cancerous cells. A number of mechanisms of transcriptional regulation as well as target gene sets have been proposed, but a consensus on the precise function of CHD8 has yet to emerge. CHD8 is one of nine members of the CHD family of chromodomain-containing proteins and a member of the type III subfamily that also includes CHD5, CHD6, CHD7, and CHD9 (Hall and Georgel 2007). CHD8 was originally identified in a yeast two-hybrid screen as a binding partner of β-catenin that inhibits transcriptional activation of β-catenin target genes (Sakamoto *et al.* 2000). Initial studies only isolated a truncated N-terminal isoform of CHD8 named Duplin (axis duplication inhibitor), which was characterized as a 749-amino acid protein that localizes to the nucleus and directly binds to the Armadillo repeats of β-catenin. This interaction competes with binding of the transcription factor Tcf to this same region of β-catenin, preventing activation of Tcf and subsequent target gene transcription. It was found that Duplin inhibits the expression of *siamois*, a gene regulated by β-catenin and Tcf that mediates axis formation upon activation of Wnt signaling. Accordingly, ventral injection of *Duplin* mRNA into *Xenopus* embryos was able to rescue the axis duplication phenotype caused by ventral injection of Wnt or β-catenin. Thus Duplin is able to counter the effects of aberrant Wnt signaling during development. Further work by this group found that inhibition of Wnt signaling is dependent on the nuclear localization of Duplin, strengthening the evidence for a role mediated by binding to transcriptional complexes (Kobayashi *et al.* 2001).

To elucidate the role of Duplin in mammalian development, Nishiyama et al. created *Duplin*$^{-/-}$ mice using a construct removing all exons (2004). Embryos

homozygous for this construct arrested growth by E8.5, and no embryos were recoverable by E9.5. *Duplin*$^{-/-}$ embryos lacked both the primitive streak and the mesoderm layer, and displayed apoptotic cells in the ectoderm layer by E7.5. Duplin was found to be expressed in wild-type mouse embryos and embryonic stem cells, but absent in newborn animals, suggesting that the role of Duplin is limited to embryonic development. Interestingly, several β-catenin target genes were not upregulated in *Duplin*$^{-/-}$ embryos as would be expected, indicating that Duplin is responsible for functions other than repression of Wnt signaling.

In order to identify how the loss of *Duplin* (by now recognized as an isoform of the *Chd8* gene consisting of its first nine exons) triggers apoptosis in developing mouse embryos, this group went on to overexpress CHD8 in NIH3T3 cells (Thompson *et al.* 2008; Nishiyama *et al.* 2009). It was observed that exogenous CHD8 expression inhibited p53-mediated apoptosis upon treatment of cells with etoposide or UV radiation. However, exogenous CHD8 did not rescue cells from p53-independent apoptosis induced by staurosporine or cycloheximide. In addition, knockdown of CHD8 by RNAi in U2OS osteosarcoma cells induced apoptosis that was rescued by pan-caspase inhibition by Z-VAD-fmk and by simultaneous RNAi-mediated depletion of p53. CHD8 knockdown led to apoptosis in *p53*$^{+/+}$ MEFs, but had no effect in *p53*$^{-/-}$ MEFs, further supporting the hypothesis that CHD8 acts through the p53 pathway.

Through analysis of a series of deletion mutants, it was discovered that the N-terminus of CHD8 directly interacts with the central core domain of p53. This interaction was necessary in order for CHD8 to repress transcription of p53 target genes such as *p21* and *Noxa*. The mechanism of transcriptional suppression was found to be recruitment of histone H1 to target gene promoters by binding to CHD8, as interaction of both of these proteins with p53 was required for repressing transcription. Finally, it was

shown that knocking out p53 rescued the mesoderm formation defect in *Chd8*$^{-/-}$ embryos and extended survival from E8.5 to E10.5, after which *Chd8*$^{-/-}$; *p53*$^{-/-}$ embryos succumbed to severe hemorrhage. As CHD8 levels were observed to be higher in early embryogenesis than in later embryonic stages or in newborn mice, the authors hypothesized that the role of CHD8 is to suppress p53-mediated apoptosis through chromatin compaction at target genes during early embryonic development when rapid cell division may otherwise trigger widespread cell death. It has been shown in multiple organisms that histone H1 plays a role in gene-specific transcriptional regulation as well as global chromatin condensation (Bouvet *et al.* 1994; Shen and Gorovsky 1996; Lee and Archer 1998; Vermaak *et al.* 1998; Fan *et al.* 2005). It is possible that a number of regulatory proteins such as CHD8 facilitate this specificity by recruiting histone H1 to sections of chromatin where transcription should be abrogated at various stages in development.

This group continued on to investigate the mechanism of CHD8 suppression of β-catenin target gene transcription and discovered a similar mechanism involving histone H1 recruitment (Nishiyama *et al.* 2012). It was found that CHD8 interacts with β-catenin and binds to the Wnt response elements (WREs) of target genes *Axin2* and *c-myc* upon stimulation of cells with Wnt3a. Recruitment of CHD8 to these promoters was dependent on the presence of β-catenin. Additionally, exogenous CHD8 expression resulted in decreased *Axin2* and *c-myc* transcription upon LiCl or Wnt3a treatment compared to control treated cells. These results supported previous evidence that CHD8 binds to the 5' ends of β-catenin target genes *Axin2*, *Dkk1*, and *Nkd2* and represses transcription of these genes in a colorectal carcinoma cell line (Thompson *et al.* 2008). Furthermore, CHD8 recruits histone H1 to β-catenin target promoters, and the interaction between CHD8 and histone H1 is required for transcriptional repression (Nishiyama *et al.* 2012).

The authors concluded that CHD8 acts during early embryogenesis to regulate the effects of Wnt signaling, possibly helping to restrict cell proliferation and axis formation. At this point, the role of CHD8 in histone H1 recruitment has only been demonstrated at p53 and β-catenin target promoters, but this mechanism may be important in regulating genes activated by other transcription factors as well.

Other investigations into the role of CHD8 have yielded evidence of functions in cell cycle regulation. Rodriguez-Paredes *et al.* found that RNAi-mediated depletion of CHD8 in human cervical carcinoma cells resulted in a modest G1 arrest (2009). A genome-wide investigation into gene expression changes 48 hours following depletion of CHD8 with a doxycycline-induced shRNA revealed downregulation of two E2F1-regulated genes expressed during the G1/S transition: cyclin E2 (*CCNE2*) and thymidylate synthetase (*TYMS*). Downregulation of these genes could not be attributed to the G1/S arrest itself as other G1/S genes including *PCNA*, *CCNA2*, and *CCNE1* were unaffected by CHD8 depletion. The role of CHD8 in the regulation of *CCNE2* but not *CCNE1* was confirmed by Caldon *et al.* who found that CHD8 was required for estrogen-mediated induction of *CCNE2* transcription (2009). Further experiments demonstrated that CHD8 associates with the promoters and 5' regions of *CCNE2* and *TYMS* as well as the elongating (phosphorylated CTD) form of RNA pol II (Rodriguez-Paredes *et al.* 2009). The authors suggested that CHD8 plays a role in facilitating transcription elongation of certain genes, similar to the proposed role of *kismet* (the Drosophila homolog of the CHD type III family) in initiating transcription elongation on a global scale (Srinivasan *et al.* 2005). The more limited scope of CHD8 targets was attributed to the division of labor between the multiple members of the CHD type III subfamily as opposed to *kismet*, which is the sole homolog of this subfamily in Drosophila (Rodriguez-Paredes *et al.* 2009).

Further work by this group confirmed the involvement of CHD8 in transcription of E2F-regulated genes (Subtil-Rodriguez *et al.* 2014). 67% of CHD8 target promoters identified in a ChIP-chip experiment contained an E2F site. Additionally, in immortalized retinal pigment epithelial (RPE1) cells, CHD8 associated with promoters of E2F-regulated genes, facilitated binding of E2F1, E2F3, and RNA pol II to these promoters, and promoted expression of E2F target genes at the G1/S transition.

A variety of additional functions have been attributed to CHD8. Through a yeast two-hybrid screen, Yamashina *et al.* found that Duplin binds to PIAS3, a STAT3 inhibitor, and overexpression of Duplin suppressed transcription of STAT3-regulated genes that are normally activated upon stimulation with leukemia-inhibitory factor (LIF) (2006). This suppression was found to be due to inhibition of STAT3 binding to DNA. This inhibition did not require the β-catenin-binding domain of Duplin and seemed to operate independently of PIAS3 despite the ability of CHD8, PIAS3, and STAT3 to form a complex. Another yeast two-hybrid screen identified the chromatin insulator CTCF as a CHD8 binding partner (Ishihara *et al.* 2006). This interaction is mediated through the BRK domains of CHD8 and the zinc-finger domain of CTCF. CHD8 binds to CTCF target sites in a CTCF-dependent manner, and CHD8 knockdown results in loss of enhancer insulation at the *H19* differentially methylated region (DMR), a known CTCF target.

CHD8 contains two tandem chromodomains near the N-terminus that are responsible for binding to methylated lysines found on histone H3 tails, specifically H3K4me2 and H3K4me3 (Yuan *et al.* 2007; Rodriguez-Paredes *et al.* 2009). Evidence has also been found supporting interaction of CHD8 with the WAR complex (WDR5, ASH2L, RbBP5) (Thompson *et al.* 2008; Menon *et al.* 2010), a critical subunit of the MLL H3K4 methyltransferase complex (Dou *et al.* 2006; Steward *et al.* 2006). H3K4me2 and

H3K4me3 marks are indicative of transcription start sites and/or transcriptional activity (Santos-Rosa *et al.* 2002; Schneider *et al.* 2003), suggesting that CHD8 binds preferentially to promoters of active or poised chromatin, either to facilitate RNA pol II elongation or to recruit histone H1 to repress transcription. Associations between CHD8 and unmodified H3K4, H3K4me1, H3K9me2, and H3K36me2 have also been examined but found to be less efficient (Yuan *et al.* 2007). H3K36me2 marks are enriched in gene bodies (Wozniak and Strahl 2014) while H3K9me2 is a transcriptionally repressive modification (Lim *et al.* 2010), therefore weak binding of these modified histones to CHD8 suggests that the activity of CHD8 is restricted to transcriptional start sites of actively transcribed genes. A role for CHD8 in RNA pol III transcription has also been demonstrated (Yuan *et al.* 2007). CHD8 associates with Staf, a transcription factor that activates Pol III transcription of the U6 snRNA, and knockdown of CHD8 by siRNA attenuated transcription of a reporter construct controlled by the U6 promoter.

While multiple groups have seen higher expression of CHD8 in cancer cells than normal adult tissue, perhaps reflecting the less differentiated nature of cancer cells (Nishiyama *et al.* 2009; Menon *et al.* 2010), other groups have observed loss of CHD8 expression in gastric and colorectal cancers (Kim *et al.* 2011; Sawada *et al.* 2013; Tahara *et al.* 2014). These cancers generally displayed high microsatellite instability (MSI-H) or CpG island methylator phenotype 1 (CIMP1). Consistent with previous findings demonstrating CHD8's role as a regulator of Wnt signaling and cell cycle gene expression, GSEA of gastric cancer tissues with low CHD8 expression revealed the Wnt/β-catenin signaling and cell cycle pathways to be the most highly enriched signatures (Tahara *et al.* 2014). Interestingly, the p53/apoptotic pathway signature was not significantly enriched in these samples as might be expected given prior evidence of CHD8's function as an inhibitor of p53-mediated apoptosis (Nishiyama *et al.* 2009). In

addition, when patient samples were stratified by CHD8 expression levels, low CHD8 expression correlated with increased depth of tumor invasion, higher incidence of lymph node metastasis, and decreased overall survival (Sawada *et al.* 2013). It is possible that the loss of CHD8 in these tumors could be attributed to random epigenetic silencing resulting from their CIMP1 and MSI-H status. In a study performed by Mulero-Navarro and Esteller, a CpG island was found at the *CHD8* transcription start site, but hypermethylation was not seen at this locus in a panel of cancer cell lines (2008). In addition, loss of CHD8 expression was seen in a number of MSI-H gastric and colorectal carcinoma samples that had not undergone mutation or loss of the *CHD8* locus (Kim *et al.* 2011). These results suggest that this promoter could be susceptible to hypermethylation in cells with a CIMP-1 phenotype, but is not normally selected for. However, knockdown of CHD8 in gastric cancer cell lines by RNAi resulted in increased proliferation, suggesting that there could in fact be selective pressure for CHD8 loss of function in these tumor types (Sawada *et al.* 2013).

It is evident that there is still much to learn about the function of CHD8 in both normal and cancerous cells. The current state of knowledge suggests the existence of two major mechanisms of activity: 1) CHD8 is recruited by transcription factors such as p53 and β-catenin to target gene promoters, and in turn recruits histone H1 to repress transcription at critical stages of development; and 2) CHD8 is recruited via its chromodomains or intermediary protein complexes to di- and tri-methylated H3K4 to repress or induce transcription. These models are not mutually exclusive. However it is intriguing that CHD8 appears to act in a pro-proliferative or pro-survival manner in most contexts but a tumor suppressor in certain gastric and colorectal carcinomas, perhaps due to its inhibitory effect on Wnt signaling. It is possible that the most active signaling pathways within the cell direct the function of CHD8 and thus the cellular reaction upon

CHD8 depletion, triggering either p53-mediated apoptosis, E2F-mediated cell cycle arrest, or increased tumor invasiveness. If CHD8 is indeed inappropriately re-expressed in cancer cells, it may prove to be a candidate for inhibition that would largely spare normal cells. Further investigation is needed however to determine the context in which CHD8 inhibition would be advantageous to the tumor and thus deleterious to the patient. For this reason we pursued investigation of the function of CHD8 as well as SIN3A in BCR-Abl+ B-ALL cells. CHD8 has never been studied in the context of a hematopoietic malignancy, and we hypothesized that CHD8 may have a role in leukemic cell differentiation analogous to its demonstrated roles in embryonic development.

We characterized *Chd8* and *Sin3a* as pro-survival genes in this mouse model of BCR-Abl+ B-ALL, confirming the results found in the RNAi screen. RNAi-mediated depletion of CHD8 resulted in cell death, but we could not confirm activation of the canonical apoptotic pathway. We were also unable to confirm aberrant expression of β-catenin target genes or cell cycle arrest upon CHD8 depletion as had been previously shown. We discovered that T-ALL cells expressing the intracellular domain of Notch (ICN) are less dependent on CHD8 expression, and ectopic expression of ICN in *K-ras*$^{LA2/+}$/*p53*$^{LSL/LSL}$ T-cell lymphoma cells partially rescues the dependency of these cells on CHD8 expression. A genome-wide interrogation of transcriptional changes in BCR-Abl+ B-ALL and T-ALL cells upon CHD8 depletion suggested that deregulation of the NF-κB pathway may be responsibe for these disparate phenotypes, and subsequent experiments provided additional evidence. We conclude that CHD8 most likely co-regulates a number of genes that converge to promote cell survival in certain signaling contexts, and that constitutive Notch signaling is able to compensate for CHD8 loss through mechanisms that are not yet fully understood.

References

Ablain J, Leiva M, Peres L, Fonsart J, Anthony E, and de Thé H. (2013). Uncoupling RARA transcriptional activation and degradation clarifies the bases for APL response to therapies. *Journal of Experimental Medicine* **210**: 647–653.

Alland L, Muhle R, Hou H, Potes J, Chin L, Schreiber-Agus N, *et al.* (1997). Role for N-CoR and histone deacetylase in Sin3-mediated transcriptional repression. *Nature* **387**: 49–55.

Arai S, Yoshimi A, Shimabe M, Ichikawa M, Nakagawa M, Imai Y, *et al.* (2011). Evi-1 is a transcriptional target of mixed-lineage leukemia oncoproteins in hematopoietic stem cells. *Blood* **117**: 6304–6314.

Ayer DE, Lawrence QA, and Eisenman RN. (1995). Mad-Max transcriptional repression is mediated by ternary complex formation with mammalian homologs of yeast repressor Sin3. *Cell* **80**: 767–776.

Bard-Chapeau EA, Gunaratne J, Kumar P, Chua BQ, Muller J, Bard FA, *et al.* (2013). EVI1 oncoprotein interacts with a large and complex network of proteins and integrates signals through protein phosphorylation. *Proc. Natl. Acad. Sci. U.S.A.* **110**: E2885–94.

Barjesteh van Waalwijk van Doorn-Khosrovani S, Erpelinck C, van Putten WLJ, Valk PJM, van der Poel-van de Luytgaarde S, Hack R, *et al.* (2003). High EVI1 expression predicts poor survival in acute myeloid leukemia: a study of 319 de novo AML patients. *Blood* **101**: 837–845.

Bernt KM, Zhu N, Sinha AU, Vempati S, Faber J, Krivtsov AV, *et al.* (2011). MLL-rearranged leukemia is dependent on aberrant H3K79 methylation by DOT1L. *Cancer Cell* **20**: 66–78.

Biondi A, Cimino G, Pieters R, and Pui C-H. (2000). Biological and therapeutic aspects of infant leukemia. *Blood* **96**: 24–33.

Borrow J, Goddard AD, Sheer D, and Solomon E. (1990). Molecular analysis of acute promyelocytic leukemia breakpoint cluster region on chromosome 17. *Science* **249**: 1577–1580.

Boulos N, Mulder HL, Calabrese CR, Morrison JB, Rehg JE, Relling MV, *et al.* (2011). Chemotherapeutic agents circumvent emergence of dasatinib-resistant BCR-ABL kinase mutations in a precise mouse model of Philadelphia chromosome-positive acute lymphoblastic leukemia. *Blood* **117**: 3585–3595.

Bouvet P, Dimitrov S, and Wolffe AP. (1994). Specific regulation of Xenopus chromosomal 5S rRNA gene transcription in vivo by histone H1. *Genes Dev* **8**: 1147–1159.

Bracken AP, Pasini D, Capra M, Prosperini E, Colli E, and Helin K. (2003). EZH2 is downstream of the pRB-E2F pathway, essential for proliferation and amplified in cancer. *EMBO J* **22**: 5323–5335.

Bradstock KF, and Gottlieb DJ. (1995). Interaction of acute leukemia cells with the bone marrow microenvironment: implications for control of minimal residual disease. *Leuk. Lymphoma* **18**: 1–16.

Caldon CE, Sergio CM, Schutte J, Boersma MN, Sutherland RL, Carroll JS, *et al.* (2009). Estrogen Regulation of Cyclin E2 Requires Cyclin D1 but Not c-Myc. *Molecular and cellular biology* **29**: 4623–4639.

Cao R, Wang L, Wang H, Xia L, Erdjument-Bromage H, Tempst P, *et al.* (2002). Role of histone H3 lysine 27 methylation in Polycomb-group silencing. *Science* **298**: 1039–1043.

Castor A, Nilsson L, Astrand-Grundström I, Buitenhuis M, Ramirez C, Anderson K, *et al.* (2005). Distinct patterns of hematopoietic stem cell involvement in acute lymphoblastic leukemia. *Nat Med* **11**: 630–637.

Challen GA, Sun D, Jeong M, Luo M, Jelinek J, Berg JS, *et al.* (2012). Dnmt3a is essential for hematopoietic stem cell differentiation. *Nat Genet* **44**: 23–31.

Chan SM, and Majeti R. (2013). Role of DNMT3A, TET2, and IDH1/2 mutations in pre-leukemic stem cells in acute myeloid leukemia. *Int J Hematol* **98**: 648–657.

Chen W, Kumar AR, Hudson WA, Li Q, Wu B, Staggs RA, *et al.* (2008). Malignant transformation initiated by Mll-AF9: gene dosage and critical target cells. *Cancer Cell* **13**: 432–440.

Chi P, Allis CD, and Wang GG. (2010). Covalent histone modifications — miswritten, misinterpreted and mis-erased in human cancers. *Nat Reviews Cancer* **10**: 457-469.

Chomienne C, Ballerini P, Balitrand N, Huang ME, Krawice I, Castaigne S, *et al.* (1990). The retinoic acid receptor alpha gene is rearranged in retinoic acid-sensitive promyelocytic leukemias. *Oncogene* **4**: 802-807.

Clark SS, McLaughlin J, Crist WM, Champlin R, and Witte ON. (1987). Unique forms of the abl tyrosine kinase distinguish Ph1-positive CML from Ph1-positive ALL. *Science* **235**: 85–88.

Corsello SM, Roti G, Ross KN, Chow KT, Galinsky I, DeAngelo DJ, *et al.* (2009). Identification of AML1-ETO modulators by chemical genomics. *Blood* **113**: 6193–6205.

Cozzio A, Passegué E, Ayton PM, Karsunky H, Cleary ML, and Weissman IL. (2003). Similar MLL-associated leukemias arising from self-renewing stem cells and short-lived myeloid progenitors. *Genes Dev* **17**: 3029–3035.

Crews LA, and Jamieson CHM. (2013). Selective elimination of leukemia stem cells: hitting a moving target. *Cancer Lett.* **338**: 15–22.

Daigle SR, Olhava EJ, Therkelsen CA, Majer CR, Sneeringer CJ, Song J, *et al.* (2011). Selective killing of mixed lineage leukemia cells by a potent small-molecule DOT1L inhibitor. *Cancer Cell* **20**: 53–65.

Dalla-Favera R, Bregni M, Erikson J, Patterson D, Gallo RC, and Croce CM. (1982). Human c-myc onc gene is located on the region of chromosome 8 that is translocated in Burkitt lymphoma cells. *Proc. Natl. Acad. Sci. U.S.A.* **79**: 7824–7827.

Dannenberg J-H, David G, Zhong S, van der Torre J, Wong WH, and Depinho RA. (2005). mSin3A corepressor regulates diverse transcriptional networks governing normal and neoplastic growth and survival. *Genes Dev* **19**: 1581–1595.

David G, Alland L, Hong SH, Wong CW, DePinho RA, and Dejean A. (1998). Histone deacetylase associated with mSin3A mediates repression by the acute promyelocytic leukemia-associated PLZF protein. *Oncogene* **16**: 2549–2556.

Dhordain P, Lin RJ, Quief S, Lantoine D, Kerckaert JP, Evans RM, *et al.* (1998). The LAZ3(BCL-6) oncoprotein recruits a SMRT/mSIN3A/histone deacetylase containing complex to mediate transcriptional repression. *Nucleic Acids Res.* **26**: 4645–4651.

Dou Y, Milne TA, Ruthenburg AJ, Lee S, Lee JW, Verdine GL, *et al.* (2006). Regulation of MLL1 H3K4 methyltransferase activity by its core components. *Nat. Struct. Mol. Biol.* **13**: 713–719.

Ezhkova E, Pasolli HA, Parker JS, Stokes N, Su I-H, Hannon G, *et al.* (2009). Ezh2 orchestrates gene expression for the stepwise differentiation of tissue-specific stem cells. *Cell* **136**: 1122–1135.2

Fan Y, Nikitina T, Zhao J, Fleury TJ, Bhattacharyya R, Bouhassira EE, *et al.* (2005). Histone H1 Depletion in Mammals Alters Global Chromatin Structure but Causes Specific Changes in Gene Regulation. *Cell* **123**: 1199–1212.

Farias EF, Petrie K, Leibovitch B, Murtagh J, Chornet MB, Schenk T, *et al.* (2010). Interference with Sin3 function induces epigenetic reprogramming and differentiation in breast cancer cells. *Proc. Natl. Acad. Sci. U.S.A.* **107**: 11811–11816.

Fathi AT, and Abdel-Wahab O. (2012). Mutations in epigenetic modifiers in myeloid malignancies and the prospect of novel epigenetic-targeted therapy. *Adv Hematol* **2012**: 469592.

Fielding AK, and Zakout GA. (2013). Treatment of Philadelphia chromosome-positive acute lymphoblastic leukemia. *Curr Hematol Malig Rep* **8**: 98–108.

Francis NJ, Kingston RE, and Woodcock CL. (2004). Chromatin compaction by a polycomb group protein complex. *Science* **306**: 1574–1577.

Goyama S, and Kurokawa M. (2010). Evi-1 as a critical regulator of leukemic cells. *Int J Hematol* **91**: 753–757.

Grembecka J, He S, Shi A, Purohit T, Muntean AG, Sorenson RJ, *et al.* (2012). Menin-MLL inhibitors reverse oncogenic activity of MLL fusion proteins in leukemia. *Nat. Chem. Biol.* **8**: 277–284.

Groffen J, Stephenson JR, Heisterkamp N, de Klein A, Bartram CR, and Grosveld G. (1984). Philadelphia chromosomal breakpoints are clustered within a limited region, bcr, on chromosome 22. *Cell* **36**: 93–99.

Hall JA, and Georgel PT. (2007). CHD proteins: a diverse family with strong ties. *Biochem. Cell Biol.* **85**: 463–476.

Hassig CA, Fleischer TC, Billin AN, Schreiber SL, and Ayer DE. (1997). Histone deacetylase activity is required for full transcriptional repression by mSin3A. *Cell* **89**: 341–347.

Hatlen MA, Wang L, and Nimer SD. (2012). AML1-ETO driven acute leukemia: insights into pathogenesis and potential therapeutic approaches. *Front Med* **6**: 248–262.

Heerema NA, Harbott J, Galimberti S, Camitta BM, Gaynon PS, Janka-Schaub G, *et al.* (2004). Secondary cytogenetic aberrations in childhood Philadelphia chromosome positive acute lymphoblastic leukemia are nonrandom and may be associated with outcome. *Leukemia* **18**: 693–702.

Heinzel T, Lavinsky RM, Mullen TM, Söderstrom M, Laherty CD, Torchia J, *et al.* (1997). A complex containing N-CoR, mSin3 and histone deacetylase mediates transcriptional repression. *Nature* **387**: 43–48.

Hess JL. (2004). MLL: a histone methyltransferase disrupted in leukemia. *Trends Mol Med* **10**: 500–507.

Hu Y, Swerdlow S, Duffy TM, Weinmann R, Lee FY, and Li S. (2006). Targeting multiple kinase pathways in leukemic progenitors and stem cells is essential for improved treatment of Ph+ leukemia in mice. *Proc. Natl. Acad. Sci. U.S.A.* **103**: 16870–16875.

Huang G, Shigesada K, Ito K, Wee HJ, Yokomizo T, and Ito Y. (2001). Dimerization with PEBP2beta protects RUNX1/AML1 from ubiquitin-proteasome-mediated degradation. *EMBO J* **20**: 723–733.

Huang S, and Brandt SJ. (2000). mSin3A regulates murine erythroleukemia cell differentiation through association with the TAL1 (or SCL) transcription factor. *Molecular and cellular biology* **20**: 2248–2259.

Ichikawa M, Asai T, Saito T, Seo S, Yamazaki I, Yamagata T, *et al.* (2004). AML-1 is required for megakaryocytic maturation and lymphocytic differentiation, but not for maintenance of hematopoietic stem cells in adult hematopoiesis. *Nat Med* **10**: 299–304.

Ichikawa M, Goyama S, Asai T, Kawazu M, Nakagawa M, Takeshita M, *et al.* (2008). AML1/Runx1 negatively regulates quiescent hematopoietic stem cells in adult hematopoiesis. *J Immunol* **180**: 4402–4408.

Imai Y, Kurokawa M, Yamaguchi Y, Izutsu K, Nitta E, Mitani K, *et al.* (2004). The corepressor mSin3A regulates phosphorylation-induced activation, intranuclear location, and stability of AML1. *Molecular and cellular biology* **24**: 1033–1043.

Ishihara K, Oshimura M, and Nakao M. (2006). CTCF-Dependent Chromatin Insulator Is Linked to Epigenetic Remodeling. *Mol. Cell* **23**: 733–742.

Jan M, and Majeti R. (2013). Clonal evolution of acute leukemia genomes. *Oncogene* **32**: 135–140.

Jeanne M, Lallemand-Breitenbach V, Ferhi O, Koken M, Le Bras M, Duffort S, *et al.* (2010). PML/RARA oxidation and arsenic binding initiate the antileukemia response of As2O3. *Cancer Cell* **18**: 88–98.

Jones PA, and Baylin SB. (2007). The epigenomics of cancer. *Cell* **128**: 683–692.

Jost E, Lin Q, Weidner CI, Wilop S, Hoffmann M, Walenda T, *et al.* (2013). Epimutations mimic genomic mutations of DNMT3A in acute myeloid leukemia. *Leukemia*.

Kakizuka A, Miller WH, Umesono K, Warrell RP, Frankel SR, Murty VV, *et al.* (1991). Chromosomal translocation t(15;17) in human acute promyelocytic leukemia fuses RAR alpha with a novel putative transcription factor, PML. *Cell* **66**: 663–674.

Kamminga LM, Bystrykh LV, de Boer A, Houwer S, Douma J, Weersing E, *et al.* (2006). The Polycomb group gene Ezh2 prevents hematopoietic stem cell exhaustion. *Blood* **107**: 2170–2179.

Kelly PN, Dakic A, Adams JM, Nutt SL, and Strasser A. (2007). Tumor Growth Need Not Be Driven by Rare Cancer Stem Cells. *Science* **317**: 337–337.

van Kemenade FJ. (2001). Coexpression of BMI-1 and EZH2 polycomb-group proteins is associated with cycling cells and degree of malignancy in B-cell non-Hodgkin lymphoma. *Blood* **97**: 3896–3901.

Khan SN, Jankowska AM, Mahfouz R, Dunbar AJ, Sugimoto Y, Hosono N, *et al.* (2013). Multiple mechanisms deregulate EZH2 and histone H3 lysine 27 epigenetic changes in myeloid malignancies. *Leukemia* **27**: 1301–1309.

Kim H, Lee JE, Cho E-J, Liu JO, and Youn H-D. (2003). Menin, a tumor suppressor, represses JunD-mediated transcriptional activity by association with an mSin3A-histone deacetylase complex. *Cancer Res.* **63**: 6135–6139.

Kim MS, Chung NG, Kang MR, Yoo NJ, and Lee SH. (2011). Genetic and expressional alterations of CHD genes in gastric and colorectal cancers. *Histopathology* **58**: 660–668.

Knutson SK, Wigle TJ, Warholic NM, Sneeringer CJ, Allain CJ, Klaus CR, *et al.* (2012). A selective inhibitor of EZH2 blocks H3K27 methylation and kills mutant lymphoma cells. *Nat. Chem. Biol.* **8**: 890–896.

Kobayashi M. (2001). Nuclear Localization of Duplin, a beta -Catenin-binding Protein, Is Essential for Its Inhibitory Activity on the Wnt Signaling Pathway. *Journal of Biological Chemistry* **277**: 5816–5822.

Koh CP, Wang CQ, Ng CEL, Ito Y, Araki M, Tergaonkar V, *et al.* (2013). RUNX1 meets MLL: epigenetic regulation of hematopoiesis by two leukemia genes. *Leukemia* **27**: 1793–1802.

Koskinen PJ, Ayer DE, and Eisenman RN. (1995). Repression of Myc-Ras cotransformation by Mad is mediated by multiple protein-protein interactions. *Cell Growth Differ.* **6**: 623–629.

Krause DS, Fulzele K, Catic A, Sun CC, Dombkowski D, Hurley MP, *et al.* (2013). Differential regulation of myeloid leukemias by the bone marrow microenvironment. *Nat Med* **19**: 1513–1517.

Krivtsov AV, and Armstrong SA. (2007). MLL translocations, histone modifications and leukaemia stem-cell development. *Nat Rev Cancer* **7**: 823–833.

Krivtsov AV, Figueroa ME, Sinha AU, Stubbs MC, Feng Z, Valk PJM, *et al.* (2013). Cell of origin determines clinically relevant subtypes of MLL-rearranged AML. *Leukemia* **27**: 852–860.

Krivtsov AV, Twomey D, Feng Z, Stubbs MC, Wang Y, Faber J, *et al.* (2006). Transformation from committed progenitor to leukaemia stem cell initiated by MLL-AF9. *Nature* **442**: 818–822.

Kumano K, and Kurokawa M. (2010). The role of Runx1/AML1 and Evi-1 in the regulation of hematopoietic stem cells. *J. Cell. Physiol.* **222**: 282–285.

Kurzrock R, Kantarjian HM, Druker BJ, and Talpaz M. (2003). Philadelphia chromosome-positive leukemias: from basic mechanisms to molecular therapeutics. *Ann. Intern. Med.* **138**: 819–830.

Laherty CD, Yang WM, Sun JM, Davie JR, Seto E, and Eisenman RN. (1997). Histone deacetylases associated with the mSin3 corepressor mediate mad transcriptional repression. *Cell* **89**: 349–356.

Lai A, Kennedy BK, Barbie DA, Bertos NR, Yang XJ, Theberge MC, *et al.* (2001). RBP1 recruits the mSIN3-histone deacetylase complex to the pocket of retinoblastoma tumor suppressor family proteins found in limited discrete regions of the nucleus at growth arrest. *Molecular and cellular biology* **21**: 2918–2932.

Lallemand-Breitenbach V, Jeanne M, Benhenda S, Nasr R, Lei M, Peres L, *et al.* (2008). Arsenic degrades PML or PML-RARalpha through a SUMO-triggered RNF4/ubiquitin-mediated pathway. *Nat Cell Biol* **10**: 547–555.

Lawrence MS, Stojanov P, Mermel CH, Robinson JT, Garraway LA, Golub TR, *et al.* (2014). Discovery and saturation analysis of cancer genes across 21 tumour types. *Nature* **505**: 495–501.

Lee HL, and Archer TK. (1998). Prolonged glucocorticoid exposure dephosphorylates histone H1 and inactivates the MMTV promoter. *EMBO J* **17**: 1454–1466.

Ley TJ, Ding L, Walter MJ, McLellan MD, Lamprecht T, Larson DE, *et al.* (2010). DNMT3A mutations in acute myeloid leukemia. *N Engl J Med* **363**: 2424–2433.

Lim S, Metzger E, Schüle R, Kirfel J, and Buettner R. (2010). Epigenetic regulation of cancer growth by histone demethylases. *Int. J. Cancer* **127**: 1991–1998.

Liu-Dumlao T, Kantarjian H, Thomas DA, O'Brien S, and Ravandi F. (2012). Philadelphia-positive acute lymphoblastic leukemia: current treatment options. *Curr Oncol Rep* **14**: 387–394.

Lund K, Adams PD, and Copland M. (2013). EZH2 in normal and malignant hematopoiesis. *Leukemia* **28**: 44–49.

Lutterbach B, Westendorf JJ, Linggi B, Isaac S, Seto E, and Hiebert SW. (2000). A mechanism of repression by acute myeloid leukemia-1, the target of multiple chromosomal translocations in acute leukemia. *J Biol Chem* **275**: 651–656.

Lutterbach B, Westendorf JJ, Linggi B, Patten A, Moniwa M, Davie JR, *et al.* (1998). ETO, a target of t(8;21) in acute leukemia, interacts with the N-CoR and mSin3 corepressors. *Molecular and cellular biology* **18**: 7176–7184.

Maicas M, Vázquez I, Vicente C, García-Sánchez MA, Marcotegui N, Urquiza L, *et al.* (2013). Functional characterization of the promoter region of the human EVI1 gene in acute myeloid leukemia: RUNX1 and ELK1 directly regulate its transcription. *Oncogene* **32**: 2069–2078.

McCabe MT, Ott HM, Ganji G, Korenchuk S, Thompson C, Van Aller GS, *et al.* (2012). EZH2 inhibition as a therapeutic strategy for lymphoma with EZH2-activating mutations. *Nature* **492**: 108–112.

Meacham C. (2012). In vivo pool based shRNA screens to identify modulators of disease progression in hematopoietic malignancies. MIT thesis.

Menon T, Yates JA, and Bochar DA. (2010). Regulation of Androgen-Responsive Transcription by the Chromatin Remodeling Factor CHD8. *Mol. Endocrinol.* **24**: 1165–1174.

Meyer C, Schneider B, Jakob S, Strehl S, Attarbaschi A, Schnittger S, *et al.* (2006). The MLL recombinome of acute leukemias. *Leukemia* **20**: 777–784.

Min IM, Waterfall JJ, Core LJ, Munroe RJ, Schimenti J, and Lis JT. (2011). Regulating RNA polymerase pausing and transcription elongation in embryonic stem cells. *Genes Dev* **25**: 742–754.

Minucci S, and Pelicci PG. (2006). Histone deacetylase inhibitors and the promise of epigenetic (and more) treatments for cancer. *Nat Rev Cancer* **6**: 38–51.

Miranda TB, Cortez CC, Yoo CB, Liang G, Abe M, Kelly TK, *et al.* (2009). DZNep is a global histone methylation inhibitor that reactivates developmental genes not silenced by DNA methylation. *Molecular Cancer Therapeutics* **8**: 1579–1588.

Mitani K, Ogawa S, Tanaka T, Miyoshi H, Kurokawa M, Mano H, *et al.* (1994). Generation of the AML1-EVI-1 fusion gene in the t(3;21)(q26;q22) causes blastic crisis in chronic myelocytic leukemia. *EMBO J* **13**: 504–510.

Morin RD, Johnson NA, Severson TM, Mungall AJ, An J, Goya R, *et al.* (2010). Somatic mutations altering EZH2 (Tyr641) in follicular and diffuse large B-cell lymphomas of germinal-center origin. *Nat Genet* **42**: 181–185.

Morishita K, Parganas E, William CL, Whittaker MH, Drabkin H, Oval J, *et al.* (1992). Activation of EVI1 gene expression in human acute myelogenous leukemias by translocations spanning 300-400 kilobases on chromosome band 3q26. *Proc. Natl. Acad. Sci. U.S.A.* **89**: 3937–3941.

Morishita K, Parker DS, Mucenski ML, Jenkins NA, Copeland NG, and Ihle JN. (1988). Retroviral activation of a novel gene encoding a zinc finger protein in IL-3-dependent myeloid leukemia cell lines. *Cell* **54**: 831–840.

Mucenski ML, Taylor BA, Ihle JN, Hartley JW, Morse HC, Jenkins NA, *et al.* (1988). Identification of a common ecotropic viral integration site, Evi-1, in the DNA of AKXD murine myeloid tumors. *Molecular and cellular biology* **8**: 301–308.

Mulero-Navarro S, and Esteller M. (2008). Chromatin remodeling factor CHD5 is silenced by promoter CpG island hypermethylation in human cancer. *Epigenetics* **3**: 210–215.

Mullighan CG, Miller CB, Radtke I, Phillips LA, Dalton J, Ma J, *et al.* (2008). BCR-ABL1 lymphoblastic leukaemia is characterized by the deletion of Ikaros. *Nature* **453**: 110–114.

Mullighan CG, Phillips LA, Su X, Ma J, Miller CB, Shurtleff SA, *et al.* (2008). Genomic analysis of the clonal origins of relapsed acute lymphoblastic leukemia. *Science* **322**: 1377–1380.

Mullighan CG, Williams RT, Downing JR, and Sherr CJ. (2008). Failure of CDKN2A/B (INK4A/B-ARF)-mediated tumor suppression and resistance to targeted therapy in acute lymphoblastic leukemia induced by BCR-ABL. *Genes Dev* **22**: 1411–1415.

Mummery A, Narendran A, and Lee KY. (2011). Targeting epigenetics through histone deacetylase inhibitors in acute lymphoblastic leukemia. *Curr Cancer Drug Targets* **11**: 882–893.

Murphy M, Ahn J, Walker KK, Hoffman WH, Evans RM, Levine AJ, *et al.* (1999). Transcriptional repression by wild-type p53 utilizes histone deacetylases, mediated by interaction with mSin3a. *Genes Dev* **13**: 2490–2501.

Nagy L, Kao HY, Chakravarti D, Lin RJ, Hassig CA, Ayer DE, *et al.* (1997). Nuclear receptor repression mediated by a complex containing SMRT, mSin3A, and histone deacetylase. *Cell* **89**: 373–380.

Nasr R, Guillemin M-C, Ferhi O, Soilihi H, Peres L, Berthier C, *et al.* (2008). Eradication of acute promyelocytic leukemia-initiating cells through PML-RARA degradation. *Nat Med* **14**: 1333–1342.

Nimer SD, and Moore MAS. (2004). Effects of the leukemia-associated AML1-ETO protein on hematopoietic stem and progenitor cells. *Oncogene* **23**: 4249–4254.

Nishiyama M, Nakayama K, Tsunematsu R, Tsukiyama T, Kikuchi A, and Nakayama KI. (2004). Early embryonic death in mice lacking the beta-catenin-binding protein Duplin. *Molecular and cellular biology* **24**: 8386–8394.

Nishiyama M, Oshikawa K, Tsukada Y-I, Nakagawa T, Iemura S-I, Natsume T, *et al.* (2009). CHD8 suppresses p53-mediated apoptosis through histone H1 recruitment during early embryogenesis. *Nat Cell Biol* **11**: 172–182.

Nishiyama M, Skoultchi AI, and Nakayama KI. (2012). Histone H1 recruitment by CHD8 is essential for suppression of the Wnt-β-catenin signaling pathway. *Molecular and cellular biology* **32**: 501–512.

Okuda T, van Deursen J, Hiebert SW, Grosveld G, and Downing JR. (1996). AML1, the target of multiple chromosomal translocations in human leukemia, is essential for normal fetal liver hematopoiesis. *Cell* **84**: 321–330.

Pluk H, Dorey K, and Superti-Furga G. (2002). Autoinhibition of c-Abl. *Cell* **108**: 247–259.

Popovic R, and Licht JD. (2012). Emerging Epigenetic Targets and Therapies in Cancer Medicine. *Cancer Discov* **2**: 405–413.

Ravandi F, and Estrov Z. (2006). Eradication of leukemia stem cells as a new goal of therapy in leukemia. *Clin. Cancer Res.* **12**: 340–344.

Ravandi F, O'Brien S, Thomas D, Faderl S, Jones D, Garris R, *et al.* (2010). First report of phase 2 study of dasatinib with hyper-CVAD for the frontline treatment of patients with Philadelphia chromosome-positive (Ph+) acute lymphoblastic leukemia. *Blood* **116**: 2070–2077.

Rehe K, Wilson K, Bomken S, Williamson D, Irving J, Boer den ML, *et al.* (2012). Acute B lymphoblastic leukaemia-propagating cells are present at high frequency in diverse lymphoblast populations. *EMBO Mol Med* **5**: 38–51.

Rodríguez-Paredes M, Ceballos-Chávez M, Esteller M, García-Domínguez M, and Reyes JC. (2009). The chromatin remodeling factor CHD8 interacts with elongating RNA polymerase II and controls expression of the cyclin E2 gene. *Nucleic Acids Res.* **37**: 2449–2460.

Rosenberg G. (2007). The mechanisms of action of valproate in neuropsychiatric disorders: can we see the forest for the trees? *Cell. Mol. Life Sci.* **64**: 2090–2103.

Sakamoto I, Kishida S, Fukui A, Kishida M, Yamamoto H, Hino S, *et al.* (2000). A novel beta-catenin-binding protein inhibits beta-catenin-dependent Tcf activation and axis formation. *J Biol Chem* **275**: 32871–32878.

dos Santos GA, Kats L, and Pandolfi PP. (2013). Synergy against PML-RARa: targeting transcription, proteolysis, differentiation, and self-renewal in acute promyelocytic leukemia. *Journal of Experimental Medicine* **210**: 2793–2802.

Santos-Rosa H, Schneider R, Bannister AJ, Sherriff J, Bernstein BE, Emre NCT, *et al.* (2002). Active genes are tri-methylated at K4 of histone H3. *Nature* **419**: 407–411.

Sato T, Goyama S, Kataoka K, Nasu R, Tsuruta-Kishino T, Kagoya Y, *et al.* (2014). Evi1 defines leukemia-initiating capacity and tyrosine kinase inhibitor resistance in chronic myeloid leukemia. *Oncogene* **0**.

Sawada G, Ueo H, Matsumura T, Uchi R, Ishibashi M, Mima K, *et al.* (2013). CHD8 is an independent prognostic indicator that regulates Wnt/β-catenin signaling and the cell cycle in gastric cancer. *Oncol Rep* **30**: 1137–1142.

Schnabel CA, Jacobs Y, and Cleary ML. (2000). HoxA9-mediated immortalization of myeloid progenitors requires functional interactions with TALE cofactors Pbx and Meis. *Oncogene* **19**: 608–616.

Schneider R, Bannister AJ, Myers FA, Thorne AW, Crane-Robinson C, and Kouzarides T. (2003). Histone H3 lysine 4 methylation patterns in higher eukaryotic genes. *Nat Cell Biol* **6**: 73–77.

Schreiber-Agus N, Chin L, Chen K, Torres R, Rao G, Guida P, *et al.* (1995). An amino-terminal domain of Mxi1 mediates anti-Myc oncogenic activity and interacts with a homolog of the yeast transcriptional repressor SIN3. *Cell* **80**: 777–786.

Shackleton M, Quintana E, Fearon ER, and Morrison SJ. (2009). Heterogeneity in cancer: cancer stem cells versus clonal evolution. *Cell* **138**: 822–829.

Shen X, and Gorovsky MA. (1996). Linker histone H1 regulates specific gene expression but not global transcription in vivo. *Cell* **86**: 475–483.

Sloma I, Jiang X, Eaves AC, and Eaves CJ. (2010). Insights into the stem cells of chronic myeloid leukemia. *Leukemia* **24**: 1823–1833.

Sneeringer CJ, Scott MP, Kuntz KW, Knutson SK, Pollock RM, Richon VM, *et al.* (2010). Coordinated activities of wild-type plus mutant EZH2 drive tumor-associated hypertrimethylation of lysine 27 on histone H3 (H3K27) in human B-cell lymphomas. *Proc. Natl. Acad. Sci. U.S.A.* **107**: 20980–20985.

Srinivasan S. (2005). The Drosophila trithorax group protein Kismet facilitates an early step in transcriptional elongation by RNA Polymerase II. *Development* **132**: 1623–1635.

Steward MM, Lee J-S, O'Donovan A, Wyatt M, Bernstein BE, and Shilatifard A. (2006). Molecular regulation of H3K4 trimethylation by ASH2L, a shared subunit of MLL complexes. *Nat. Struct. Mol. Biol.* **13**: 852–854.

Subtil-Rodríguez A, Vázquez-Chávez E, Ceballos-Chávez M, Rodríguez-Paredes M, Martín-Subero JI, Esteller M, *et al.* (2014). The chromatin remodeller CHD8 is required for E2F-dependent transcription activation of S-phase genes. *Nucleic Acids Res.* **42**: 2185–2196.

Tahara T, Yamamoto E, Suzuki H, Maruyama R, Chung W, Garriga J, *et al.* (2014). Fusobacterium in colonic flora and molecular features of colorectal carcinoma. *Cancer Res.* **74**: 1311–1318.

Talpaz M, Shah NP, Kantarjian H, Donato N, Nicoll J, Paquette R, *et al.* (2006). Dasatinib in imatinib-resistant Philadelphia chromosome-positive leukemias. *N Engl J Med* **354**: 2531–2541.

Tan J, Yang X, Zhuang L, Jiang X, Chen W, Lee PL, *et al.* (2007). Pharmacologic disruption of Polycomb-repressive complex 2-mediated gene repression selectively induces apoptosis in cancer cells. *Genes Dev* **21**: 1050–1063.

Tatham MH, Geoffroy M-C, Shen L, Plechanovova A, Hattersley N, Jaffray EG, *et al.* (2008). RNF4 is a poly-SUMO-specific E3 ubiquitin ligase required for arsenic-induced PML degradation. *Nat Cell Biol* **10**: 538–546.

Taub R, Kirsch I, Morton C, Lenoir G, Swan D, Tronick S, *et al.* (1982). Translocation of the c-myc gene into the immunoglobulin heavy chain locus in human Burkitt lymphoma and murine plasmacytoma cells. *Proc. Natl. Acad. Sci. U.S.A.* **79**: 7837–7841.

de Thé H, and Chen Z. (2010). Acute promyelocytic leukaemia: novel insights into the mechanisms of cure. *Nat Rev Cancer* **10**: 775–783.

de Thé H, Lavau C, Marchio A, Chomienne C, Degos L, and Dejean A. (1991). The PML-RAR alpha fusion mRNA generated by the t(15;17) translocation in acute promyelocytic leukemia encodes a functionally altered RAR. *Cell* **66**: 675–684.

de Thé H, Le Bras M, and Lallemand-Breitenbach V. (2012). The cell biology of disease: Acute promyelocytic leukemia, arsenic, and PML bodies. *The Journal of Cell Biology* **198**: 11–21.

Thompson BA, Tremblay V, Lin G, and Bochar DA. (2008). CHD8 is an ATP-dependent chromatin remodeling factor that regulates beta-catenin target genes. *Molecular and cellular biology* **28**: 3894–3904.

Vermaak D, Steinbach OC, Dimitrov S, Rupp RA, and Wolffe AP. (1998). The globular domain of histone H1 is sufficient to direct specific gene repression in early Xenopus embryos. *Curr. Biol.* **8**: 533–536.

Viré E, Brenner C, Deplus R, Blanchon L, Fraga M, Didelot C, *et al.* (2006). The Polycomb group protein EZH2 directly controls DNA methylation. *Nature* **439**: 871–874.

Vogelstein B, Papadopoulos N, Velculescu VE, Zhou S, Diaz LA, and Kinzler KW. (2013). Cancer genome landscapes. *Science* **339**: 1546–1558.

Wang J, Hoshino T, Redner RL, Kajigaya S, and Liu JM. (1998). ETO, fusion partner in t(8;21) acute myeloid leukemia, represses transcription by interaction with the human N-CoR/mSin3/HDAC1 complex. *Proc. Natl. Acad. Sci. U.S.A.* **95**: 10860–10865.

Wang PY, Young F, Chen CY, Stevens BM, Neering SJ, Rossi RM, *et al.* (2008). The biologic properties of leukemias arising from BCR/ABL-mediated transformation vary as a function of developmental origin and activity of the p19ARF gene. *Blood* **112**: 4184–4192.

Wang Q, Stacy T, Binder M, Marin-Padilla M, Sharpe AH, and Speck NA. (1996). Disruption of the Cbfa2 gene causes necrosis and hemorrhaging in the central nervous system and blocks definitive hematopoiesis. *Proc. Natl. Acad. Sci. U.S.A.* **93**: 3444–3449.

Wang Z-Y, and Chen Z. (2008). Acute promyelocytic leukemia: from highly fatal to highly curable. *Blood* **111**: 2505–2515.

Williams RT, Besten den W, and Sherr CJ. (2007). Cytokine-dependent imatinib resistance in mouse BCR-ABL+, Arf-null lymphoblastic leukemia. *Genes Dev* **21**: 2283–2287.

Williams RT, and Sherr CJ. (2008). The INK4-ARF (CDKN2A/B) Locus in Hematopoiesis and BCR-ABL-induced Leukemias. *Cold Spring Harb. Symp. Quant. Biol.* **73**: 461–467.

Wozniak GG, and Strahl BD. (2014). Hitting the 'mark': Interpreting lysine methylation in the context of active transcription. *Biochim. Biophys. Acta*.

Yamashina K, Yamamoto H, Chayama K, Nakajima K, and Kikuchi A. (2006). Suppression of STAT3 Activity by Duplin, Which Is a Negative Regulator of the Wnt Signal. *J. Biochem.* **139**: 305–314.

Yang G, Thompson MA, Brandt SJ, and Hiebert SW. (2007). Histone deacetylase inhibitors induce the degradation of the t(8;21) fusion oncoprotein. *Oncogene* **26**: 91–101.

Young RM, and Staudt LM. (2013). Targeting pathological B cell receptor signalling in lymphoid malignancies. *Nat Rev Drug Discov* **12**: 229–243.

Yuan CC, Zhao X, Florens L, Swanson SK, Washburn MP, and Hernandez N. (2007). CHD8 Associates with Human Staf and Contributes to Efficient U6 RNA Polymerase III Transcription. *Molecular and cellular biology* **27**: 8729–8738.

Yuasa H, Oike Y, Iwama A, Nishikata I, Sugiyama D, Perkins A, *et al.* (2005). Oncogenic transcription factor Evi1 regulates hematopoietic stem cell proliferation through GATA-2 expression. *EMBO J* **24**: 1976–1987.

Zhang X-W, Yan X-J, Zhou Z-R, Yang F-F, Wu Z-Y, Sun H-B, *et al.* (2010). Arsenic trioxide controls the fate of the PML-RARalpha oncoprotein by directly binding PML. *Science* **328**: 240–243.

Zhang Y, Chen A, Yan X-M, and Huang G. (2012). Disordered epigenetic regulation in MLL-related leukemia. *Int J Hematol* **96**: 428–437.

Zhao X, Jankovic V, Gural A, Huang G, Pardanani A, Menendez S, *et al.* (2008). Methylation of RUNX1 by PRMT1 abrogates SIN3A binding and potentiates its transcriptional activity. *Genes Dev* **22**: 640–653.

Zheng P-Z, Wang K-K, Zhang Q-Y, Huang Q-H, Du Y-Z, Zhang Q-H, *et al.* (2005). Systems analysis of transcriptome and proteome in retinoic acid/arsenic trioxide-induced cell differentiation/apoptosis of promyelocytic leukemia. *Proc. Natl. Acad. Sci. U.S.A.* **102**: 7653–7658.

Zuber J, Shi J, Wang E, Rappaport AR, Herrmann H, Sison EA, *et al.* (2011). RNAi screen identifies Brd4 as a therapeutic target in acute myeloid leukaemia. *Nature* **478**: 524–528.

Chapter 2: Results

Author Contributions

Jennifer Shingleton and Michael Hemann designed the experiments. Jennifer Shingleton performed the experiments and wrote the manuscript.

CHD8 and SIN3A depletion are detrimental to growth of BCR-Abl+ B-ALL cells *in vitro* and *in vivo*

To validate that the deleterious effects of these shRNAs are due to knockdown of the intended target genes, additional constructs targeting *Chd8* and *Sin3a* were designed and tested by GFP competition assays (**Fig. 1A**). In these assays, a population of cells is partially transduced with a retroviral vector expressing the shRNA of interest linked to a GFP marker in order to allow identification of shRNA-expressing cells by flow cytometry. As in the screen, if the shRNA confers a growth advantage, the percentage of GFP+ cells will increase over time. Alternatively, if the shRNA is detrimental to the cell either through induction of apoptosis or cell cycle arrest, the percentage of GFP+ cells will decrease. As with the original shRNAs identified by the screen, these new shRNAs also led to significant decreases in CHD8 and SIN3A expression at the protein level (**Fig. 1B**). Consistent with an on-target effect, these additional constructs lead to depletion of transduced BCR-Abl+ B-ALL cells over time, both in the *in vitro* and *in vivo* settings (**Fig. 1C, D**). Depletion of sh*Chd8*- and sh*Sin3a*-expressing cells was observed in all lymphatic tissues examined (spleen, bone marrow, and peripheral blood). These results support the conclusion that the detrimental effects of CHD8 and SIN3A knockdown are cell-autonomous and independent of the tumor microenvironment. Interestingly, while sh*Chd8*-0 appears to confer its deleterious phenotype more rapidly than sh*Chd8*-1 *in vitro*, cells expressing sh*Chd8*-1 deplete to a similar extent when examined over a longer period of time (**Fig. 1E**).

Figure 1:

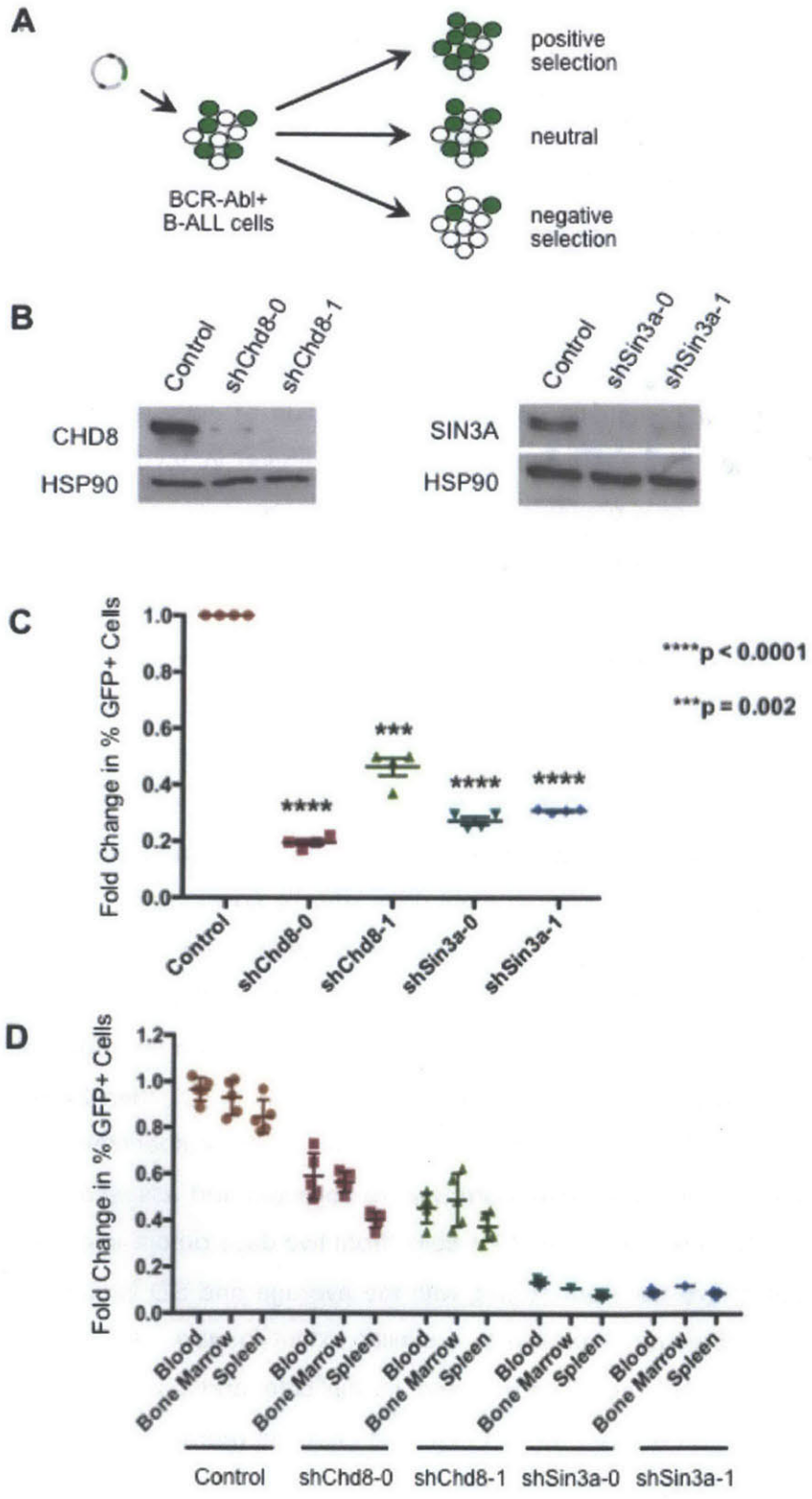
A
positive selection
neutral
negative selection
BCR-Abl+ B-ALL cells
B
Control
shChd8-0
shChd8-1
CHD8
HSP90
Control
shSin3a-0
shSin3a-1
SIN3A
HSP90
C
Fold Change in % GFP+ Cells
****p < 0.0001
***p = 0.002
Control
shChd8-0
shChd8-1
shSin3a-0
shSin3a-1
D
Fold Change in % GFP+ Cells
Blood
Bone Marrow
Spleen
Control
shChd8-0
shChd8-1
shSin3a-0
shSin3a-1

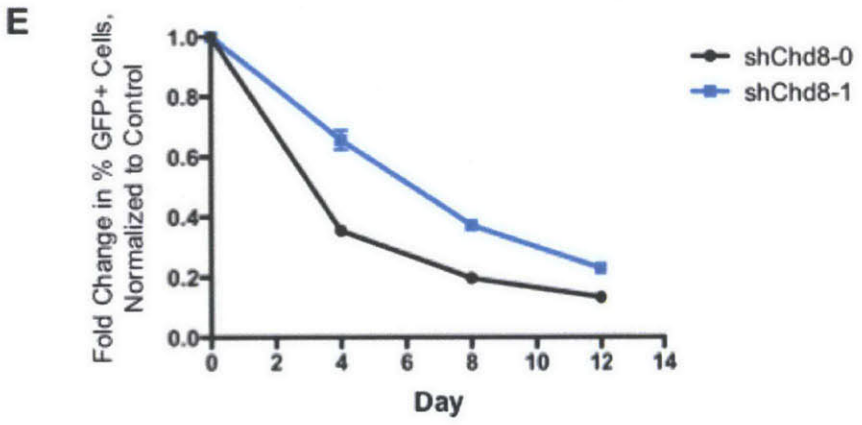

Figure 1: BCR-Abl+ B-ALL cells are dependent on expression of CHD8 and SIN3A. **(A)** Schematic of the GFP growth competition assay. A population of cells is partially transduced with an shRNA linked to a GFP marker. The fold change in %GFP+ cells indicates whether the shRNA confers a growth/survival advantage (positive selection) or disadvantage (negative selection). **(B)** Western blot confirming CHD8 and SIN3A knockdown in BCR-Abl+ B-ALL cells by distinct shRNAs. BCR-Abl+ B-ALL cells were retrovirally transduced with shRNAs targeting *Chd8* or *Sin3a*, or a vector control, then selected with puromycin before collecting for protein analysis. HSP90 was used as a loading control. **(C)** Knockdown of CHD8 and SIN3A in BCR-Abl+ B-ALL cells results in depletion in *in vitro* GFP growth competition assays. BCR-Abl+ B-ALL cells were partially transduced with the indicated constructs containing a GFP marker and plated in triplicate. The percentage of transduced cells was assessed eight days later by flow cytometry, and the fold change in %GFP+ cells was calculated. Shown are average fold changes of each of four experiments normalized to vector controls and the SEM. **(D)** CHD8 and SIN3A knockdown in BCR-Abl+ B-ALL cells result in depletion in an *in vivo* growth competition assay. Cells were partially transduced with the indicated constructs as in (C), then $2x10^6$ cells were injected into mice via the tail vein. Upon morbidity, mice were euthanized and leukemic cells from the blood, spleen, and bone marrow were collected and assessed for %GFP+ cells. Shown are the fold changes in %GFP+ cells (from two days before injection to time of morbidity) for each of five mice per cohort, with the average and SD indicated. **(E)** Both shRNAs targeting *Chd8* cause depletion to a similar extent *in vitro*. As in (C), partially transduced BCR-Abl+ B-ALL cells were plated in triplicate and assessed for %GFP+ cells by flow cytometry. Shown are the average fold changes (normalized to the vector control) and SEM of three replicate experiments.

The model of BCR-Abl+ B-ALL utilized in this study is extremely aggressive, giving rise to terminal disease less than two weeks following tail vein injection of 2 million cells into immunocompetent syngeneic mice. This model is also highly enriched for leukemia-initiating cells (LICs). When Williams and colleagues transplanted 2000 of these cells into syngeneic mice, the recipients survived approximately 17 days (Williams *et al.* 2007). Furthermore, when only 20 cells were injected, all recipients were moribund by 23 days, indicating that a significant percentage of the transplanted cell population has the potential to seed disease in immunocompetent mice. We predicted that depletion of CHD8 or SIN3A in transplanted BCR-Abl+ B-ALL cells would increase time to disease due to attenuation of cell viability and tumor growth. Following retroviral infection of BCR-Abl+ B-ALL cells with a GFP-labeled shRNA targeting *Chd8* or *Sin3a* or a GFP-expressing empty vector control, cells were sorted to obtain pure GFP-expressing populations. Approximately 20 cells were transplanted by tail vein injection into each of 45 C57BL/6 mice (15 mice per cohort), and time to disease was monitored by flow cytometry analysis of blood samples. Time to terminal disease was indeed extended significantly in mice injected with CHD8- or SIN3A-depleted cells (**Fig. 2A**). Disease penetrance was decreased as well, with only 2 mice in both the sh*Chd8* and sh*Sin3a* cohorts succumbing to disease, as compared with 10 mice in the control cohort. When mice reached morbidity, cells from the spleen, bone marrow, and blood were collected and analyzed by flow cytometry for GFP expression. Interestingly, cells collected from mice in the control cohort expressed GFP, but cells harvested from mice injected with CHD8- or SIN3A-depleted cells were GFP-negative (**Fig. 2B**). These results indicate that disease onset in these mice was caused by the outgrowth of a small number of GFP-negative cells contaminating the injected population.

Figure 2:

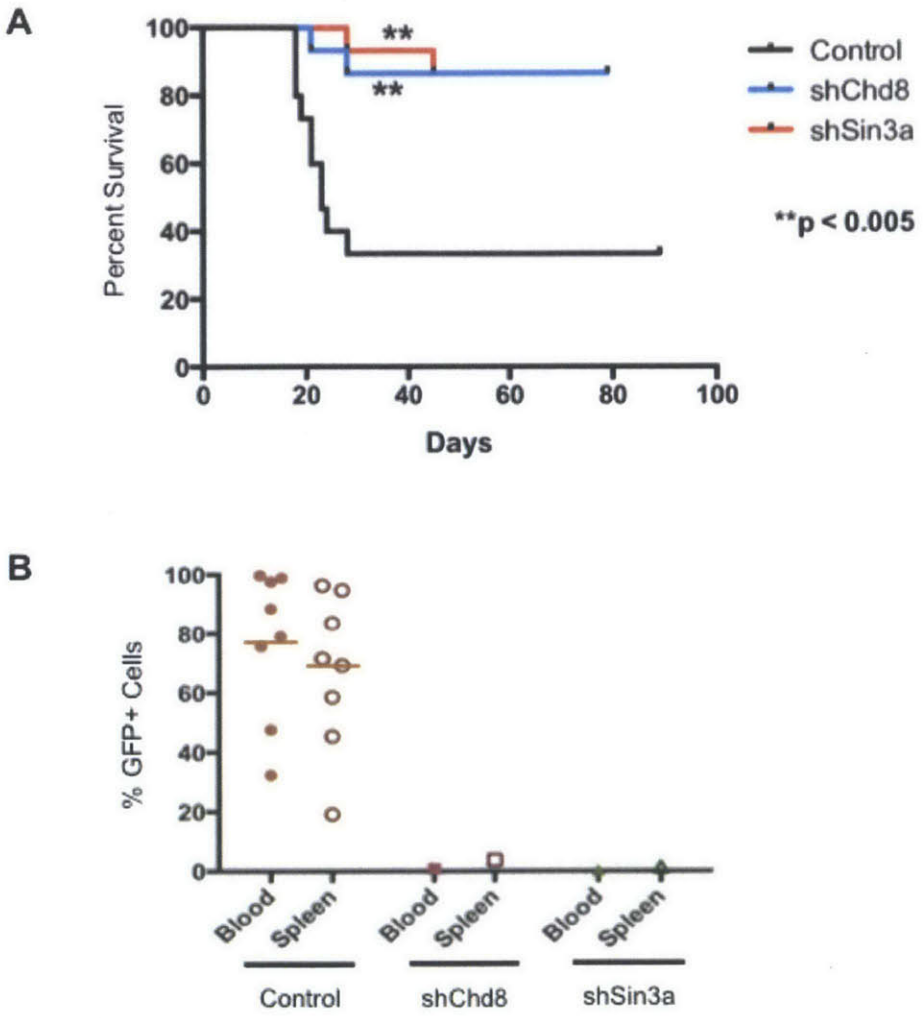

Figure 2: CHD8- and SIN3A- depleted cells are less able to seed disease *in vivo*. Pure populations of BCR-Abl+ B-ALL cells transduced with the indicated constructs were injected into mice via the tail vein (20 cells per mouse, 15 mice per cohort). **(A)** Percent survival over time. **(B)** Upon morbidity, mice were euthanized and leukemic cells were collected from the blood and spleen and analyzed by flow cytometry for GFP expression. Closed symbols = blood samples; open symbols = spleen samples. The means for control blood and spleen samples are indicated.

Untransformed pre-B cells require CHD8 and SIN3A for survival

Previously, it had been observed that CHD8 is overexpressed in murine cancer cell lines compared to corresponding normal tissues (Nishiyama *et al.* 2009), perhaps reflecting the less differentiated nature of most tumors. To determine if this phenomenon could be observed in the B-cell lineage, bone marrow was harvested from healthy adult C57BL/6 mice and stained with fluorescently labeled antibodies in order to identify and collect pre-B cells ($B220^{+}IgM^{-}CD11b^{-}$) by FACS. After sorting, protein lysates were generated from these cells and CHD8 as well as SIN3A protein levels were measured by western blot. Unexpectedly, CHD8 and SIN3A levels in these untransformed pre-B cells were comparable or even higher than those seen in BCR-Abl+ B-ALL cells (**Fig. 3A**). The dependence of these cells on CHD8 and SIN3A expression was also tested by a growth competition assay *in vitro* (**Fig. 3B**). While expression levels of CHD8 and SIN3A in these cells may be similar, biological differences between the cell types might make untransformed pre-B cells less reliant on these proteins for survival. Untransformed pre-B cells were retrovirally infected with both shRNAs targeting *Chd8* or *Sin3a*, as well as a vector control, and the percentage of infected cells (marked by GFP expression) was measured over time by flow cytometry. Because untransformed pre-B cells are more refractory to retroviral infection than BCR-Abl+ B-ALL cells, these cells received two rounds of retroviral infection on subsequent days before beginning the assay. Untransformed pre-B cells expressing sh*Chd8* or sh*Sin3a* depleted *in vitro* to a similar extent as BCR-Abl+ B-ALL cells. This indicates that in the B lymphoid lineage, dependence on expression of these proteins is not limited to malignant cells since untransformed pre-B cells also depend on CHD8 and SIN3A expression for growth and survival.

Figure 3:

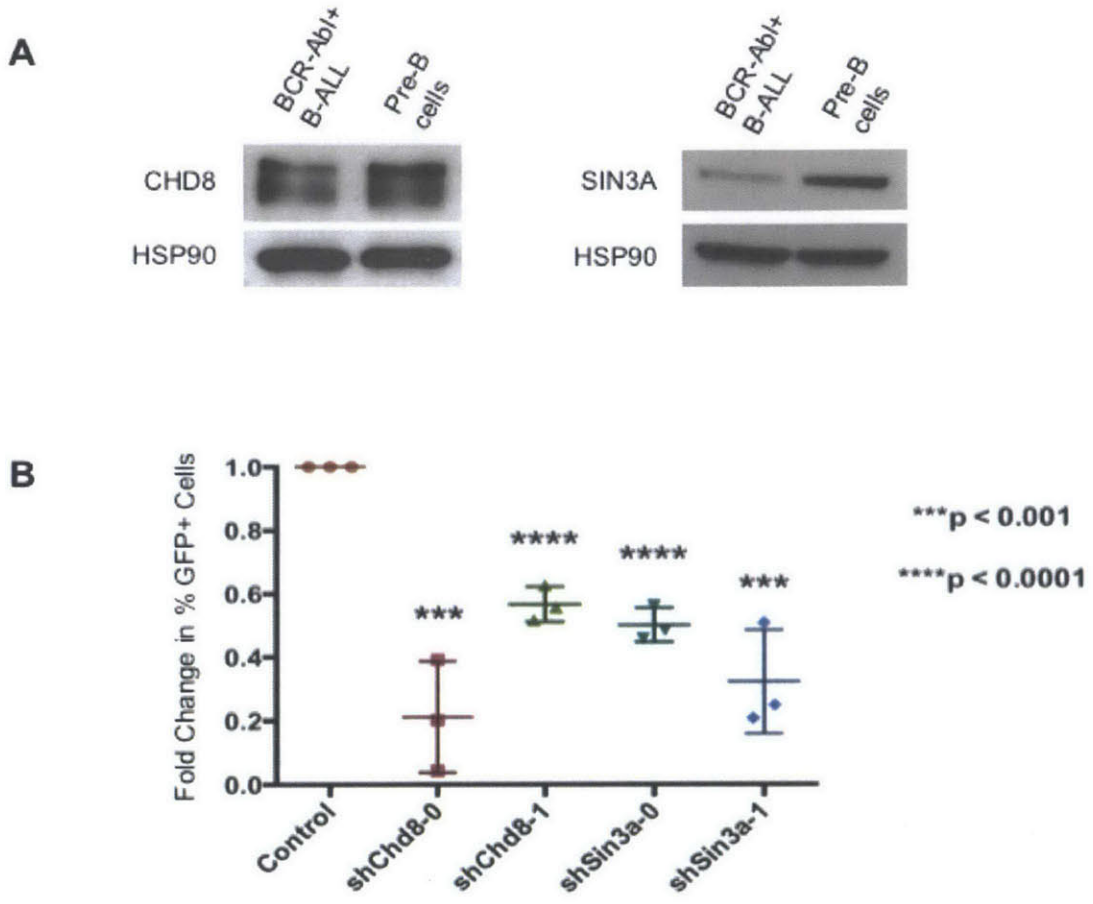

Figure 3: Untransformed pre-B cells express CHD8 and SIN3A at similar levels as BCR-Abl+ B-ALL cells and are dependent on their expression for survival. (A) Normal pre-B cells were sorted from tissue harvested from the bone marrow of an adult C57BL/6 mouse based on surface marker staining ($B220^{+}IgM^{-}CD11b^{-}$). Lysate was generated for protein analysis and compared to a lysate of BCR-Abl+ B-ALL cells. HSP90 was used as a loading control. **(B)** Pre-B cells were retrovirally transduced on two consecutive days with the indicated constructs containing a GFP marker and plated in triplicate (Day 0). The percentage of GFP+ cells was assessed over time by flow cytometry. Shown are the fold changes in %GFP+ cells (Day 8/Day 0) normalized to the vector control, with the average and SD indicated.

An inducible RNAi vector allows examination of gene function in a temporally controlled manner

SIN3A is a protein with a large number of interacting partners that control the expression of a vast number of genes (Dannenberg *et al.* 2005). SIN3A has been demonstrated to interact with the transcription factors RUNX1 and PU.1, both regulators of hematopoietic development, to facilitate transcriptional repression (Suzuki *et al.* 2003; Zhao *et al.* 2008). SIN3A has also been shown to interact with p53 to recruit HDACs and facilitate transcriptional repression of target genes including regulators of mitosis and cellular differentiation (Murphy *et al.* 1999; Chun *et al.* 2003; Lin *et al.* 2005). Additionally, disruption of specific protein interactions with SIN3A can lead to differentiation of breast cancer cells and sensitization to therapy (Farias *et al.* 2010). Because SIN3A's mechanism of action is already well-established, further efforts were focused on discovering the molecular effects of CHD8, which are more obscure and have never been examined in hematopoietic malignancies.

In order to study the downstream molecular effects of *Chd8* knockdown in a temporally controlled manner, shRNAs targeting *Chd8* were cloned into the doxycycline-inducible retroviral vector TRMPVIR (Zuber *et al.* 2010). This vector utilizes a Tet-On system to control the transcription of an shRNA construct. A reverse Tet-transactivator (rtTA) and the fluorescent protein Venus are constitutively expressed under the control of a PGK promoter. Upon the addition of doxycycline, rtTA binds to a Tet-response element (TRE) upstream of the shRNA and a dsRed marker, inducing their expression. This activation also induces further transcription of rtTA, creating a positive feedback loop that continues to drive shRNA expression. shRNA-expressing cells are identified by flow cytometry after doxycycline administration as $Venus^{+}dsRed^{+}$ events (**Fig. 4A**).

When transduced into BCR-Abl+ B-ALL cells, TRMPVIR-sh*Chd8*-1 leads to a marked reduction of CHD8 expression by 24 hours following treatment with 200 ng/mL doxycycline, while CHD8 levels in cells transduced with TRMPVIR expressing a Renilla luciferase shRNA (shRen) are not affected (**Fig. 4B**). Cells were also transduced with TRMPVIR-sh*Chd8*-0; however upon doxycycline treatment a substantial portion of the Venus+ population does not express dsRed (not shown). Given the less efficient nature of sh*Chd8*-0 in this system, all subsequent inducible RNAi experiments were performed with sh*Chd8*-1.

CHD8 depletion leads to cell death without a preceding cell cycle arrest

Others have found that CHD8 depletion leads to a decrease in the expression of the *CCNE2* and *TYMS* genes and a subsequent cell cycle arrest at the G1/S transition (Rodriguez-Paredes *et al.* 2009). We examined *CCNE2* as well as *CCNE1* expression by qPCR in BCR-Abl+ B-ALL cells expressing TRMPVIR-sh*Chd8*-1 or the luciferase control. Surprisingly, the mRNA expression levels of of *CCNE1* and *CCNE2* were found to be slightly higher in CHD8-depleted cells after 48 hours of doxycycline (**Fig. 4C**). This result seemed counter to the expected outcome in that a decrease in cyclin expression rather than an increase would be expected to be detrimental to cell cycle progression. To determine if this change in *CCNE1* and *CCNE2* levels correlated with a change in cell cycle profile, cell cycle analysis was carried out on these populations. Samples were collected at 0, 24, 48, and 72 hours following doxycycline administration, fixed with ethanol, and stained with propidium iodide. Flow cytometry analysis revealed no significant change in the cell cycle profile upon CHD8 depletion (**Fig. 4D**), indicating that

dysregulation of *CCNE1* and *CCNE2* upon CHD8 depletion does not lead to a G1/S arrest in BCR-Abl+ B-ALL cells.

Figure 4:

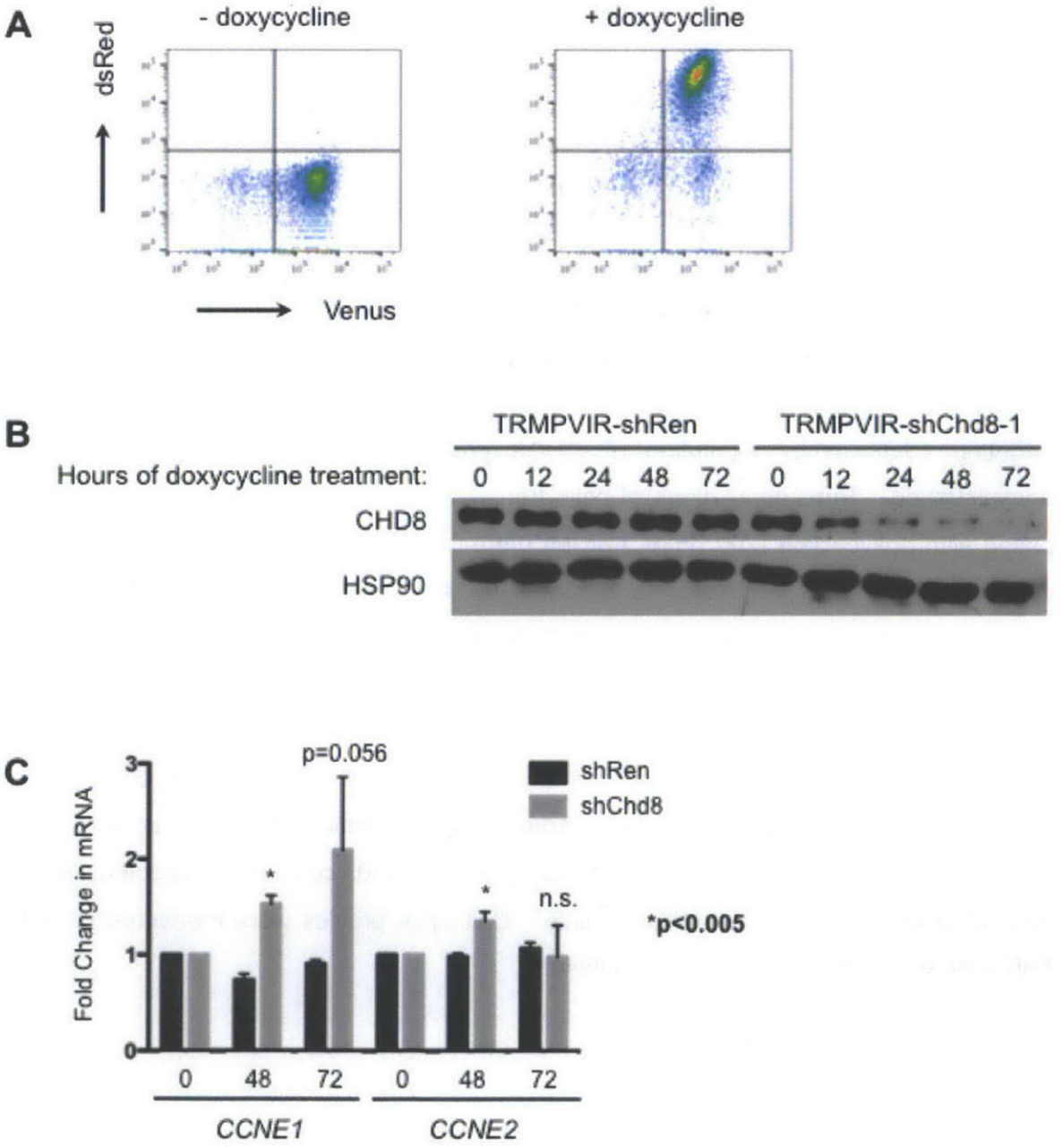

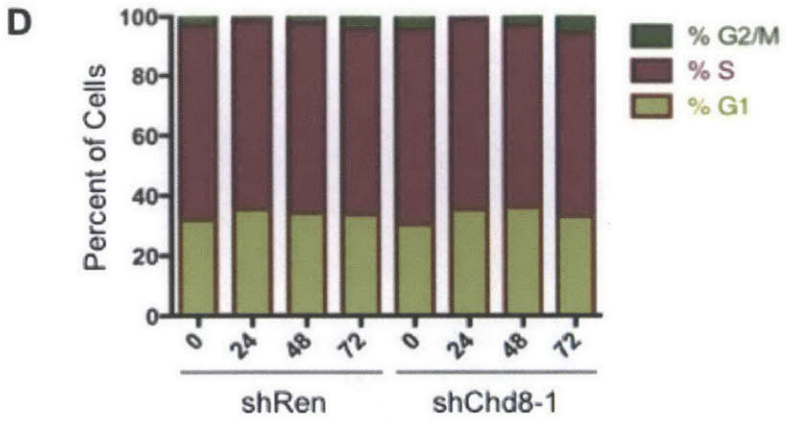

Figure 4: A doxycycline-inducible shRNA vector (TRMPVIR) allows temporal control of shRNA induction following transduction into BCR-Abl+ B-ALL cells. **(A)** Cells expressing TRMPVIR-shRen were sorted by Venus expression and treated with doxycycline (200 ng/mL). After 24 hours, cells were assessed for induction of dsRed and the shRNA by flow cytometry. **(B)** BCR-Abl+ B-ALL cells expressing an inducible shRNA targeting *Chd8* exhibit depletion of CHD8 protein over time following doxycycline administration. Pure populations of cells transduced with the indicated constructs were plated with doxycycline (200 ng/mL) or left untreated. At the indicated times, cells were collected and lysates generated for analysis by western blot. HSP90 was used as a loading control. **(C)** Modest increases in *CCNE1* and *CCNE2* expression are observed in BCR-Abl+ B-ALL cells upon *Chd8* knockdown. Triplicate RT and qPCR reactions were run on the indicated samples. Shown are the averages and standard deviations. **(D)** Induction of sh*Chd8* by doxycycline does not lead to a change in cell cycle profile in BCR-Abl+ B-ALL cells. Pure populations of cells transduced with the indicated constructs were plated with or without doxycycline. At the indicated times, $1x10^6$ cells were collected, fixed in ethanol, and stained with propidium iodide. Cell cycle profiles were measured on a BD FACScan and analyzed with ModFit software.

However, these results do not preclude the possibility that CHD8 depletion leads to a prolonged doubling time in these cells, lengthening each stage of the cell cycle rather than arresting in a particular stage. CHD8 depletion could also lead to cell death without a preceding cell cycle arrest. To test these last two possibilities, we retrovirally infected cells with a puromycin-selectable vector expressing one of two sh*Chd8* constructs or a vector control. Following puromycin selection, 2.5×10^5 live cells per construct were plated in triplicate. The total numbers of live and dead cells per plate were quantified at 24-hour intervals by hemocytometer with trypan blue stain exclusion. Both sh*Chd8* constructs caused a decrease in the apparent growth rates of BCR-Abl+ B-ALL cells, and an increase in the percentages of dead cells (**Fig. 5A, B**). Taken together, these results argue that the depletion observed in the growth competition assays is due to cell death rather than slowed proliferation.

It has been shown that *Chd8* knockdown in U2OS cells leads to an increased incidence of apoptosis that can be rescued with simultaneous knockdown of p53 (Nishiyama *et al.* 2009). To determine if canonical apoptosis is responsible for the death seen in CHD8-depleted populations, protein lysates were generated from BCR-Abl+ B-ALL cells expressing TRMPVIR-sh*Chd8*-1 collected 12, 24, 48, and 72 hours after doxycycline treatment, as well as an untreated control. These lysates were run on a polyacrylamide gel and blotted with an antibody that recognizes both pro- and cleaved caspase 3. A lysate from a cell line treated with the platinum-based chemotherapy agent phenanthriplatin served as a positive control for cleaved caspase 3. While a weak 35 kDa (procaspase 3) and a stronger 17 kDa (cleaved caspase 3) band were observed in the positive control lane, only the 35 kDa band was observed in the TRMPVIR-sh*Chd8*-1 lanes, suggesting that canonical apoptotic signaling through caspase 3 cleavage is not

playing a major role in the phenotype of CHD8-depleted BCR-Abl+ B-ALL cells (**Fig. 5C**).

To determine if cell death is being initiated through an alternative caspase cascade, cells expressing TRMPVIR-sh*Chd8*-1 or the luciferase control were treated with doxycycline and the pan-caspase inhibitor Z-VAD-fmk. This molecule was chosen due to its broad-spectrum effects on a number of caspases. At 40μM, Z-VAD-fmk is able to partially suppress apoptosis in BCR-Abl+ B-ALL cells upon doxorubicin treatment, and the vehicle control-treated cells maintain viability at this concentration of DMSO (0.2%; Singh *et al.* 2014; **Supplementary Fig. 1**). There was no decrease in %Venus^{+}dsRed^{+} cells between Z-VAD-fmk- and vehicle control-treated cells expressing sh*Chd8*-1 (**Fig. 5D**). However, this result does not preclude the occurrence of caspase-independent forms of cell death such as necroptosis.

Figure 5:

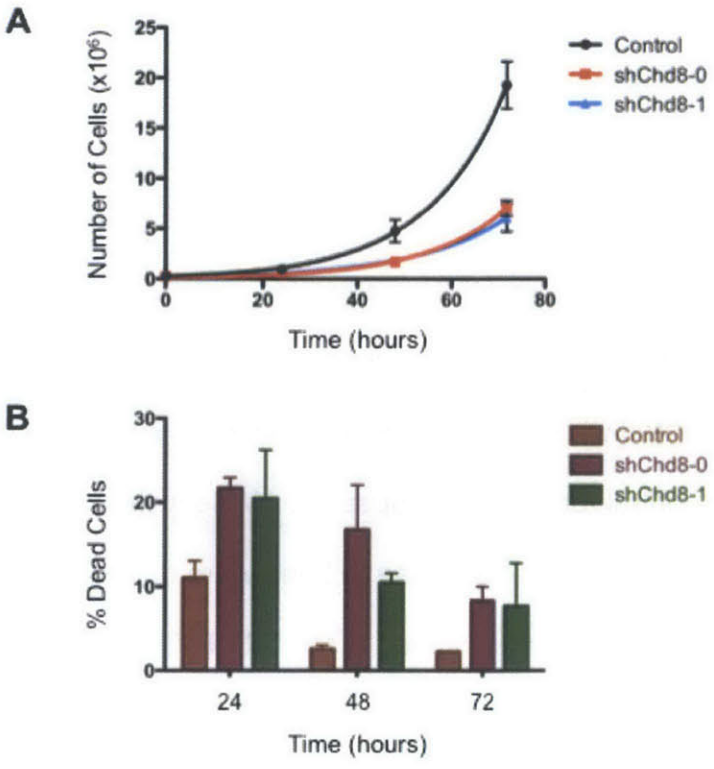

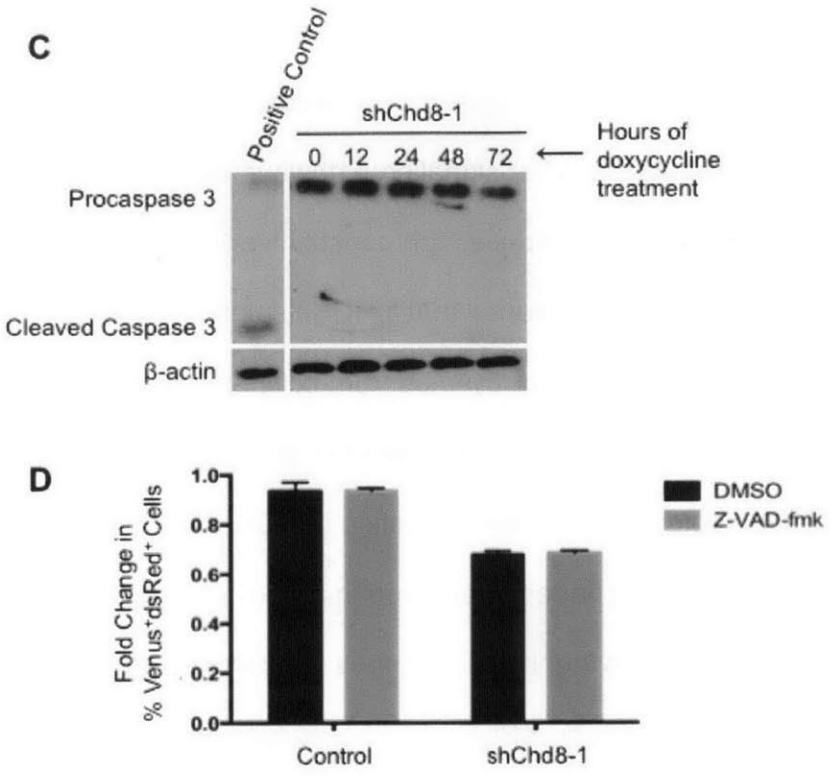

Figure 5: BCR-Abl+ B-ALL cells exhibit decreased apparent growth rates upon CHD8 depletion. Cells were transduced with the indicated constructs in the MLP vector and selected with puromycin. $2.5x10^5$ selected cells were plated in triplicate and counted at 24-hour intervals by hemocytometer. Shown are **(A)** the average numbers of live cells and standard deviations, and **(B)** the percent of dead cells as assessed by trypan blue stain exclusion from one representative experiment. **(C)** No caspase 3 cleavage is observed upon induction of sh*Chd8*-1. A pure population of BCR-Abl+ B-ALL cells expressing TRMPVIR-sh*Chd8*-1 was plated with or without doxycycline and collected at the indicated times. Protein lysates were generated and analyzed by western blot for the presence of cleaved (17 kDa) and pro-caspase 3 (35 kDa). β-actin was used as a loading control. Image cropped to align discontinuous lanes from the same membrane. **(D)** Pan-caspase inhibition by treatment with Z-VAD-fmk does not prevent cell death upon CHD8 knockdown. BCR-Abl+ B-ALL cells transduced with TRMPVIR-shRen or TRMPVIR-sh*Chd8*-1 were plated in triplicate with doxycycline and Z-VAD-fmk or DMSO vehicle control. The percentage of Venus+dsRed+ cells was assessed every two days by flow cytometry, and the fold change from time of plating to the end of the assay (eight days) was calculated. Shown are averages and SD of triplicate wells.

Regulation of the Wnt pathway

While CHD8 depletion does not appear to trigger the canonical apoptotic pathway, CHD8 may have a role in regulating other signaling pathways active in BCR-Abl+ B-ALL cells. BCR-Abl has been shown to induce high constitutive β-catenin activity in leukemia cells (Minami *et al.* 2008), so we reasoned that CHD8 depletion may diminish the transcriptional effects of this pathway. Lysates from cells expressing TRMPVIR-shRen or TRMPVIR-sh*Chd8*-1 were probed by western blot for the presence of β-catenin to determine if CHD8 depletion alters Wnt signaling in BCR-Abl+ B-ALL cells. Constitutive β-catenin expression was indeed observed in all samples, even upon sh*Chd8* induction (**Fig. 6A**). Additionally, no significant changes in expression of the β-catenin target genes *Axin2* or *Nkd2* was seen by qPCR at 72 hours following shRNA induction (**Fig. 6B**). These results suggest that the functional targets of CHD8 may be context-specific, as negative transcriptional regulation of Wnt signaling by CHD8 has been observed in other cancer types (Nishiyama *et al.* 2012; Sawada *et al.* 2013).

Figure 6:

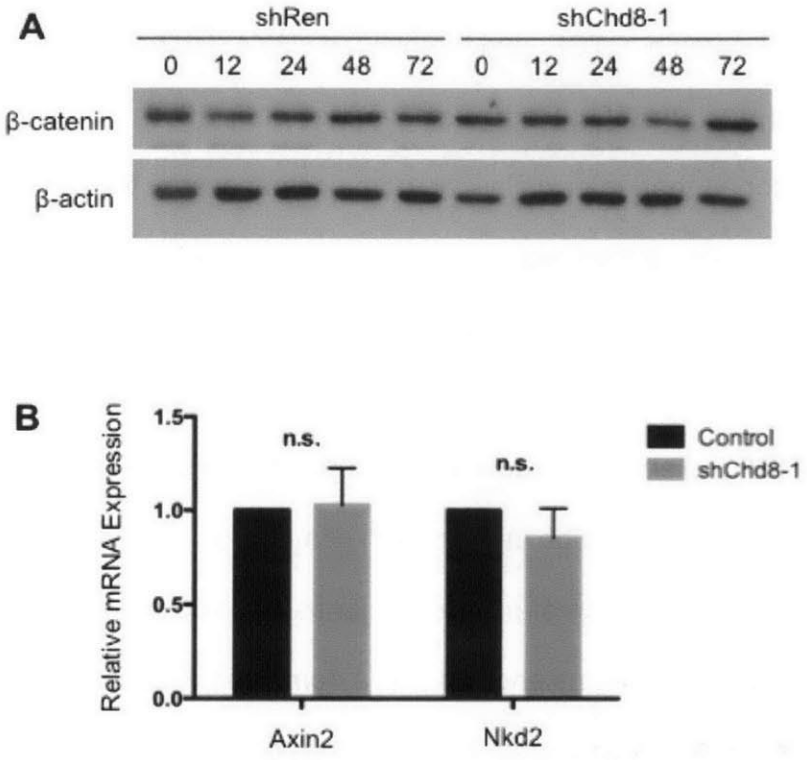

Figure 6: CHD8 does not regulate Wnt signaling in BCR-Abl+ B-ALL cells. (A) β-catenin is constitutively expressed in BCR-Abl+ B-ALL cells and its stabilization does not change upon CHD8 depletion. Cells transduced with the indicated constructs in the TRMPVIR vector were sorted for Venus expression then treated with doxycycline or left untreated. At the indicated times, cells were collected and lysates generated for analysis by western blot. β-actin was used as a loading control. **(B)** CHD8 depletion does not lead to upregulation of the β-catenin target genes *Axin2* or *Nkd2*. mRNA was extracted from BCR-Abl+ B-ALL cells expressing TRMPVIR-shRen or TRMPVIR-sh*Chd8*-1 (untreated and following 72hrs of doxycycline treatment). Following normalization to the endogenous control (tubulin), ΔC_T values for *Axin2* and *Nkd2* in doxycycline-treated samples were normalized to those of untreated samples. Relative expression values in TRMPVIR-sh*Chd8*-1 samples were then normalized to the corresponding TRMPVIR-shRen relative expression values. Shown are averages and SD of three biological replicates.

Ectopic expression of CHD8 N-terminal domains

Given that a number of CHD8 domains have been shown to interact with specific binding partners including p53, β-catenin, CTCF, and methylated H3K4 (Ishihara *et al.* 2006; Yuan *et al.* 2007; Nishiyama *et al.* 2009; Rodriguez-Paredes *et al.* 2009; Nishiyama *et al.* 2012), we reasoned that determining the domains necessary for CHD8 function in BCR-Abl+ B-ALL cells might inform important pro-survival roles. Previously, others have found that overexpression of a 110 kDa truncated N-terminal isoform of murine CHD8 called Duplin was able to rescue cells from p53-mediated apoptosis as effectively as the full-length CHD8 protein (Nishiyama *et al.* 2009). Both p53- and histone H1-interaction domains were found to be in the region common to both isoforms, and Duplin was found to exist at the promoters of p53 target genes and suppress their expression. Subsequent work by these authors showed that a domain in this isoform also facilitated binding to β-catenin (Nishiyama *et al.* 2012). Duplin contains the first of the two tandem chromodomains in CHD8, but not the helicase/ATPase domain, C-terminal helicase domain, or BRK domains (**Fig. 7A**) (Hall and Georgel 2007; Nishiyama *et al.* 2009). Given these results, we hypothesized that overexpression of this isoform might be able to rescue the sh*Chd8* phenotype in BCR-Abl+ B-ALL cells. *Duplin* cDNA was PCR-amplified from BCR-Abl+ B-ALL cDNA and cloned into an MSCV-IRES-GFP (MIG) retroviral vector. BCR-Abl+ B-ALL cells were transduced with this MIG-*Duplin* construct or a vector control, and then sorted for GFP expression. Transduction with MIG-*Duplin* led to high expression of the protein as expected, however endogenous expression of Duplin was not observed in untransduced cells even at very long exposures (**Fig. 7B**). The *Duplin* sequence was therefore probably amplified from the full-length endogenous *Chd8* cDNA rather than an endogenous *Duplin* cDNA. Previous

studies did not measure Duplin expression in blood, so it is possible that only the full-length isoform is expressed in murine lymphoid cells. However, we were also unable to detect multiple isoforms of *Chd8* by qPCR in other murine tissues including brain, liver, lung, and kidney. Pairs of primers amplifying regions located in the 5' or 3' ends of the gene led to equivalent C_T measurements by qPCR (**Fig. 7C**). If the *Duplin* isoform was transcribed at significant levels, differences in these measurements would have been observed. Although this isoform may not normally be expressed, we reasoned that if the domains found in Duplin are important for CHD8 function in BCR-Abl+ B-ALL cells, Duplin overexpression would still be able to prevent the depletion of sh*Chd8*-expressing cells in a growth competition assay. While sh*Chd8*-0 binds within the *Duplin* sequence, sh*Chd8*-1 only targets the full-length isoform, so sh*Chd8*-1 was selected for use in rescue experiments to preclude knockdown of the exogenous *Duplin* construct. sh*Chd8*-1 linked to a tdTomato marker or a tdTomato-expressing vector control was used to partially transduce populations of BCR-Abl+ B-ALL cells expressing *Duplin* cDNA or a GFP+ vector control mixed with GFP- cells. This setup allowed us to use the GFP- population as an internal control to ensure that cells expressing sh*Chd8* alone depleted as expected (data not shown). As seen in **Fig. 7D**, exogenous expression of Duplin was unable to prevent depletion of sh*Chd8*-expressing cells, suggesting that the domains found in Duplin are not sufficient to rescue the effects of CHD8 depletion. We wished to perform similar rescue experiments with the full-length CHD8 protein, but the large size of this cDNA (7.75 kb) made it challenging to clone and express in BCR-Abl+ B-ALL cells. We were able to insert the full-length cDNA sequence into a retroviral vector, but cells transduced with this construct did not express higher protein levels even though we observed increased mRNA expression by qPCR (**Supplementary Fig. 2**).

Figure 7:

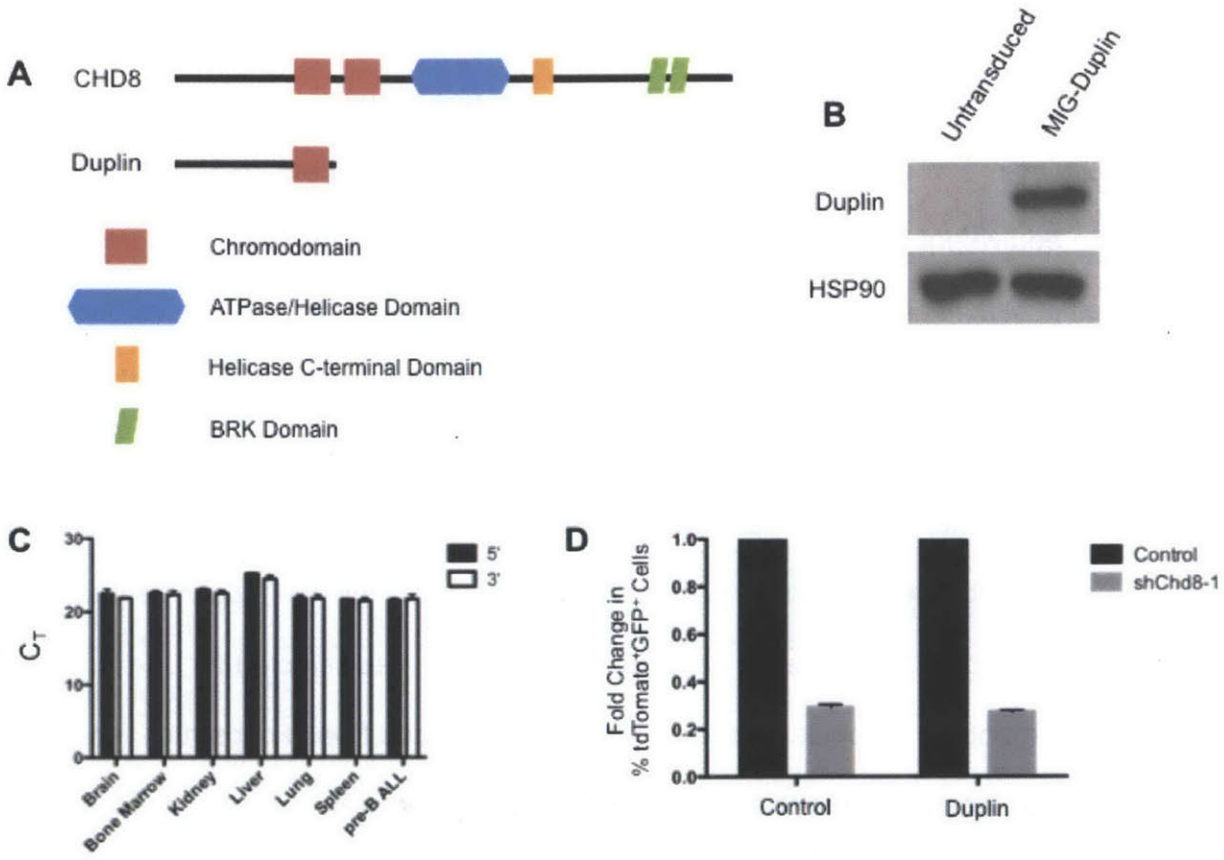

Figure 7: Ectopic expression of Duplin does not increase survival of sh*Chd8*-expressing BCR-Abl+ B ALL cells. **(A)** Functional domains found in CHD8 and the N-terminal isoform Duplin. See text for references. **(B)** Exogenous expression of Duplin isoform in BCR-Abl+ B-ALL cells. Lysates were generated from cells transduced with MIG-Duplin and sorted by GFP expression. This lysate was run alongside lysate from untransduced BCR-Abl+ B-ALL cells and probed for Duplin (110 kDa). HSP90 was used as a loading control. **(C)** qPCR performed with primer pairs amplifying regions near the 5' or 3' ends of *Chd8* yield similar C_T values in multiple healthy mouse tissues, suggesting no endogenous Duplin expression. **(D)** Exogenous expression of Duplin does not rescue the CHD8 knockdown phenotype. BCR-Abl+ B-ALL cells were partially transduced with MIG-Duplin or MIG vector control. Cells were then partially transduced with MLT-sh*Chd8*-1 or the MLT vector control expressing tdTomato. The percentage of tdTomato$^+$GFP$^+$ cells was assessed over time by flow cytometry. The fold change in percent tdTomato$^+$GFP$^+$ cells (out of all GFP+ cells) normalized to MLT vector controls is shown for a representative experiment.

Differential requirement for CHD8 expression in additional hematopoietic malignancies

To determine whether dependency on CHD8 expression extends to other types of hematopoietic malignancies, we turned to another cancer of the B cell lineage, a murine model of Burkitt's lymphoma. In this model, the c-*myc* proto-oncogene is under the transcriptional control of the μ-Ig heavy chain enhancer (Eμ-*myc*), mimicking the t(8;14)(q24;q32) chromosomal translocation that causes this disease in humans (Dalla-Favera *et al.* 1982; Taub *et al.* 1982; Adams *et al.* 1985). We transduced these cells with both shRNAs targeting *Chd8* and confirmed knockdown by western blot (**Fig. 8A**). As with BCR-Abl+ B-ALL cells, Eμ-*myc Arf*$^{-/-}$ cells expressing these shRNAs deplete in *in vitro* growth competition assays (**Fig. 8B**), and growth curves of pure populations of shRNA-expressing cells display decreased proliferation rates and increased numbers of dead cells compared with cells expressing vector controls (**Fig. 8C, D**).

Next we tested the dependency of two murine T-cell malignancies on CHD8 expression. We obtained a spontaneous T-cell lymphoma cell line derived from a *K-ras*$^{LA2/+}$; *p53*$^{LSL/LSL}$ mouse (hereafter referred to as KP). The *K-ras*^{LA2} allele confers expression of an oncogenic G12D mutation upon spontaneous homologous recombination *in vivo* (Johnson *et al.* 2001). Additionally, a stop cassette inserted between the first two exons in both copies of *p53* (*p53*$^{LSL/LSL}$) creates functionally *p53*$^{-/-}$ cells (Ventura *et al.* 2007). We also obtained a transplantable model of T-ALL in which the intracellular domain of Notch (ICN) is ectopically expressed (Top Notch; Beverly *et al.* 2005). Expression of this transgene results in constitutive activation of the Notch signaling pathway and misregulated transcription of target genes.

Figure 8:

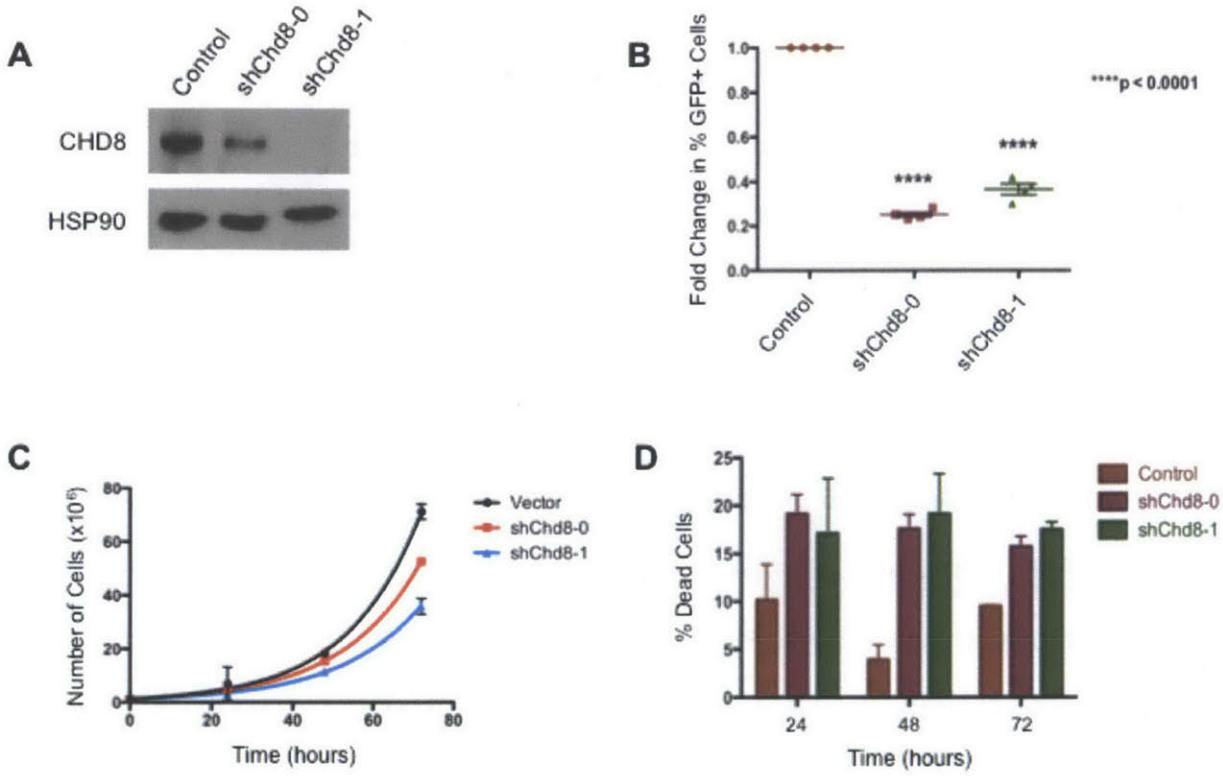

Figure 8: A B-cell lymphoma cell line is also dependent on CHD8 expression for survival. **(A)** Western blot confirming knockdown of CHD8 in Eμ-myc *Arf*$^{-/-}$ lymphoma cells by two distinct shRNAs. Eμ-myc cells lymphoma retrovirally transduced with shRNAs targeting *Chd8* or an MLP vector control were selected with puromycin then collected for protein analysis. HSP90 was used as a loading control. **(B)** Results of four growth competition assays in Eμ-myc *Arf*$^{-/-}$ lymphoma cells. As in Fig. 1C, Eμ-myc cells partially transduced with the indicated constructs containing a GFP marker were plated in triplicate. The %GFP+ cells was assessed eight days later by flow cytometry. Shown are averages of four independent experiments and SEM. **(C)** CHD8 depletion by RNAi leads to a decrease in apparent growth rate of Eμ-myc *Arf*$^{-/-}$ lymphoma cells. As in (A), cells transduced with the indicated constructs in MLP were selected with puromycin. $2.5x10^5$ cells were plated in triplicate and counted by hemocytometer at 24-hour intervals. Shown are the average numbers of live cells and standard deviations, and **(D)** percent dead cells as assessed by trypan blue stain exclusion.

Knockdown of CHD8 expression by shRNA was confirmed in both cell lines by western blot (**Fig. 9A, B**). Interestingly, Top Notch cells expressing sh*Chd8*-1 did not deplete in *in vitro* growth competition assays (**Fig. 9C**). While sh*Chd8*-0 expression caused depletion that met the cut-off for statistical significance, this depletion was less than that seen in BCR-Abl+ B-ALL cells. These results suggest that this cell line is somehow able to compensate for CHD8 knockdown. KP lymphoma cells depleted upon CHD8 knockdown in this assay, but to a lesser extent than either B cell malignancy (**Fig. 9D**). Our findings are consistent with the results of a recent study performed by Knoechel and colleagues (2014). The authors discovered that human T-ALL cells dependent on Notch1 were not dependent on CHD8 expression for survival; however, syngeneic cells that had downregulated ICN after chronic *in vitro* exposure to a γ-secretase inhibitor were negatively affected by RNAi-mediated depletion of CHD8. Constitutive ICN expression appeared to compensate for the loss of CHD8 expression in these cells. We hypothesized that Notch signaling activity was driving cell survival in Top Notch and KP lymphoma cells, partially rescuing the detrimental effect of CHD8 knockdown. To confirm the ability of increased Notch signaling to rescue the CHD8-knockdown phenotype, KP lymphoma cells were transduced with retroviral vectors expressing ICN and a GFP marker, or a GFP marker alone (Aster *et al.* 2000). Ectopic ICN expression is lethal to B cells (Zweidler-McKay *et al.* 2005), so they were not used for these experiments. Cells were sorted to obtain a pure GFP-expressing population, and then partially transduced with retroviral vectors encoding one of two sh*Chd8* constructs in a tdTomato-expressing vector, or a tdTomato+ vector control. Cells were plated and analyzed by flow cytometry to assess the change in the proportion of tdTomato+ cells in each population over time. While cells expressing sh*Chd8* on the GFP+ vector control background depleted to a significant extent, cells expressing

sh*Chd8* on the ICN-transduced background were partially rescued from depletion (**Fig. 9E**). This result indicates that constitutive Notch signaling can attenuate the detrimental effects of CHD8 knockdown in KP lymphoma cells, possibly by overriding a reduction in survival or growth signals caused by CHD8 depletion that constitutive K-ras, BCR-Abl, and Myc signaling are unable to compensate for.

Figure 9:

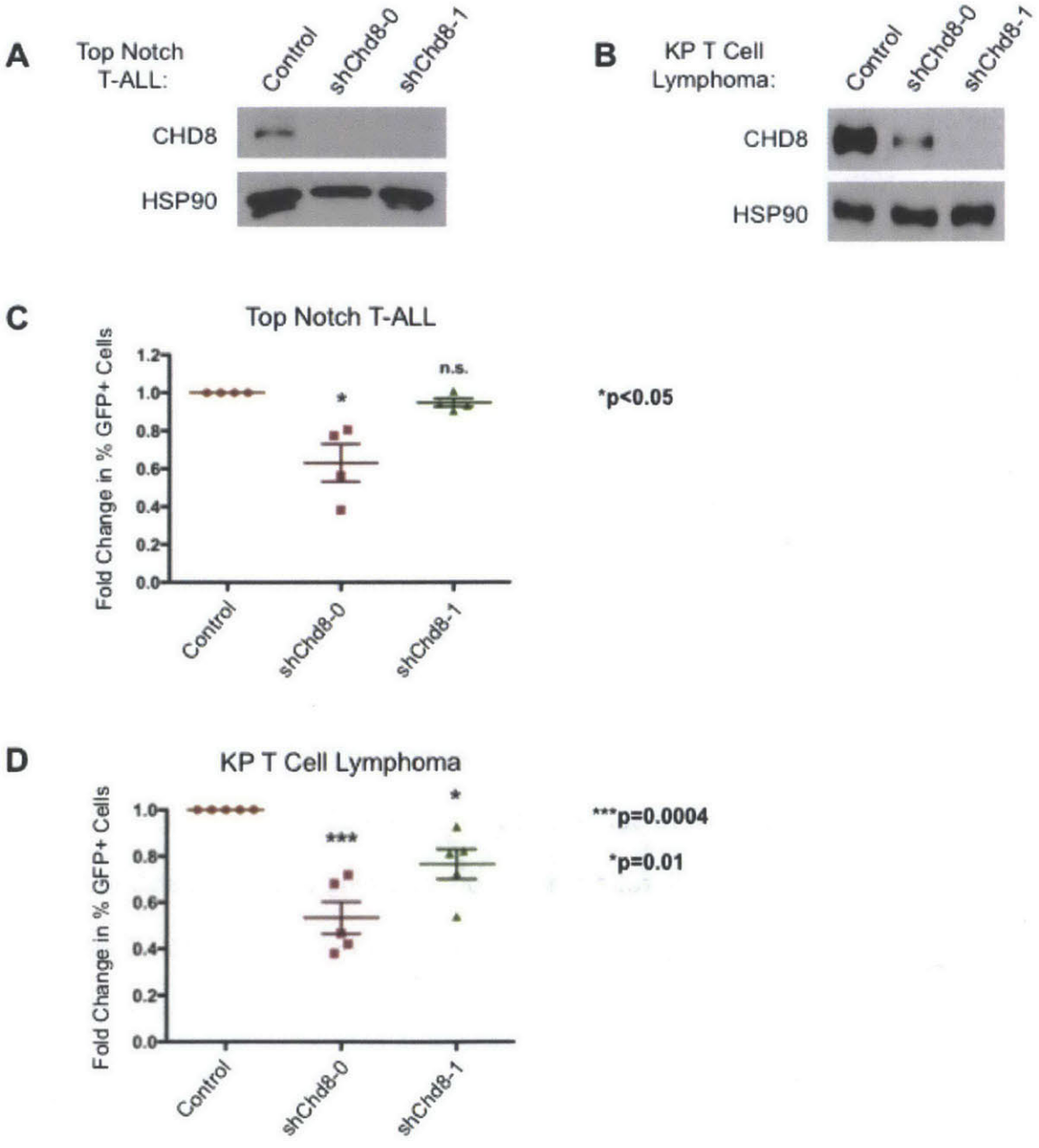

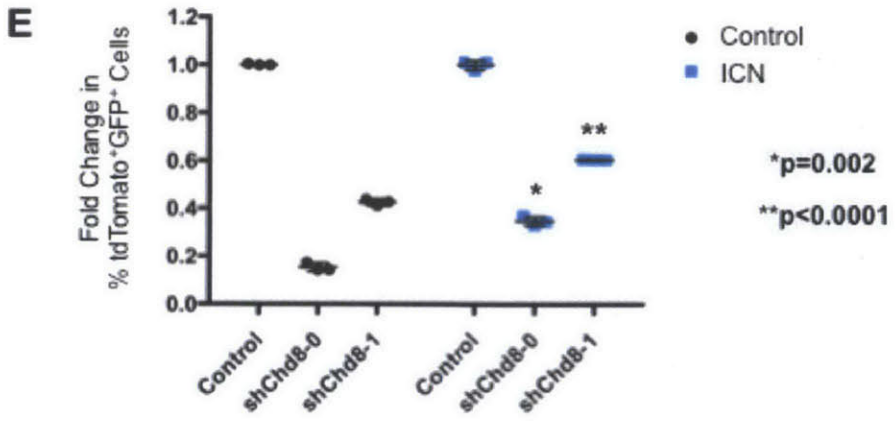

Figure 9: T cell malignancies are less dependent on CHD8 expression than B cell malignancies. Western blot confirming knockdown of CHD8 in **(A)** Top Notch T-ALL and **(B)** *K-Ras*$^{LA2/+}$/*p53*$^{LSL/LSL}$ (KP) T cell lymphoma cells by distinct shRNAs. Cells were retrovirally transduced with the indicated constructs and sorted or selected with puromycin before collecting for protein analysis. HSP90 was used as a loading control. Top Notch **(C)** and KP lymphoma **(D)** cells were partially transduced with the indicated constructs in MLP. Cells were seeded in triplicate and the percentage of transduced cells was assessed eight days later by flow cytometry. Shown are the average fold changes of each of four (Top Notch) or five (KP lymphoma) experiments and the SEM. **(E)** Exogenous ICN expression partially rescues CHD8 depletion phenotype. KP lymphoma cells were retrovirally transduced with a construct containing ICN cDNA and a GFP marker, or a vector control, then sorted by GFP expression to obtain pure populations of transduced cells. Both sorted populations were then partially transduced with tdTomato-labeled *Chd8* shRNAs or a vector control, then plated in triplicate. The percentage of tdTomato$^+$GFP$^+$ cells was assessed over time by flow cytometry. Shown are fold changes in tdTomato$^+$GFP$^+$ cells from a representative experiment, normalized to the average fold change of each MLT control.

Alternatively, CHD8 could be playing a role in regulating expression of hematopoietic lineage genes. CHD8 depletion could alter the expression of B and T cell lineage genes, promoting the progression of BCR-Abl+ B-ALL cells toward a more differentiated state or inducing the expression of T-cell lineage genes such as *Dtx1* and *Hes1* that would prove detrimental to B lymphocytes. To test the first hypothesis, cells expressing TRMPVIR-sh*Chd8*-1 or the luciferase control were stained for two cell surface markers expressed at different stages of the B cell lineage. CD25 (the alpha chain of the IL-2 receptor) begins to be expressed in pre-B cells, while B220 is expressed beginning in the prepro-B stage and its expression increases as cells progress through the B cell lineage (Hardy *et al.* 2007). The BCR-Abl+ B-ALL cell line expresses B220 but not CD25 due to its less differentiated state. If CHD8 depletion were leading these cells to advance to the pre-B cell stage, gain of CD25 expression would be observed; however CD25 status remained unchanged even after 96 hours of doxycycline administration (**Fig. 10A**). B220 status also remained unchanged, indicating that these cells are not losing their B lymphocyte identity to revert to a common lymphocyte progenitor stage upon CHD8 depletion (**Fig. 10B**). However, further investigation into expression of other cell surface markers and stage-specific genes will be necessary to rule out the possibility of alterations in differentiation status.

To test for the induction of T-cell lineage genes upon CHD8 depletion, qPCR was run on mRNA from BCR-Abl+ B-ALL cells expressing TRMPVIR-sh*Chd8*-1 or TRMPVIR-shRen following doxycycline treatment. No upregulation of the T lymphocyte genes and Notch targets *Dtx1* or *Hes1* was observed up to 72 hours following sh*Chd8* induction (**Fig. 10C**), indicating that CHD8 depletion is not causing depletion of these cells through inappropriate expression of these T-cell lineage genes.

Figure 10:

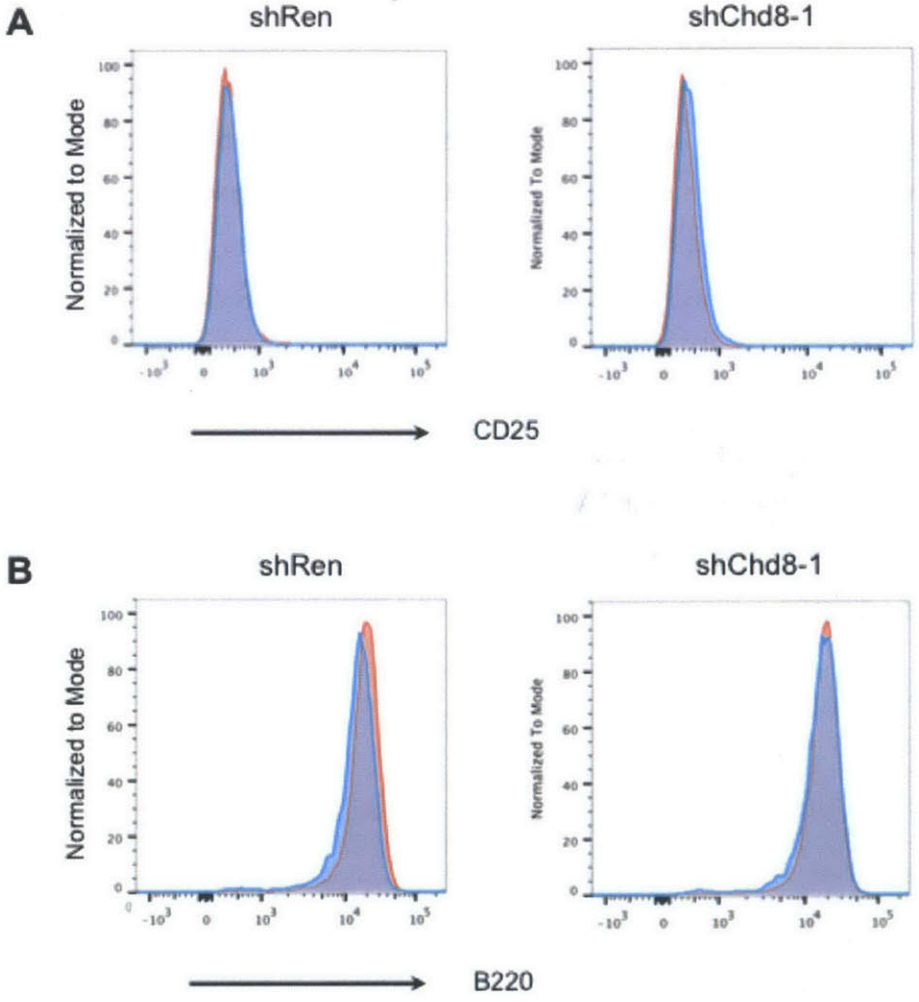
A
shRen
shChd8-1
Normalized to Mode
Normalized To Mode
CD25
B
shRen
shChd8-1
Normalized to Mode
Normalized To Mode
B220
C
Relative mRNA Expression
2.0
1.5
1.0
0.5
0.0
n.s.
n.s.
Control
shChd8
Dtx1
Hes1

Figure 10: CHD8 depletion does not alter surface expression of B lymphocyte markers, or induce transcription of Notch1 target genes in BCR-Abl+ B-ALL cells. BCR-Abl+ B-ALL cells transduced with TRMPVIR-shRen or TRMPVIR-sh*Chd8*-1 were collected after exposure to doxycycline (200 ng/mL) for 96 hours, stained with APC-conjugated antibodies for CD25 **(A)** or B220 **(B)** and compared to untreated cells. Untreated cells are indicated in red, 96-hour samples are indicated in blue. Results of staining with APC-conjugated antibody isotype controls are shown in Supplementary Fig. 4. **(C)** CHD8 depletion does not alter the expression of T-cell lineage genes *Dtx1* or *Hes1* in BCR-Abl+ B-ALL cells. As in Fig. 6B, mRNA was extracted from BCR-Abl+ B-ALL cells expressing TRMPVIR-shRen or TRMPVIR-sh*Chd8*-1, both untreated and following 72hrs of doxycycline treatment. Tubulin was used as an endogenous control, and ΔC_T values for *Dtx1* and *Hes1* in doxycycline-treated samples were normalized to those of untreated samples. Relative expression values in TRMPVIR-sh*Chd8*-1 samples were then normalized to the corresponding TRMPVIR-shRen relative expression values. Shown are averages and SD of three biological replicates.

Genome-wide analysis of CHD8 transcriptional targets

As a protein able to associate with di- and trimethylated H3K4, CHD8 has the potential to bind to the promoter of virtually any actively transcribed gene and alter its transcription. Previous studies have demonstrated CHD8 binding to approximately 2,000 active promoters (Subtil-Rodriguez *et al.* 2014) including promoters of E2F-, p53-, and β-catenin target genes (Thompson *et al.* 2008; Nishiyama *et al.* 2009; Nishiyama *et al.* 2012), RNA Pol III-transcribed genes (Yuan *et al.* 2007), cyclin E2 (Rodriguez-Paredes *et al.* 2009), HOXA2 (Yates *et al.* 2010), and androgen receptor target genes (Menon *et al.* 2010). To identify and compare the transcriptional targets of CHD8 in BCR-Abl+ B-ALL and Top Notch T-ALL cells in a high-throughput manner, we carried out RNA-Seq. Biological triplicates were generated by retrovirally transducing three separate populations of BCR-Abl+ B-ALL cells or Top Notch cells with TRMPVIR-sh*Chd8*-1 or TRMPVIR-shRen, and then sorting by Venus expression. Beverly and colleagues generated the Top Notch mouse model with a Tet-operable ICN construct (2005). In this system, expression of a tTA construct in T-cell progenitor cells activates expression of ICN in the absence of doxycycline, and mice develop disease within weeks after birth. If doxycycline is administered from birth, ICN transcription is inhibited and mice remain disease-free. Similarly, if leukemic mice are given doxycycline, tumors regress. However, disease invariably relapses while on doxycycline as tumor cells reactivate the ICN transgene. ICN in these relapse-derived cells are now insensitive to the presence of doxycycline and give rise to leukemia in naïve recipients with identical latency with or without doxycycline treatment. We found that, like the relapse-derived cells, our stock of Top Notch cells express ICN regardless of the presence of doxycycline, allowing the use of this inducible RNAi construct to knock down CHD8 expression without interfering with

ICN transgene expression (**Supplementary Fig. 5**). Sorted TRMPVIR-expressing cells were treated with 200 ng/mL doxycycline and collected after 24 hours. This time point was chosen to capture the immediate rather than downstream targets of CHD8. Samples were analyzed by flow cytometry to ensure induction of dsRed expression at the time of collection (data not shown). mRNA was extracted from each sample and sequenced using the Illumina HiSeq platform. Analysis of sequencing results showed that *Chd8* expression was indeed diminished in sh*Chd8*-expressing cell lines upon doxycycline treatment (data not shown). As expected, while most genes were expressed at similar levels in both cell types, a number of genes showed differential expression (**Fig. 11A**). When the set of differentially expressed genes was analyzed by GSEA (Gene Set Enrichment Analysis), this list was shown to be highly enriched for genes involved in B cell receptor signaling and genes expressed in fetal thymocyte progenitors (**Fig. 11B**). In addition, BCR-Abl+ B-ALL and T-ALL cells expressed very high levels of *Abl* and *Notch1* transcripts, respectively.

Figure 11:

A

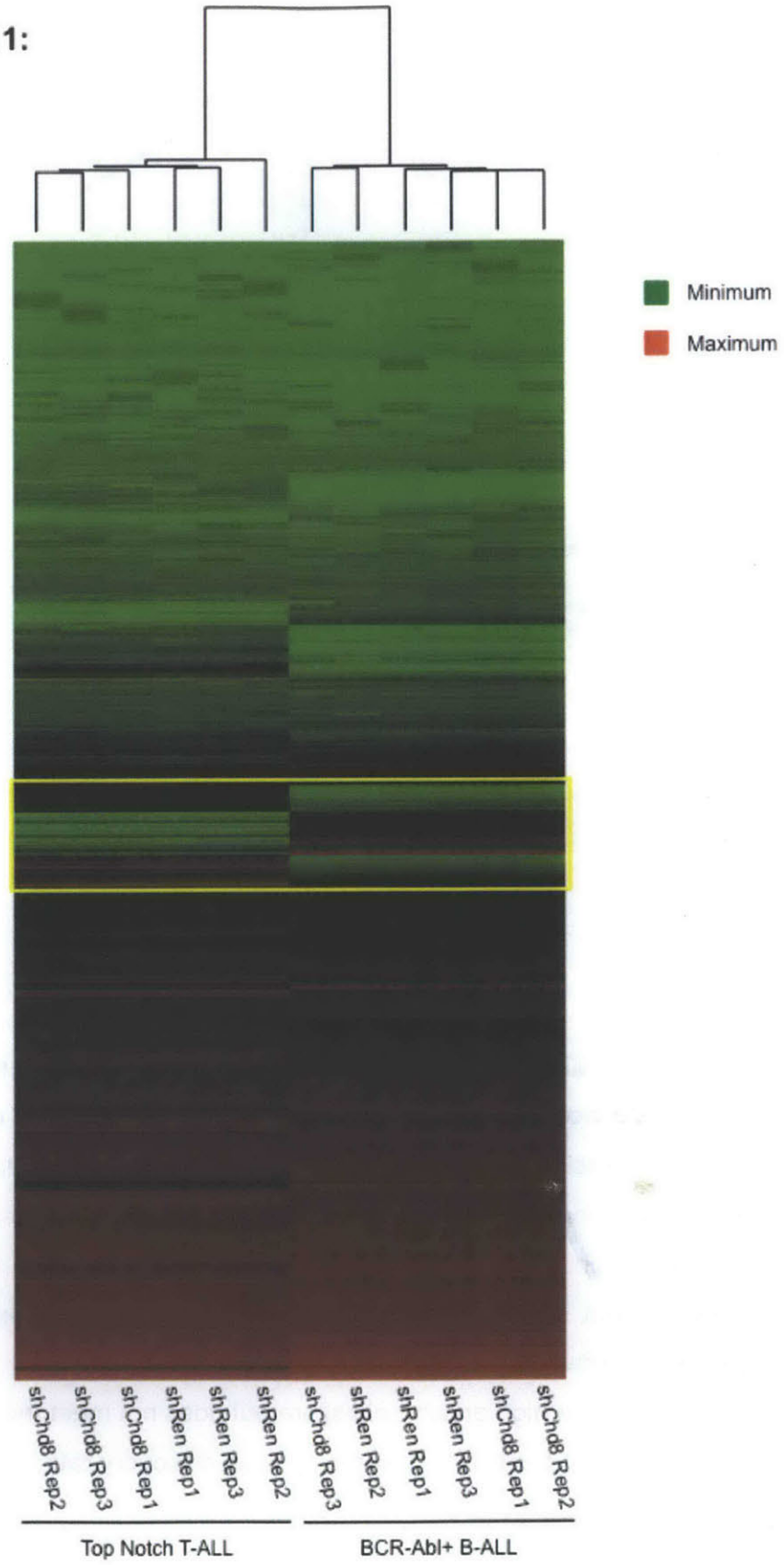
Minimum
Maximum
shChd8 Rep2
shChd8 Rep3
shChd8 Rep1
shRen Rep1
shRen Rep3
shRen Rep2
shChd8 Rep3
shRen Rep2
shRen Rep1
shRen Rep3
shChd8 Rep1
shChd8 Rep2
Top Notch T-ALL
BCR-Abl+ B-ALL

B Higher Expression in BCR-Abl+ B-ALL:

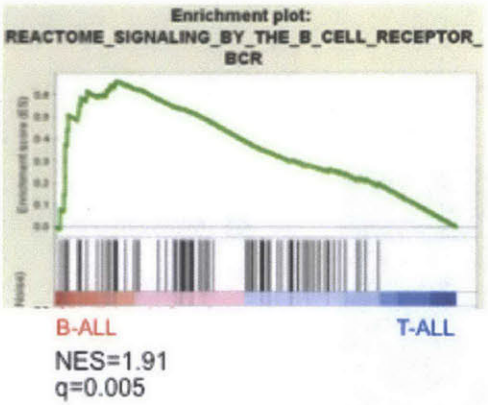

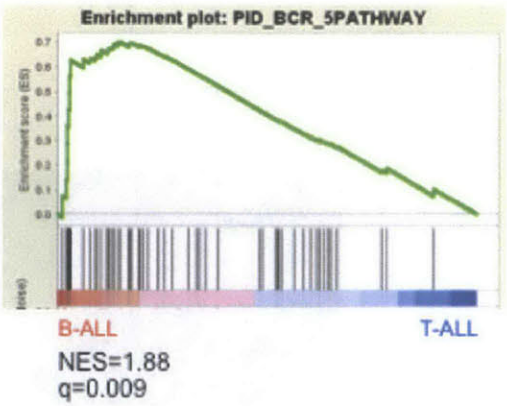

Higher Expression in Top Notch T-ALL:

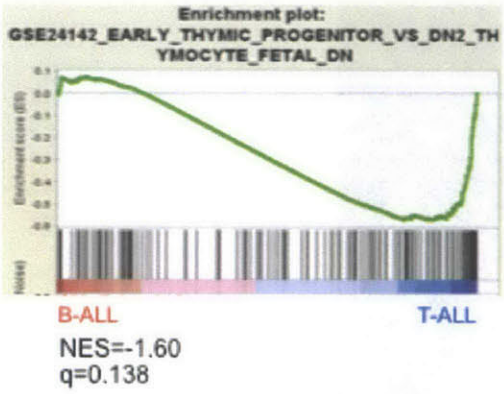

Figure 11: BCR-Abl+ B-ALL and Top Notch T-ALL RNA-Seq results cluster samples based on cell type, but do not show large gene expression differences upon CHD8 depletion. **(A)** Gene expression profiles in BCR-Abl+ B-ALL and Top Notch cell lines cluster by cell type. Expression values were normalized by the mean. Lineage-specific differences in gene expression are outlined in yellow. **(B)** GSEA of genes differentially expressed in BCR-Abl+ B-ALL and Top Notch T-ALL cells shows enrichment for genes involved in B cell receptor signaling and genes expressed in fetal thymocyte progenitors. A Notch pathway signature has a high enrichment score but does not meet the FDR cut-off for significance. NES, normalized enrichment score; q, false discovery rate.

CHD8 as a co-regulator of the NF-κB pathway

While no single gene met the requirement for significantly altered expression upon CHD8 knockdown by the more rigorous multi-hypothesis testing, GSEA yielded a number of putative hits that were components or targets of the NF-κB pathway, including *Btk*, *TNFα*, *Fas*, *Irak2*, *Ltb*, *Prf1*, and *TGFβ2*. We performed individual analysis of gene expression by qPCR on cDNA generated from replicate TRMPVIR-sh*Chd8*-1 time course experiments, this time selecting the 72-hour timepoint rather than the 24-hour timepoint used in the RNA-Seq experiment in an attempt to measure a larger change in gene expression. Our results revealed modest changes in a subset of these genes upon CHD8 knockdown, some of which differed between BCR-Abl+ B-ALL cells and Top Notch cells (**Fig. 12A**). One of these hits, *Btk* (Bruton's tyrosine kinase), appeared to be modestly upregulated upon CHD8 depletion in BCR-Abl+ B-ALL cells, although this change did not meet the requirement for significance by a multi-hypothesis t test. BTK is an integral member of the signal transduction pathway that links antigen binding-mediated activation of the B cell receptor to activation of the NF-κB pathway (Young and Staudt 2013). Interestingly, this gene is not expressed in the T cell lineage, making it an attractive candidate to account for the different dependencies of these two cell lines to CHD8 expression. However, BTK inhibition has been under investigation as a new therapy in various B cell malignancies (Ponader and Burger 2014), which would contradict our results of putative negative regulation of *Btk* by CHD8. However, these malignancies are typically derived from mature B cells with fully rearranged B cell receptors, so it is possible that BTK may have a different function in a pre-B cell leukemia such as BCR-Abl+ B-ALL. To directly test this hypothesis, we turned to a small molecule inhibitor of BTK (ibrutinib) that is currently undergoing clinical trials (Ponader

and Burger 2014). To determine if BTK inhibition could alter the CHD8-knockdown phenotype in BCR-Abl+ B-ALL cells, we treated pure populations of TRMPVIR-sh*Chd8*-1 or TRMPVIR-shRen transduced cells with 5.0μM ibrutinib (LD30, **Supplementary Fig. 6**) and 200 ng/mL doxycycline. This dose of ibrutinib was selected as it clearly confers a biological effect yet does not kill the majority of cells. Ibrutinib did not alter the detrimental effect of CHD8 depletion, suggesting that deregulation of *Btk* expression does not contribute to the CHD8 knockdown phenotype in BCR-Abl+ B-ALL cells (**Fig. 12B**). However, ibrutinib may also inhibit a small number of other kinases with a similar ATP-binding site (Ponader and Burger 2014), so we cannot rule out that inhibition of one or more of these kinases is overcoming the effect of BTK inhibition alone. It is still possible that *Btk* is a bone fide target for regulation by CHD8, but it appears that its increased expression upon CHD8 depletion is not the driver behind the observed phenotype.

While the results of our validation studies indicated no significant change in TNFα upon CHD8 depletion **(Fig. 12A)**, stimulation of the NF-κB pathway by treatment with TNFα may alter the dependence of BCR-Abl+ B-ALL cells on CHD8 expression. First we set out to determine if depletion of TNFα itself is detrimental to BCR-Abl+ B-ALL cells. RNAi-mediated knockdown of TNFα led to depletion of BCR-Abl+ B-ALL cells in an *in vitro* growth competition assay **(Fig. 12C)**, consistent with the phenotype conferred by CHD8 knockdown. After 6 hours of treatment with recombinant murine TNFα at 10.0 ng/mL, an increase in phospho-RelA signal is observable by western blot **(Fig. 12D)**. When phosphorylated, RelA becomes a transcriptionally active subunit of the NF-κB heterodimer along with p50, indicating activation of the NF-κB pathway (Baeuerle and Henkel 1994). This dose did modestly decrease the amount of depletion of BCR-Abl+ B-

ALL cells expressing TRMPVIR-sh*Chd8 in vitro*, but when the concentration of TNFα was increased to 100.0 ng/mL no further rescue was observed **(Fig. 12E)**. However, this result is to be expected if CHD8 is acting on the NF-κB pathway downstream of initial stimulation by TNFα. We therefore tested the effect of CHD8 knockdown on NF-κB activation as measured by levels of phosphorylated RelA. Interestingly, BCR-Abl+ B-ALL cells expressing TRMPVIR-sh*Chd8*-1 showed decreased phospho-RelA 24 hours following doxycycline administration, suggesting that NF-κB signaling is diminished upon CHD8 depletion, at least initially as these levels were partially recovered by 72 hours. Top Notch cells expressing TRMPVIR-sh*Chd8*-1 also displayed a decrease in phospho-RelA after 24 hours of doxycycline treatment. The extent of this decrease varied between replicates in both cell lines, so we could not conclude from this evidence if the magnitude of the change in NF-κB signaling upon CHD8 depletion is the mechanism determining the dependence of these cell lines on CHD8 expression. It is possible that downstream events that differ in these cell lines are the determining factor. Additional experimentation will be necessary to test this hypothesis. Taken together, the results of *in vitro* assays with ibrutinib and TNFα suggest that the transcriptional targets of CHD8 may be numerous, and replacement or inhibition of a single gene product may not be sufficient to fully rescue the detrimental effects of CHD8 depletion in these cells.

Figure 12:

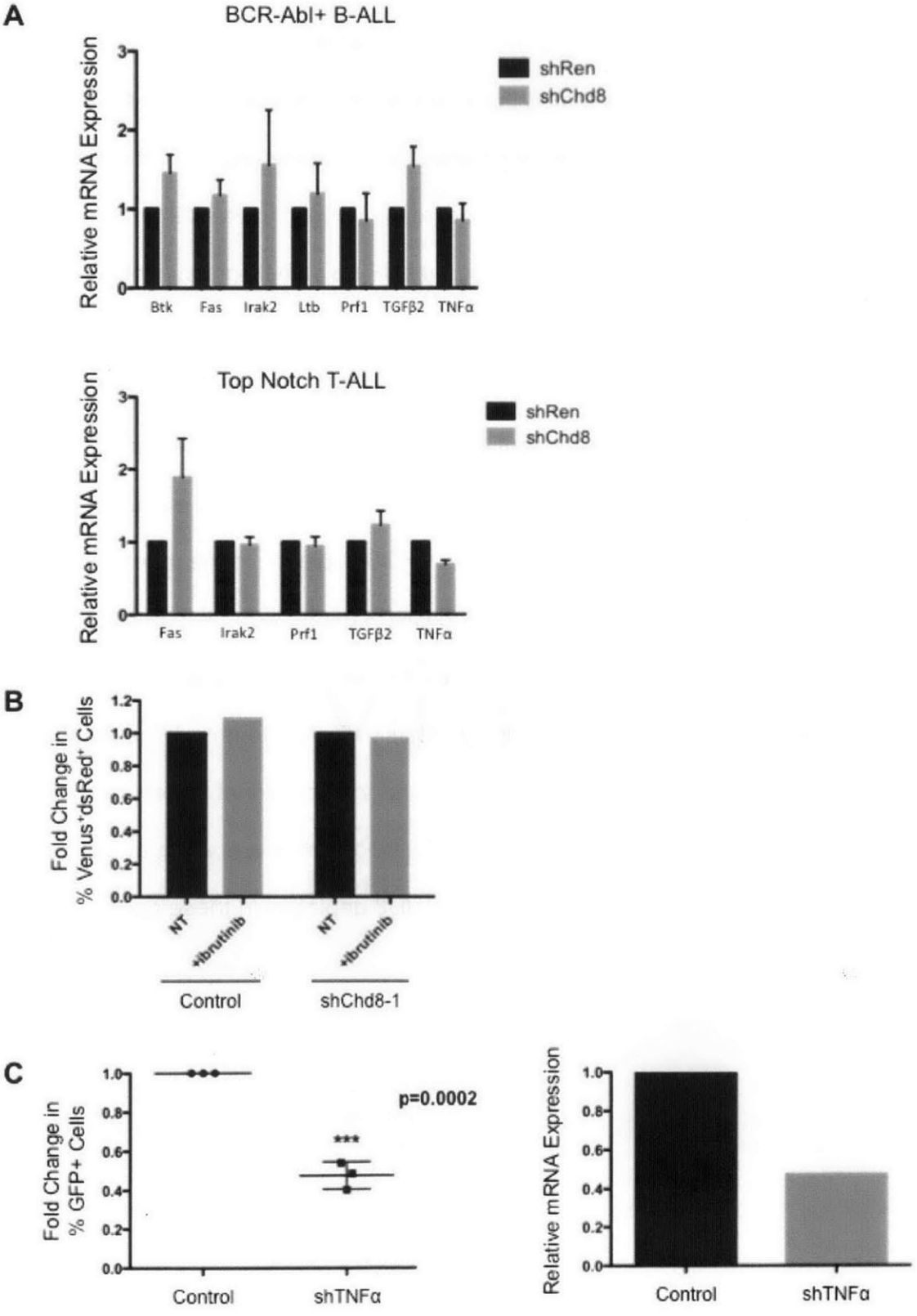
A
BCR-Abl+ B-ALL
Relative mRNA Expression
shRen
shChd8
Btk
Fas
Irak2
Ltb
Prf1
TGFβ2
TNFα
Top Notch T-ALL
Relative mRNA Expression
shRen
shChd8
Fas
Irak2
Prf1
TGFβ2
TNFα
B
Fold Change in % Venus+dsRed+ Cells
NT
+ibrutinib
NT
+ibrutinib
Control
shChd8-1
C
Fold Change in % GFP+ Cells
p=0.0002
***
Control
shTNFα
Relative mRNA Expression
Control
shTNFα

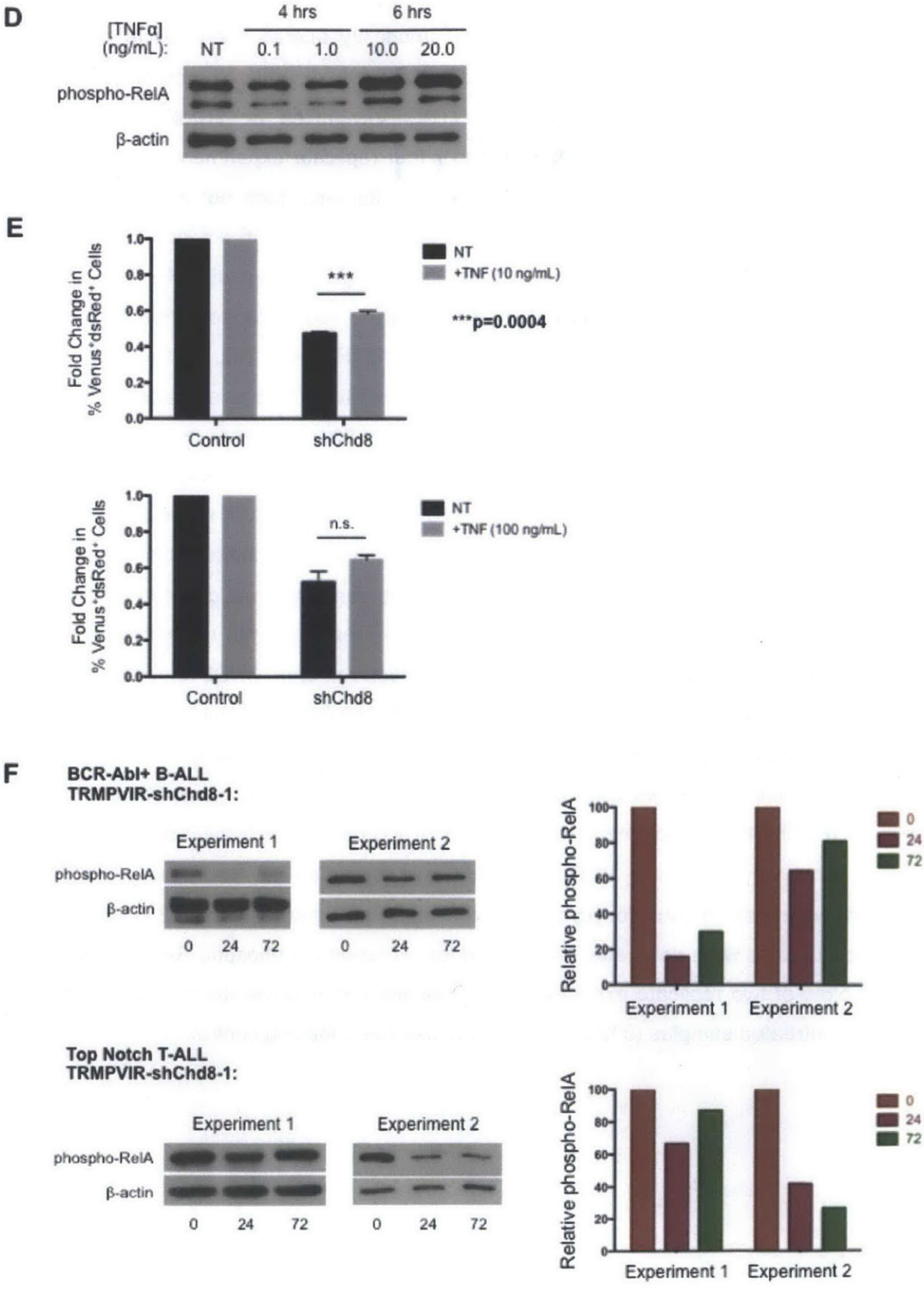
D
4 hrs
6 hrs
[TNFα] (ng/mL):
NT
0.1
1.0
10.0
20.0
phospho-RelA
β-actin
E
Fold Change in % Venus+dsRed+ Cells
1.0
0.8
0.6
0.4
0.2
0.0
***
NT
+TNF (10 ng/mL)
***p=0.0004
Control
shChd8
n.s.
NT
+TNF (100 ng/mL)
F
BCR-Abl+ B-ALL
TRMPVIR-shChd8-1:
Experiment 1
Experiment 2
phospho-RelA
β-actin
0
24
72
Relative phospho-RelA
100
80
60
40
20
0
Top Notch T-ALL
TRMPVIR-shChd8-1:

Fig. 12: CHD8 depletion modestly alters NF-κB signaling in leukemias. (A) Transcription of NF-κB pathway components is modestly altered upon CHD8 depletion. qPCR was performed on cDNA from untreated and 72hr doxycycline-treated samples from replicate experiments with cells expressing TRMPVIR-shRen or TRMPVIR-sh*Chd8*-1. Shown are averages and SEM of either three or four replicate experiments normalized to TRMPVIR-shRen. **(B)** Addition of the BTK inhibitor ibrutinib does not alter the sh*Chd8* phenotype in BCR-Abl+ B-ALL cells. TRMPVIR-shRen or TRMPVIR-sh*Chd8*-1 expressing cells were treated with ibrutinib at 5.0μM and the change in %Venus$^+$dsRed$^+$ cells was assessed by flow cytometry every two days. Results were normalized to untreated controls. **(C)** Knockdown of TNFα by RNAi leads to depletion of BCR-Abl+ B-ALL cells *in vitro*. Cells were partially transduced with a GFP-marked shRNA targeting TNFα or a vector control, and the change in %GFP+ cells was assessed over time by flow cytometry (left). Puromycin-selected populations were collected for RNA analysis by qPCR to assess efficiency of knockdown (right). **(D)** NF-κB activity is enhanced upon treatment with recombinant murine TNFα at 10.0 ng/mL. BCR-Abl+ B-ALL cells were treated with the indicated concentrations of TNFα and collected after 4 or 6 hours. Lysates were generated and probed for phospho-RelA, a transcriptionally active subunit of NF-κB. **(E)** Treatment with recombinant murine TNFα modestly rescues BCR-Abl+ B-ALL cells from depletion upon CHD8 knockdown. Pure populations of cells expressing TRMPVIR-shRen or TRMPVIR-sh*Chd8*-1 were treated with 200 ng/mL doxycycline and TNFα at 10.0 ng/mL or 100 ng/mL. Change in %Venus$^+$dsRed$^+$ cells was assessed every two days by flow cytometry. Results were normalized to shRen controls. **(F)** CHD8 depletion leads to decreased NF-κB pathway activation as measured by levels of phosphorylated RelA. BCR-Abl+ B-ALL and Top Notch cells expressing TRMPVIR-sh*Chd8*-1 were treated with doxycycline for the indicated times (24 and 72 hours) or left untreated. Lysates were generated and probed for expression of phospho-RelA. Shown are western blots of two replicate experiments per cell line and quantifications of band density relative to untreated samples (0 hrs). β-actin was used as a loading control.

Supplementary Figures

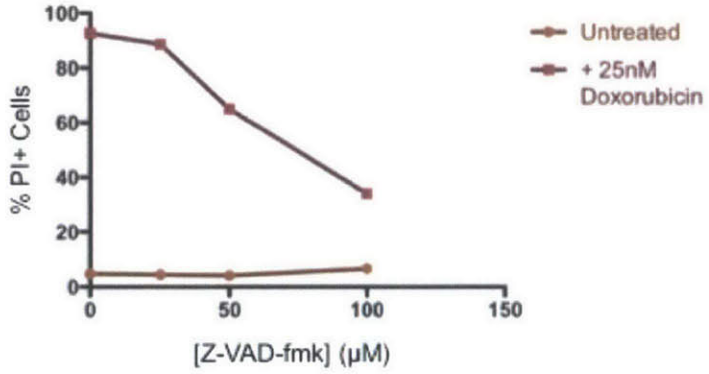

Supplementary Figure 1: Z-VAD-fmk prevents apoptosis in BCR-Abl+ B-ALL cells treated with doxorubicin. Cells were dosed with Z-VAD-fmk at the indicated concentrations and 1 hour later treated with doxorubicin (25nM) or left untreated to measure effect of DMSO vehicle on viability. After 24 hours doxorubicin was diluted 1:2 and the concentration of Z-VAD-fmk maintained. After 48 hours viability was assessed by PI incorporation. Shown is the percentage of PI+ (dead) cells.

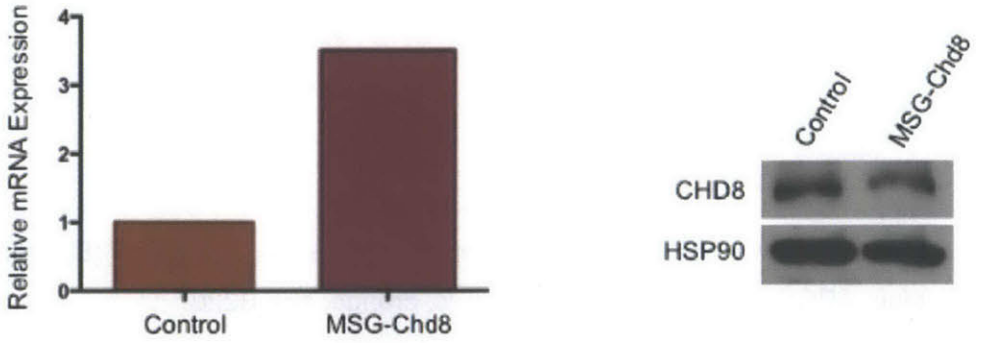

Supplementary Fig. 2: BCR-Abl+ B-ALL cells transduced with MSG-*Chd8* show increased mRNA expression (left) but fail to express higher levels of CHD8 protein (right). Cells were transduced with the indicated construct and sorted for GFP expression. mRNA was extracted for qPCR analysis with primers amplifying a region at the 3' end of *Chd8*. Lysates were generated and probed for expression of CHD8. HSP90 was used as a loading control.

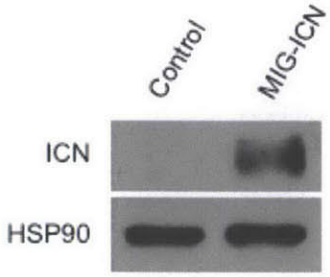

Supplementary Figure 3: Ectopic expression of ICN in *K-ras*$^{LA2/+}$; *p53*$^{LSL/LSL}$ T cell lymphoma cells transduced with MIG-ICN. HSP90 was used as a loading control.

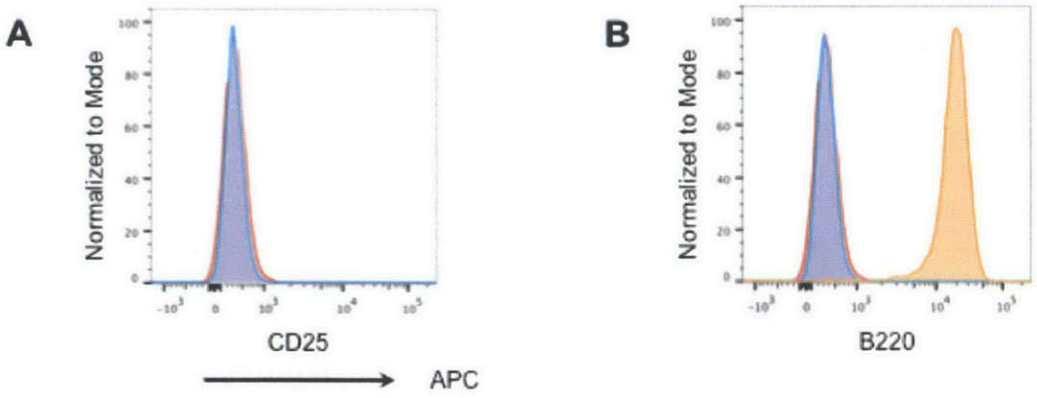

Supplementary Figure 4: Antibody isotype controls for CD25 **(A)** and B220 **(B)**. Red, unstained cells; blue, APC-conjugated isotype controls; orange, anti-B220.

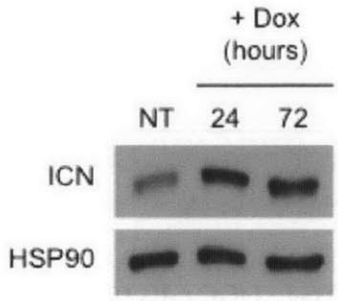

Supplementary Figure 5: Top Notch cells express ICN regardless of doxycycline treatment. Top Notch cells were transduced with TRMPVIR-shRen, sorted by Venus expression, and treated with doxycycline (200 ng/mL). At the indicated times, cells were collected and lysates generated for protein analysis. HSP90 was used as a loading control.

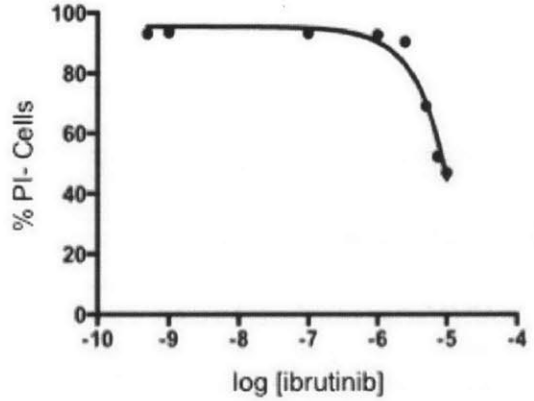

Supplementary Figure 6: Dose response curve of ibrutinib in BCR-Abl+ B-ALL cells. Cells were treated with the indicated doses for 48 hours before assessing viability by PI incorporation. Shown is the percentage of PI-negative (live) cells as a function of [ibrutnib].

Supplementary Tables

Supplementary Table 1: shRNA sequences

Target	Sequence
Chd8-0	TGCTGTTGACAGTGAGCGCCGATGTAACTGGTCCAATAAATAGTGAAGCC ACAGATGTATTTATTGGACCAGTTACATCGGTGCCTACTGCCTCGGA
Chd8-1	TGCTGTTGACAGTGAGCGCCACAATGATGGAGCTACGAAATAGTGAAGC CACAGATGTATTTCGTAGCTCCATCATTGTGTTGCCTACTGCCTCGGA
Sin3A-0	TGCTGTTGACAGTGAGCGCGGATGTTGATGTAGAAGATTATAGTGAAGCC ACAGATGTATAATCTTCTACATCAACATCCGTGCCTACTGCCTCGGA
Sin3A-1	TGCTGTTGACAGTGAGCGATTCATTCAAAGTCAAGGTCAATAGTGAAGCC ACAGATGTATTGACCTTGACTTTGAATGAACTGCCTACTGCCTCGGA
TNFα	TGCTGTTGACAGTGAGCGACACCACCATCAAGGACTCAAATAGTGAAGC CACAGATGTATTTGAGTCCTTGATGGTGGTGCTGCCTACTGCCTCGGA

Supplementary Table 2: PCR primers

Name	Sequence
XhoI Fw	CAGAAGGCTCGAGAAGGTATATTGCTGTTGACAGTGAGCG
EcoRI Rv	CTAAAGTAGCCCCTTGAATTCCGAGGCAGTAGGCA
Chd8 Fw	TGAATTGCGGCCGCATCGTAATGGCAGACCCCATCAT
Chd8 Rv	CCTAGTCAATTGCAAGTCTGGATCAGTCGTCAGCATCTTCACT
Duplin Fw	CGCCGGAATTAGATCTCTCGAGGACTGACTGAGCGGCCGCATAGATG GCAGACCCCATCATGGATCTTT
Duplin Rv	CGTTAGGGGGGGGGGGCGGAATTCATAGCTAGGTCAATTGTGGCTCA TGTTCTCCGCGCCCAACTCAC

Supplementary Table 3: Antibodies

Target	Source	Dilution
β-actin	Cell Signaling 4967	1:3000
β-catenin	Cell Signaling 9582	1:1000
CHD8 (C-terminus)	Abcam ab84527	1:1000
CHD8 (N-terminus)	Bethyl A301-224A	1:4000
HSP90	BD Biosciences 610418	1:4000
Notch1	Santa Cruz sc-6014	1:3000
RelA (phospho-Ser536)	Cell Signaling 3033	1:1000
SIN3A	Santa Cruz sc-5299	1:1000

Supplementary Table 4: qPCR primers

Primer Name	Sequence
Axin2 FWD	TAGGCGGAATGAAGATGGAC
Axin2 REV	CTGGTCACCCAACAAGGAGT
Btk FWD	CCAGGTCCAGAGTCTTCAGAG
Btk REV	TGGAACTTGTTTGTGTACTCAGTT
Chd8 3' FWD	GGGTCCCTGTCTCTGCATAA
Chd8 3' REV	GGTGATGATGAAGCATGGTA
Chd8 5' FWD	CCAAACTTATTTGGCCTGGA
Chd8 5' REV	GATGAATTCCCCACATCACC
Dtx1 FWD	CCTGAACATCCCAACCCAGG
Dtx1 REV	GCAATCTCAGCACCTTTCGG
Fas FWD	CATGCACAGAAGGGAAGGAGT
Fas REV	GTTTCCACCTCTAAACCATGC
Hes1 FWD	GCCTATCATGGAGAAGAGGCG
Hes1 REV	GGAATGCCGGGAGCTATCTT
Irak2 FWD	TCGCCATGGCTTGCTACATC
Irak2 REV	ACGTAGGAAGCGAACTGCAT
Ltb FWD	CAGCTGCGGATTCTACACCA
Ltb REV	CATCCAAGCGCCTATGAGGT
Nkd2 FWD	AGCAAGACCCTTCGAAGTGAA
Nkd2 REV	CAATCTCTGTTCTGCCACGA
Prf1 FWD	GGTGGGACTTCAGCTTTCCA
Prf1 REV	GAGCAGGGACAGGTCGTG
Sin3A FWD	AAGAGTGGCGAGAAGCTCAG
Sin3A REV	TGCTTGAAGTTGATGCCTTG
TGFβ2 FWD	AAGAGAGAAGGCGCTGAGAG

TGFβ2 REV	TTCTCTCCGCAGATGGGTTG
TNFα FWD	ATGGCCTCCCTCTCATCAGT
TNFα REV	CTTGTTGGTTTGCTACGACG

References

Adams JM, Harris AW, Pinkert CA, Corcoran LM, Alexander WS, Cory S, *et al.* (1985). The c-myc oncogene driven by immunoglobulin enhancers induces lymphoid malignancy in transgenic mice. *Nature* **318**: 533–538.

Aster JC, Xu L, Karnell FG, Patriub V, Pui JC, and Pear WS. (2000). Essential Roles for Ankyrin Repeat and Transactivation Domains in Induction of T-Cell Leukemia by Notch1. *Molecular and cellular biology* **20**: 7505–7515.

Baeuerle PA, and Henkel T. (1994). Function and activation of NF-kappa B in the immune system. *Annu. Rev. Immunol.* **12**: 141–179.

Beverly LJ, Felsher DW, and Capobianco AJ. (2005). Suppression of p53 by Notch in lymphomagenesis: implications for initiation and regression. *Cancer Res.* **65**: 7159–7168.

Chun ACS, and Jin D-Y. (2003). Transcriptional regulation of mitotic checkpoint gene MAD1 by p53. *J Biol Chem* **278**: 37439–37450.

Dannenberg J-H, David G, Zhong S, van der Torre J, Wong WH, and Depinho RA. (2005). mSin3A corepressor regulates diverse transcriptional networks governing normal and neoplastic growth and survival. *Genes Dev* **19**: 1581–1595.

Dalla-Favera R, Bregni M, Erikson J, Patterson D, Gallo RC, and Croce CM. (1982). Human c-myc onc gene is located on the region of chromosome 8 that is translocated in Burkitt lymphoma cells. *Proc. Natl. Acad. Sci. U.S.A.* **79**: 7824–7827.

Farias EF, Petrie K, Leibovitch B, Murtagh J, Chornet MB, Schenk T, *et al.* (2010). Interference with Sin3 function induces epigenetic reprogramming and differentiation in breast cancer cells. *Proc. Natl. Acad. Sci. U.S.A.* **107**: 11811–11816.

Hall JA, and Georgel PT. (2007). CHD proteins: a diverse family with strong ties. *Biochem. Cell Biol.* **85**: 463–476.

Hardy RR, Kincade PW, and Dorshkind K. (2007). The protean nature of cells in the B lymphocyte lineage. *Immunity* **26**: 703–714.

Ishihara K, Oshimura M, and Nakao M. (2006). CTCF-Dependent Chromatin Insulator Is Linked to Epigenetic Remodeling. *Mol. Cell* **23**: 733–742.

Johnson L, Mercer K, Greenbaum D, Bronson RT, Crowley D, Tuveson DA, *et al.* (2001). Somatic activation of the K-ras oncogene causes early onset lung cancer in mice. *Nature* **410**: 1111–1116.

Knoechel B, Roderick JE, Williamson KE, Zhu J, Lohr JG, Cotton MJ, *et al.* (2014). An epigenetic mechanism of resistance to targeted therapy in T cell acute lymphoblastic leukemia. *Nat Genet* **46**: 364–370.

Lin T, Chao C, Saito S, Mazur SJ, Murphy ME, Appella E, *et al.* (2005). p53 induces differentiation of mouse embryonic stem cells by suppressing Nanog expression. *Nat Cell Biol* **7**: 165–171.

Meacham C. (2012). In vivo pool based shRNA screens to identify modulators of disease progression in hematopoietic malignancies. MIT thesis.

Menon T, Yates JA, and Bochar DA. (2010). Regulation of Androgen-Responsive Transcription by the Chromatin Remodeling Factor CHD8. *Mol. Endocrinol.* **24**: 1165–1174.

Minami Y, Stuart SA, Ikawa T, Jiang Y, Banno A, Hunton IC, *et al.* (2008). BCR-ABL-transformed GMP as myeloid leukemic stem cells. *Proc. Natl. Acad. Sci. U.S.A.* **105**: 17967–17972.

Murphy M, Ahn J, Walker KK, Hoffman WH, Evans RM, Levine AJ, *et al.* (1999). Transcriptional repression by wild-type p53 utilizes histone deacetylases, mediated by interaction with mSin3a. *Genes Dev* **13**: 2490–2501.

Nishiyama M, Oshikawa K, Tsukada Y-I, Nakagawa T, Iemura S-I, Natsume T, *et al.* (2009). CHD8 suppresses p53-mediated apoptosis through histone H1 recruitment during early embryogenesis. *Nat Cell Biol* **11**: 172–182.

Nishiyama M, Skoultchi AI, and Nakayama KI. (2012). Histone H1 recruitment by CHD8 is essential for suppression of the Wnt-β-catenin signaling pathway. *Molecular and cellular biology* **32**: 501–512.

Ponader S, and Burger JA. (2014). Bruton's Tyrosine Kinase: From X-Linked Agammaglobulinemia Toward Targeted Therapy for B-Cell Malignancies. *J. Clin. Oncol.*

Rodríguez-Paredes M, Ceballos-Chávez M, Esteller M, García-Domínguez M, and Reyes JC. (2009). The chromatin remodeling factor CHD8 interacts with elongating RNA polymerase II and controls expression of the cyclin E2 gene. *Nucleic Acids Res.* **37**: 2449–2460.

Sawada G, Ueo H, Matsumura T, Uchi R, Ishibashi M, Mima K, *et al.* (2013). CHD8 is an independent prognostic indicator that regulates Wnt/β-catenin signaling and the cell cycle in gastric cancer. *Oncol Rep* **30**: 1137–1142.

Singh H, Shelat AA, Singh A, Boulos N, Williams RT, and Guy RK. (2014). A screening-based approach to circumvent tumor microenvironment-driven intrinsic resistance to BCR-ABL+ inhibitors in Ph+ acute lymphoblastic leukemia. *J Biomol Screen* **19**: 158–167.

Subtil-Rodríguez A, Vázquez-Chávez E, Ceballos-Chávez M, Rodríguez-Paredes M, Martín-Subero JI, Esteller M, *et al.* (2014). The chromatin remodeller CHD8 is required for E2F-dependent transcription activation of S-phase genes. *Nucleic Acids Res.* **42**: 2185–2196.

Suzuki M, Yamada T, Kihara-Negishi F, Sakurai T, and Oikawa T. (2003). Direct association between PU.1 and MeCP2 that recruits mSin3A-HDAC complex for PU.1-mediated transcriptional repression. *Oncogene* **22**: 8688–8698.

Taub R, Kirsch I, Morton C, Lenoir G, Swan D, Tronick S, *et al.* (1982). Translocation of the c-myc gene into the immunoglobulin heavy chain locus in human Burkitt lymphoma and murine plasmacytoma cells. *Proc. Natl. Acad. Sci. U.S.A.* **79**: 7837–7841.

Thompson BA, Tremblay V, Lin G, and Bochar DA. (2008). CHD8 is an ATP-dependent chromatin remodeling factor that regulates beta-catenin target genes. *Molecular and cellular biology* **28**: 3894–3904.

Ventura A, Kirsch DG, McLaughlin ME, Tuveson DA, Grimm J, Lintault L, *et al.* (2007). Restoration of p53 function leads to tumour regression in vivo. *Nature* **445**: 661–665.

Williams RT, Besten den W, and Sherr CJ. (2007). Cytokine-dependent imatinib resistance in mouse BCR-ABL+, Arf-null lymphoblastic leukemia. *Genes Dev* **21**: 2283–2287.

Yates JA, Menon T, Thompson BA, and Bochar DA. (2010). Regulation of HOXA2 gene expression by the ATP-dependent chromatin remodeling enzyme CHD8. *FEBS Lett.* **584**: 689–693.

Young RM, and Staudt LM. (2013). Targeting pathological B cell receptor signalling in lymphoid malignancies. *Nat Rev Drug Discov* **12**: 229–243.

Yuan CC, Zhao X, Florens L, Swanson SK, Washburn MP, and Hernandez N. (2007). CHD8 Associates with Human Staf and Contributes to Efficient U6 RNA Polymerase III Transcription. *Molecular and cellular biology* **27**: 8729–8738.

Zhao X, Jankovic V, Gural A, Huang G, Pardanani A, Menendez S, *et al.* (2008). Methylation of RUNX1 by PRMT1 abrogates SIN3A binding and potentiates its transcriptional activity. *Genes Dev* **22**: 640–653.

Zuber J, McJunkin K, Fellmann C, Dow LE, Taylor MJ, Hannon GJ, *et al.* (2010). Toolkit for evaluating genes required for proliferation and survival using tetracycline-regulated RNAi. *Nat Biotechnol* **29**: 79–83.

Zweidler-McKay PA, He Y, Xu L, Rodriguez CG, Karnell FG, Carpenter AC, *et al.* (2005). Notch signaling is a potent inducer of growth arrest and apoptosis in a wide range of B-cell malignancies. *Blood* **106**: 3898–3906.

Materials and Methods

Cell Culture

BCR-Abl+ B-ALL and Top Notch T-ALL cells were cultured in RPMI-1640 (HyClone) supplemented with 10% FBS, 5μM β-mercaptoethanol, and 4mM L-glutamine. BCR-Abl+ B-ALL cells were a gift from Charles Sherr and Top Notch cells were a gift from Anthony Capobianco. Eu-*myc Arf*$^{-/-}$ cells were cultured in 45% DMEM/45% IMDM (HyClone) supplemented with 10% FBS, 5μM β-mercaptoethanol, and 2mM L-glutamine. *K-ras*$^{LA2/+}$; *p53*$^{LSL/LSL}$ T-ALL cells (a gift from Tyler Jacks) were cultured in IMDM supplemented with 10% FBS and 10μM β-mercaptoethanol. Pre-B cells were harvested from the bone marrow of a healthy C57BL/6 mouse, stained with fluorescently-conjugated anti-B220 (BioLegend), anti-CD11b (eBioscience), and anti-IgM antibodies (eBioscience) and sorted to obtain B220^{+}CD11b^{-}IgM^{-} cells. Pre-B cells were cultured in 45% DMEM/45% IMDM supplemented with 10% FBS, 5μM β-mercaptoethanol, 2mM L-glutamine, recombinant murine IL-7 (1.0 ng/mL), and recombinant murine SCF (1.0 ng/mL) (Peprotech) on a feeder layer of bone marrow stromal cells. 293T cells were cultured in DMEM supplemented with 10% FBS. All cells were incubated at 37°C and 5% CO_2.

shRNAs and plasmids

shRNA sequences were designed and cloned as previously described (Dickins *et al.* 2005). Oligo sequences are listed in Supplementary Table 1 and were PCR-amplified with XhoI and EcoRI primers (sequences listed in Supplementary Table 2). shRNAs were cloned into MSCV/LTRmir30-PGK-puromycin^{r}-IRES-GFP (MLP) or

MSCV/LTRmir30-SV40-GFP (MLS) for GFP competition assays, and TRMPVIR (TRE-dsRed-miR30/shRNA-PGK-Venus-IRES-rtTA3) (Zuber *et al.* 2010) for inducible RNAi studies. MIG (MSCV-IRES-GFP) and MIG-ICN (a gift from Warren Pear) were used for rescue assays. The Gibson Assembly® method (New England BioLabs) was used to clone *Duplin*. mRNA was extracted from BCR-Abl+ B-ALL cells using a Qiagen RNEasy kit and reverse-transcribed with oligo-dT primers and the ThermoScript RT-PCR system (Life Technologies). cDNA was PCR-amplified using Phusion polymerase (New England BioLabs) with primers flanking the *Duplin* sequence and containing Gibson Assembly® overhang sequences (listed in Supplementary Table 2). Following gel purification, the PCR product was ligated into MIG that had been modified by inserting Not1 and Mfe1 sites between the existing EcoRI and XhoI restriction sites using the following sequences:

Forward: 5' TCGAGGACTGACTGAGCGGCCGCTTCGGTCTAGCAATTGACCTAGCTATG 3'

Reverse: 5' AATTCATAGCTAGGTCAATTGCTAGACCGAAGCGGCCGCTCAGTCAGTCC 3'

Clones were sequence-verified by Sanger sequencing. *Chd8* cloning was carried out by PCR-amplification of cDNA from BCR-Abl+ B-ALL cells using the primers listed in Supplementary Table 2. Following gel purification, the PCR product was digested and ligated into a MSG (MSCV-SV40-GFP) retroviral vector that had been modified by inserting NotI and MfeI sites. Clones were sequence-verified by Sanger sequencing. To generate retroviruses, 293T cells were transfected with plasmids using the calcium phosphate method (Swift *et al.* 2001).

Western blotting and qPCR

To confirm target knockdown, cells pellets were generated following puromycin selection

(MLP) or doxycycline treatment of sorted cells (TRMPVIR). *K-ras*$^{LA2/+}$; *p53*$^{LSL/LSL}$ cells were sorted following transduction with MLS. Lysates for western blotting were generated by incubating cell pellets in RIPA lysis buffer (1% NP-40, 0.1% SDS, 50 mM Tris-HCl, pH 7.4, 150 mM NaCl, 0.5% sodium deoxycholate, 1 mM EDTA) with vortexing, followed by centrifugation at 13,000 rpm for 15 minutes. Samples were mixed with 4X SDS sample buffer (Boston BioProducts), run on an SDS-PAGE gel, then transferred to a PVDF membrane (Millipore). Antibodies and dilutions are listed in Supplementary Table 3. mRNA for qPCR analysis was extracted using a Qiagen RNEasy kit and reverse-transcribed using random hexamer primers and MMLV-RT (New England BioLabs). qPCR primer sequences can be found in Supplementary Table 4. qPCR was performed using Fast SYBR® Green Master Mix and a StepOnePlus™ Real-Time PCR System (Applied Biosystems).

Growth competition assays and survival experiments

Following partial infection of cells with the indicated retroviruses, cells were seeded in 6-well plates in triplicate. The percentage of GFP+ cells was determined on days 2, 6, and 10 after infection using a Becton Dickinson FACScan flow cytometer. To carry out *in vivo* competition assays, 2 x 10^6 partially transduced cells were injected into C57BL/6 mice via the tail vein. Upon disease presentation, leukemia cells were harvested from the spleen, bone marrow, and peripheral blood and analyzed on a FACScan flow cytometer to determine the percentage of GFP+ cells. Propidium iodide incorporation was used to quantify dead cells and exclude from analysis. For survival experiments, cells transduced with the indicated constructs in the MLS vector were sorted by GFP expression and approximately 20 GFP+ cells per mouse were injected into the tail vein. Upon disease presentation, cells were harvested from the spleen, bone marrow, and

peripheral blood and analyzed by flow cytometry to determine the percentage of GFP+ cells.

Growth curves and cell cycle analysis

Cells were retrovirally infected with MLP, MLP-sh*Chd8*-0, or MLP-sh*Chd8*-1 and selected with puromycin. The indicated numbers of selected cells were seeded in triplicate, and the total numbers of live and dead cells in each plate were counted at the indicated time points using a hemocytometer and trypan blue incorporation. For cell cycle analysis, BCR-Abl+ B-ALL cells were retrovirally infected with TRMPVIR-shRen or TRMPVIR-sh*Chd8*-1 and sorted by Venus expression. Sorted cells were plated and treated with doxycycline (200 ng/mL), and samples were collected at the indicated time points and fixed in ethanol. Cells were stained with propidium iodide and analyzed on a FACScan flow cytometer. Cell cycle profiles were created with ModFit LT software (Verity Software).

RNA-Seq analysis

BCR-Abl+ B-ALL cells and Top Notch T-ALL cells were each retrovirally infected with TRMPVIR-shRen or TRMPVIR-sh*Chd8*-1 and sorted by Venus expression as above. Sorted cells were treated with doxycycline (200 ng/mL, Sigma) and collected after 24 hours. Biological triplicates were created with three separate plasmid transfections and subsequent retroviral infections. mRNA was extracted from each sample using a Qiagen RNEasy kit and submitted for high-throughput sequencing on the Illumina Hi-Seq platform. Gene expression values were normalized to the mean expression value of each sample. For each cell line, genes were sorted by signal-to-noise ratio and analyzed by GSEA (Broad Institute). Putative hits were validated individually by qPCR as

described above; additionally TRMPVIR-sh*Chd8*-1 results were normalized to those of TRMPVIR-shRen. Primer sequences are listed in Supplementary Table 4.

Pan-caspase inhibition assay

Cells were transduced with TRMPVIR-shRen or TRMPVIR-shChd8-1 and sorted by Venus expression. Cells were plated and treated with doxycycline (200 ng/mL) and Z-VAD-fmk (40μM, R&D Systems) or 0.2% DMSO as vehicle control. Each condition was plated in triplicate wells. Every two days the percentage of live $Venus^{+}dsRed^{+}$ cells in each well was assessed on a Becton Dickinson LSR II, and doxycycline and Z-VAD-fmk were re-administered to maintain a consistent concentration of 200 ng/mL and 40μM, respectively.

Recombinant TNFα rescue assay

BCR-Abl+ B-ALL cells partially transduced with TRMPVIR-shRen or TRMPVIR-shChd8-1 were plated and treated with doxycycline alone (200 ng/mL) or doxycycline plus recombinant murine TNFα (10 ng/mL or 100 ng/mL, Peprotech). Doxycycline was re-administered every 48 hours and TNFα every 24 hours to maintain consistent exposure. Every two days cells were assessed for the percentage of live $Venus^{+}dsRed^{+}$ cells on a Becton Dickinson LSR II.

Cell surface marker staining

5×10^5 BCR-Abl+ B-ALL cells were collected at the indicated time points, stained with APC-conjugated anti-B220 (553092), anti-CD25 (557192), and isotype controls (551139, 550884) (BD Biosciences), and analyzed on a Becton Dickinson LSR II. Histograms were generated using FlowJo software.

Ibrutinib rescue assay

BCR-Abl+ B-ALL cells were transduced with TRMPVIR-shRen or TRMPVIR-sh*Chd8*-1 and sorted to obtain pure Venus+ populations. Cells were plated and treated with doxycycline (200 ng/mL) and ibrutinib (5μM, Selleck Chemicals) or doxycycline alone. Every two days cells were assessed for percentage of live $Venus^{+}dsRed^{+}$ cells on a Becton Dickinson LSR II. Cells were split as needed and maintained on 200 ng/mL doxycycline and 5μM ibrutinib.

Statistical analysis

Student's t tests and survival analyses were performed with GraphPad Prism software.

References

Dickins RA, Hemann MT, Zilfou JT, Simpson DR, Ibarra I, Hannon GJ, *et al.* (2005). Probing tumor phenotypes using stable and regulated synthetic microRNA precursors. *Nat Genet* **37**: 1289–1295.

Swift S, Lorens J, Achacoso P, and Nolan GP. (2001). Rapid production of retroviruses for efficient gene delivery to mammalian cells using 293T cell-based systems. *Curr Protoc Immunol* **Chapter 10**: Unit 10.17C–10.17.29.

Zuber J, McJunkin K, Fellmann C, Dow LE, Taylor MJ, Hannon GJ, *et al.* (2010). Toolkit for evaluating genes required for proliferation and survival using tetracycline-regulated RNAi. *Nat Biotechnol* **29**: 79–83.

Chapter 3: Discussion

From our results it is clear that CHD8 is necessary for survival of B lymphoid cells, both malignant and untransformed. We established that this dependency occurs in both the *in vitro* and *in vivo* settings, indicating that CHD8 functions in a cell-autonomous manner. Additionally, its depletion does not alter the interaction of BCR-Abl+ B-ALL cells with their microenvironment. Although the RNAi screen that identified CHD8 and SIN3A as modulators of leukemia progression was originally designed to identify *in vivo*-specific factors, we appreciate that interesting targets for inhibition can also be factors that have effects in both settings.

CHD8 expression and dependency in normal versus leukemic pre-B cells

We began our investigation into the function of CHD8 in pre-B ALL by looking to evidence provided by prior studies. It had been reported that CHD8 expression is higher in cancer cell lines than in corresponding normal tissues (Nishiyama *et al.* 2009). However, we measured similar expression levels of CHD8 in both pre-B ALL cells and untransformed pre-B cells isolated from the bone marrow of a healthy mouse. Accordingly, when CHD8 was knocked down in these untransformed pre-B cells, we observed depletion of transduced cells in growth competition assays similar to what we see in pre-B ALL cells. The difference in CHD8 expression between normal pre-B cells and other tissues could be attributed to variances between cell types. Nishiyama and colleagues only compared *Chd8* mRNA expression between normal and cancerous cells in the neuronal and hepatocyte lineages. These investigators also examined relative *Chd8* expression in various healthy mouse tissues; however their qPCR results were normalized to *Gapdh* expression, which we have observed to be variable between tissue

types. Without a more consistent standard for normalization and a more comprehensive interrogation of matched tumor-normal tissues, it is difficult to draw generalizable conclusions about relative *Chd8* expression between different cell types.

CHD8 and central signaling pathways

We next examined the effects of CHD8 depletion on leukemic cell proliferation. Others have shown that CHD8 knockdown in cervical carcinoma cells leads to G1 arrest facilitated by downregulation of *CCNE2* and *TYMS*, genes required for transition into S phase (Rodriguez-Paredes *et al.* 2009). However, when we examined cell cycle profiles of BCR-Abl+ B-ALL cells upon CHD8 knockdown, we observed no difference in profiles between control and CHD8-depleted cells. We also did not observe a change in *CCNE2* expression after CHD8 depletion in contrast to this previous study. It is possible that the differences between our results and those of Rodriguez-Paredes *et al.* are due to the distinct signaling contexts present in our pre-B ALL cells relative to the cervical carcinoma cells used in their study.

We observed propidium iodide incorporation by flow cytometry upon CHD8 depletion, indicating cell death. However, we were unable to detect caspase 3 cleavage upon CHD8 depletion, a marker of canonical apoptosis. We subsequently tested the involvement of alternative caspase cascades by treating pre-B ALL cells with the pan-caspase inhibitor Z-VAD-fmk upon CHD8 knockdown. We still observed no change in depletion of sh*Chd8*-expressing cells treated with Z-VAD-fmk versus vehicle control. Again, our findings contrast with those of Nishiyama *et al.* who demonstrated that CHD8 depletion in U2OS osteosarcoma cells led to canonical apoptosis and could be rescued

by Z-VAD-fmk (2009). Our results suggest that a caspase-independent cell death program is activated upon CHD8 depletion. Possible caspase-independent cell death pathways induced by CHD8 depletion include necroptosis, autophagy, and death induced by oxidative stress (Jäättelä and Tschopp 2003; Linkermann and Green 2014). Alternatively, CHD8 depletion could lead to caspase-dependent (but caspase 3-independent) apoptosis under normal conditions, but caspase inhibition by Z-VAD-fmk forces cells to activate other death pathways. Further experiments exploring caspase-independent forms of cell death will be necessary to clarify this phenotype and could shed additional light on the normal function of CHD8.

CHD8 was initially discovered in a screen for proteins that interact with components of the Wnt pathway (Sakamoto *et al.* 2000). Further studies confirmed interaction with β-catenin and negative transcriptional regulation of β-catenin target genes (Kobayashi *et al.* 2001; Thompson *et al.* 2008). Unlike the HeLa cells utilized by Nishiyama and colleagues (2012) our BCR-Abl+ B-ALL cells exhibit constitutive Wnt signaling as seen by stabilization of β-catenin in the absence of stimulation by LiCl or recombinant Wnt3a. In addition, we did not observe negative regulation of the β-catenin target genes *Axin2* and *Nkd2* upon CHD8 depletion. However qPCR measurement of what could be modest transcriptional changes in a large number of target genes may not be the optimal assay. A more sensitive assay for β-catenin function such as a reporter construct may allow us to observe and reproducibly quantify an impact on β-catenin promoter binding upon CHD8 knockdown. Nishiyama *et al.* carried out most experiments with cells that exogenously expressed CHD8 rather than by knocking down the endogenous gene, so perhaps this method magnified the effects of CHD8 on the Wnt pathway (2012). However a study of gastric cancer, which often relies on constitutive

Wnt signaling, has shown that there is likely selection for loss of CHD8 function in these tumor types (Sawada *et al.* 2013). This suggests that CHD8 knockdown should have noticeable effects on the Wnt pathway in these tumors. Alternatively, it is possible that pre-B ALL cells have found a way to uncouple CHD8 from Wnt pathway regulation, allowing both high CHD8 expression and constitutive Wnt signaling to co-exist.

Ectopic CHD8 expression

The large size of the *Chd8* transcript (7.75 kb) led to challenges in subcloning the cDNA sequence, subsequent retroviral infections, and final expression of the full-length protein. Although we were able to insert the full-length cDNA sequence into the MSG vector and found evidence of increased *Chd8* mRNA levels in transduced cells, we were ultimately unable to express the protein at higher levels in BCR-Abl+ B-ALL cells. It may be that the amount of CHD8 within these cells is already very high, so additional ectopic expression does not significantly add to the total amount of protein. Without confirmation of ectopic expression, we were unable to proceed with rescue experiments co-expressing the cDNA and shRNAs targeting the *Chd8* 3' UTR, or a mutated cDNA that avoids recognition by sh*Chd8*. These experiments would have added confirmation that this phenotype is indeed caused by knockdown of CHD8 rather than interference with expression of other proteins.

A number of studies have observed expression of an N-terminal truncated CHD8 isoform termed Duplin (Sakamoto 2000; Nishiyama 2009). We were able to express the Duplin isoform in BCR-Abl+ B-ALL cells; however it did not compensate for knockdown of full-length CHD8, suggesting that domains unique to full-length CHD8 are crucial to its

function in these cells. The second chromodomain, absent in Duplin, has been shown to enable binding to histone H3 (Rodriguez-Paredes *et al.* 2009), and the BRK domains at the C-terminus have been demonstrated to interact with the chromatin insulator CTCF (Ishihara *et al.* 2006). It is curious that in contrast to results of previous studies, endogenous Duplin expression was not found in pre-B ALL cells or in other normal mouse tissues by qPCR. Bioinformatics databases currently only show truncated isoforms of CHD8 in rat, so it is likely that murine Duplin is an experimental artifact that is not physiologically expressed.

CHD8 and B cell differentiation

We hypothesized that CHD8 may be important for regulation of hematopoietic development given the fact that other chromatin-modifying proteins implicated in leukemia have demonstrated roles in differentiation. BCR-Abl+ B-ALL cells exhibit surface markers most consistent with a pro-B cell state in that they are $CD127^{+}BP1^{+}CD19^{+}B220^{+}CD25^{-}$. We hypothesized that CHD8 depletion could be forcing cellular differentiation, represented by an increase in CD25, resulting in cell death. However we did not observe a shift in CD25 expression in these cells upon CHD8 depletion. Although this result did not confirm our hypothesis, additional markers of B cell development (e.g. loss of CD34 or gain of CD20) could be tested to detect changes in other genes important for B lymphoid differentiation.

The results of our experiments with a murine Burkitt's lymphoma cell line demonstrate that B cell malignancies at other stages of differentiation are also dependent on CHD8 expression for survival. Burkitt's lymphoma is a disease

characterized by chromosomal translocations that place the Myc proto-oncogene under the transcriptional control of an immunoglobulin enhancer region, usually IgH (Hecht and Aster 2000). The disease is composed of rapidly proliferating mature germinal center B cells that express IgM and have undergone somatic hypermutation. The dependence of these cells on CHD8 expression suggests that either mature B cells normally retain expression of CHD8 as do less differentiated B cells, or lymphoma cells re-express this protein upon transformation. Isolation of normal mature B cells and characterization of CHD8 expression should be sufficient to answer this question. It would also be interesting to determine if mature B cell malignancies with different genetic backgrounds such as diffuse large B cell lymphoma (DLBCL) and follicular lymphoma are dependent on CHD8 expression for survival as well.

Dependency on CHD8 expression in T-cell malignancies

Previous work by our group has highlighted genes whose effect on survival is context-specific between B and T cell malignancies (Meacham 2012). For example, the chromatin-modifying protein PHF6 is required for survival of BCR-Abl+ B-ALL cells, but loss-of-function mutations are selected for in T-ALL (Van Vlierberghe *et al.* 2010). In addition, factors such as HES1 that promote T lineage development are often fatal when ectopically expressed in the B cell lineage (Zweidler-McKay *et al.* 2005). With this in mind, we looked for differences in B and T cell lineage dependence on CHD8. We employed a constitutively active Notch-driven mouse model of T-ALL (Top Notch) and a cell line derived from a spontaneous murine T cell lymphoma that expresses mutant *K-ras* (KP). We found that the Top Notch T-ALL was significantly less dependent on

CHD8 expression, whereas the KP T cell lymphoma displayed an intermediate phenotype upon CHD8 depletion. Therefore we hypothesized that constitutive signaling through the Notch pathway may be sufficient to rescue cells from the detrimental effects of CHD8 depletion. Because ectopic intracellular Notch (ICN) expression would be lethal to BCR-Abl+ B-ALL cells (Zweidler-McKay *et al.* 2005), we carried out these experiments in the KP lymphoma cell line.

The results of these studies suggest that constitutive Notch signaling is able to partially compensate for CHD8 knockdown. The recent work by Knoechel and colleagues is consistent with this result (2014). The authors found that when chronically treated with low levels of γ-secretase inhibitor (GSI), a subset of Notch-dependent T-ALL cells tolerated treatment by downregulating this pathway (termed "persister cells"). This phenomenon was reversible as cells re-expressed ICN and Notch target genes upon withdrawal of GSI, suggesting an epigenetic mechanism of regulation. In addition, persister cells not only downregulated ICN expression, but also exhibited more compact chromatin and higher levels of repressive chromatin modifications. To identify chromatin-modifying proteins necessary for survival of these altered cells, the authors screened an shRNA library targeting this category of genes in the two populations. While many targets were required for survival of both populations, a subset were found to be "preferentially required" for one cell state over the other. CHD8 was found to be more necessary for the survival of persister cells than the syngeneic cells that had never been exposed to GSI and thus continued to exhibit high levels of ICN and a more open chromatin conformation.

While Knoechel and colleagues did not investigate the mechanism of action of CHD8 in this system, its identification in this screen raises a number of possibilities.

First, CHD8 could be necessary to facilitate the chromatin compaction seen in persister cells, consistent with the model of histone H1 recruitment proposed by Nishiyama and colleagues (2009; 2012). However chromatin compaction alone may not confer a significant advantage to persister cells. Initially, Myc levels decreased after loss of Notch signaling, but then were partially restored, indicating that a compensation mechanism must exist in these cells to correct for the absence of Notch-mediated transcription (Knoechel *et al.* 2014). For example, the acetylated histone-binding protein Brd4, another screen hit preferentially required for persister cell survival, was found to facilitate expression of Myc as well as BCL2 in this chromatin state. Furthermore, persister cells were more sensitive to inhibition of Brd4 by the small molecule JQ1 than GSI-naïve cells. BCL2 and Myc expression levels were found to be downregulated by JQ1 treatment in a dose-dependent manner in persister but not naïve cells. These results suggest that chromatin-modifying proteins that compensate for chromatin compaction by promoting transcription are required for persister cell survival. However the possibility that CHD8-mediated chromatin compaction promotes survival of persister cells cannot be ruled out based on the current evidence.

Alternatively, CHD8 could act to enhance global transcription in the state of chromatin compaction seen in the persister cells. CHD8 has been shown to bind to H3K4me2/3 though its tandem chromodomains (Rodriguez-Paredes *et al.* 2009). H3K4me2/3 is enriched at promoters of actively transcribed genes, so CHD8 has the potential to bind to these modified histones and recruit other components of the transcriptional machinery and/or make these regions more accessible to transcription factors. In this scenario, when CHD8 is depleted in persister cells, transcription of a large set of genes is modestly decreased and cells are unable to survive. This model

has precedent in the action of the proto-oncogene Myc, which has been shown to bind to large portions of the genome yet has relatively weak effects on transcript levels of particular genes (Eilers and Eisenman 2008; Lin *et al.* 2012). A similar function has been proposed for CHD7, another CHD type III family member (Schnetz *et al.* 2009; 2010). These studies found that CHD7 associates with over 10,000 sites in the genome, many of them distal enhancer elements enriched for H3K4me1 marks, and modestly represses expression of actively transcribed genes. Interestingly, Knoechel *et al.* identified CHD7 as preferentially required in GSI-naïve cells that express high levels of ICN and have a more open chromatin conformation (2014). Perhaps CHD7 rather than CHD8 helps facilitate ICN-mediated transcription through binding to H3K4me1 at enhancer elements of Notch target genes, explaining the mild phenotype of Top Notch cells upon CHD8 depletion. Significant depletion of Top Notch cells in growth competition assays upon CHD7 knockdown would support this hypothesis.

CHD8 as a global regulator of transcription

The results of our genome-wide transcriptional analysis of BCR-Abl+ B-ALL and Top Notch cells are also consistent with this model of large-scale gene regulation. RNA-Seq showed no statistically significant transcriptional changes of particular genes in either cell line upon CHD8 depletion. CHD8 could exhibit a global effect on mRNA expression that standard RNA-Seq analysis might misinterpret. Lovén *et al.* reported that standard RNA-Seq and microarray normalization procedures can misrepresent global transcriptional effects of genes such as Myc (2012). These standard procedures assume that all cell states yield equal amounts of RNA per cell and that the perturbation

under investigation has a pronounced transcriptional effect on a limited set of genes. Thus these assumptions can lead to misinterpretation of widespread but modest effects such as the increased transcription of a large percentage of genes by Myc. If CHD8 binds to active promoters marked by H3K4me2/3 and helps facilitate recruitment of transcription factors, then the levels of many actively transcribed genes are potentially altered upon CHD8 knockdown, resulting in decreased fitness and ultimately death. The recent work by Subtil-Rodriguez *et al.* confers additional support for this model (2014). This study demonstrated that CHD8 binds to nearly 2,000 gene promoters. Notably, these promoters are enriched for H3K4me2/3 marks, and CHD8 binding at these sites activates transcription. However, this model of transcriptional enhancement seems to conflict with the paradigm of CHD8-facilitated transcriptional repression through recruitment of histone H1 to active promoter regions (Nishiyama *et al.* 2009; 2012). It may be that the transcription factor that binds to CHD8 in each situation determines its function. Further examination into changes in global transcription upon CHD8 depletion in both BCR-Abl+ B-ALL and Top Notch T-ALL cells will be needed to test this model.

While it has proved challenging to define a discrete set of genes that display statistically significant change in expression upon CHD8 depletion, we have observed evidence of a role for CHD8 in the regulation of NF-κB target genes. BCR-Abl+ B-ALL cells are sensitive to RNAi-mediated depletion of TNFα, and addition of recombinant TNFα was able to partially alleviate the sh*Chd8* phenotype. After CHD8 depletion we observed a decrease in levels of phosphorylated RelA in both BCR-Abl+ B-ALL and Top Notch cells, indicating decreased activation of the NF-κB pathway. The different dependencies of these two cell lines on CHD8 function could be due to variable responses to decreased NF-κB signaling. It may be that CHD8 is acting on the NF-κB

pathway in a similar manner in both cell types, but Top Notch cells are able to compensate for the decrease in NF-κB signaling through constitutive Notch signaling, or are intrinsically less reliant on this pathway for survival. The precise mechanism of compensation by Notch is yet to be determined. Our work calls for further investigation into the link between CHD8 and NF-κB, as it is possible that CHD8 could be functioning at promoters of NF-κB target genes to regulate transcription.

RNAi screening identifies epigenetic regulators as potential drug targets

Previous work by our group identified *Chd8* and *Sin3a* as positive regulators of disease progression in a mouse model of Ph+ B-ALL through a large-scale RNAi screen (Meacham 2012). Other RNAi screens have identified additional chromatin-modifying proteins as important factors in hematopoietic malignancies. One such screen identified the bromodomain-containing protein Brd4 as a positive regulator of disease progression in a mouse model of AML (Zuber *et al.* 2011). Accordingly, inhibition of Brd4 by the small molecule JQ1 resulted in differentiation of AML cells and increased survival in mice transplanted with this model. A separate RNAi screen also performed in a murine AML model identified the histone demethylase Jmjd1c as necessary for survival of AML cells but not normal bone marrow cells (Sroczynska *et al.* 2014). Inhibiting the effects of chromatin-modifying proteins may be an effective treatment strategy in leukemias driven by "undruggable" transcription factor oncogenes such as Myc, or a way to overcome resistance to targeted therapeutics such as GSIs and tyrosine kinase inhibitors (TKIs).

Acquired resistance to TKI therapy is a major roadblock in the effective treatment of BCR-Abl+ B-ALL. Resistance frequently arises due to mutations in the Abl ATP-

binding pocket that interfere with drug binding. The T315I "gatekeeper" mutation of Abl is particularly problematic as it prevents binding to three out of the four FDA-approved TKIs: imatinib, dasatinib, and nilotinib (Cortes *et al.* 2013). Ponatinib, a third-generation TKI, is able to inhibit BCR-Abl T315I; however use of this drug has been shown to cause serious adverse vascular events and is limited to patients who are resistant to first- or second-generation TKIs. It is abundantly clear that inhibition of targets in addition to BCR-Abl are necessary to improve disease prognosis, and targets that will synergize with TKI therapy will be especially effective. For example, recent work has shown that BCR-Abl+ B-ALL is dependent on NF-κB signaling (Hsieh and Van Etten 2014). Transduction of Bcr-Abl+ leukemic cells with dominant negative forms of IKKα, IKKβ, or IκBα conferred greater sensitivity to imatinib. With numerous potent NF-κB pathway inhibitors approved for human use or in development, one can speculate that a number of them may be effective against this disease when combined with TKI therapy.

A growing body of literature shows that inhibition of chromatin-modifying proteins is a promising field of investigation and drug development. Inhibiting these factors may serve to correct global transcriptional deregulation instigated by events such as Myc overexpression. Our work with B cell malignancies suggests that CHD8 is a potential effective drug target as long as toxicity in normal hematopoietic cells is not limiting. However, inhibiting CHD8 would not be as effective in T cell malignancies driven by Notch signaling, and could be counter-productive in certain solid tumors. When compared to the wealth of knowledge about other chromatin-modifying proteins, our understanding of the function of CHD8 is relatively incomplete. Nonetheless, it is clear that CHD8 has critical roles in cell proliferation and survival, and additional investigation

should be carried out to better define its place within central signaling pathways and global transcriptional regulation.

References

Cortes JE, Kim DW, Pinilla-Ibarz J, le Coutre P, Paquette R, Chuah C, *et al.* (2013). A phase 2 trial of ponatinib in Philadelphia chromosome-positive leukemias. *N Engl J Med* **369**: 1783–1796.

Eilers M, and Eisenman RN. (2008). Myc's broad reach. *Genes Dev* **22**: 2755–2766.

Hecht JL, and Aster JC. (2000). Molecular biology of Burkitt's lymphoma. *J. Clin. Oncol.* **18**: 3707–3721.

Hsieh M-Y, and Van Etten RA. (2014). IKK-dependent activation of NF-κB contributes to myeloid and lymphoid leukemogenesis by BCR-ABL1. *Blood* **123**: 2401–2411.

Ishihara K, Oshimura M, and Nakao M. (2006). CTCF-Dependent Chromatin Insulator Is Linked to Epigenetic Remodeling. *Mol. Cell* **23**: 733–742.

Jäättelä M, and Tschopp J. (2003). Caspase-independent cell death in T lymphocytes. *Nat Immunol* **4**: 416–423.

Knoechel B, Roderick JE, Williamson KE, Zhu J, Lohr JG, Cotton MJ, *et al.* (2014). An epigenetic mechanism of resistance to targeted therapy in T cell acute lymphoblastic leukemia. *Nat Genet* **46**: 364–370.

Kobayashi M, Kishida S, Fukui A, Michiue T, Miyamoto Y, Okamoto T, *et al.* (2002). Nuclear localization of Duplin, a beta-catenin-binding protein, is essential for its inhibitory activity on the Wnt signaling pathway. *J Biol Chem* **277**: 5816–5822.

Lin CY, Lovén J, Rahl PB, Paranal RM, Burge CB, Bradner JE, *et al.* (2012). Transcriptional amplification in tumor cells with elevated c-Myc. *Cell* **151**: 56–67.

Linkermann A, and Green DR. (2014). Necroptosis. *N Engl J Med* **370**: 455–465.

Lovén J, Orlando DA, Sigova AA, Lin CY, Rahl PB, Burge CB, *et al.* (2012). Revisiting global gene expression analysis. *Cell* **151**: 476–482.

Meacham C. (2012). In vivo pool based shRNA screens to identify modulators of disease progression in hematopoietic malignancies. MIT thesis.

Nishiyama M, Oshikawa K, Tsukada Y-I, Nakagawa T, Iemura S-I, Natsume T, *et al.* (2009). CHD8 suppresses p53-mediated apoptosis through histone H1 recruitment during early embryogenesis. *Nat Cell Biol* **11**: 172–182.

Nishiyama M, Skoultchi AI, and Nakayama KI. (2012). Histone H1 recruitment by CHD8 is essential for suppression of the Wnt-β-catenin signaling pathway. *Molecular and cellular biology* **32**: 501–512.

Rodríguez-Paredes M, Ceballos-Chávez M, Esteller M, García-Domínguez M, and Reyes JC. (2009). The chromatin remodeling factor CHD8 interacts with elongating RNA polymerase II and controls expression of the cyclin E2 gene. *Nucleic Acids Res.* **37**: 2449–2460.

Sakamoto I, Kishida S, Fukui A, Kishida M, Yamamoto H, Hino S, *et al.* (2000). A novel beta-catenin-binding protein inhibits beta-catenin-dependent Tcf activation and axis formation. *J Biol Chem* **275**: 32871–32878.

Sawada G, Ueo H, Matsumura T, Uchi R, Ishibashi M, Mima K, *et al.* (2013). CHD8 is an independent prognostic indicator that regulates Wnt/β-catenin signaling and the cell cycle in gastric cancer. *Oncol Rep* **30**: 1137–1142.

Schnetz MP, Bartels CF, Shastri K, Balasubramanian D, Zentner GE, Balaji R, *et al.* (2009). Genomic distribution of CHD7 on chromatin tracks H3K4 methylation patterns. *Genome Research* **19**: 590–601.

Schnetz MP, Handoko L, Akhtar-Zaidi B, Bartels CF, Pereira CF, Fisher AG, *et al.* (2010). CHD7 targets active gene enhancer elements to modulate ES cell-specific gene expression. *PLoS Genet.* **6**: e1001023.

Sroczynska P, Cruickshank VA, Bukowski J-P, Miyagi S, Bagger FO, Walfridsson J, *et al.* (2014). shRNA screening identifies JMJD1C as being required for leukemia maintenance. *Blood* **123**: 1870–1882.

Subtil-Rodríguez A, Vázquez-Chávez E, Ceballos-Chávez M, Rodríguez-Paredes M, Martín-Subero JI, Esteller M, *et al.* (2014). The chromatin remodeller CHD8 is required for E2F-dependent transcription activation of S-phase genes. *Nucleic Acids Res.* **42**: 2185–2196.

Thompson BA, Tremblay V, Lin G, and Bochar DA. (2008). CHD8 is an ATP-dependent chromatin remodeling factor that regulates beta-catenin target genes. *Molecular and cellular biology* **28**: 3894–3904.

Van Vlierberghe P, Palomero T, Khiabanian H, Van der Meulen J, Castillo M, Van Roy N, *et al.* (2010). PHF6 mutations in T-cell acute lymphoblastic leukemia. *Nat Genet* **42**: 338–342.

Zuber J, Shi J, Wang E, Rappaport AR, Herrmann H, Sison EA, *et al.* (2011). RNAi screen identifies Brd4 as a therapeutic target in acute myeloid leukaemia. *Nature* **478**: 524–528.

Zweidler-McKay PA, He Y, Xu L, Rodriguez CG, Karnell FG, Carpenter AC, *et al.* (2005). Notch signaling is a potent inducer of growth arrest and apoptosis in a wide range of B-cell malignancies. *Blood* **106**: 3898–3906.